

SORPTION OF ARSENIC BY IRON SULFIDE MADE BY SULFATE-REDUCING
BACTERIA: IMPLICATIONS FOR BIOREMEDIATION

Except where reference is made to the work of others, the work described in this thesis is my own or was done in collaboration with my advisory committee. This thesis does not include proprietary or classified information.

Prakash Dhakal

Certificate of Approval:

Ming-Kuo Lee
Professor
Geology and Geography

James A. Saunders, Chair
Professor
Geology and Geography

Lorraine W. Wolf
Professor
Geology and Geography

George T. Flowers
Dean
Graduate School

SORPTION OF ARSENIC BY IRON SULFIDE MADE BY SULFATE-REDUCING
BACTERIA: IMPLICATIONS FOR BIOREMEDIATION

Prakash Dhakal

A Thesis

Submitted to

the Graduate Faculty of

Auburn University

in Partial Fulfillment of the

Requirement for the

Degree of

Master of Science

Auburn, Alabama
December 19, 2008

SORPTION OF ARSENIC BY IRON SULFIDE MADE BY SULFATE-REDUCING
BACTERIA: IMPLICATIONS FOR BIOREMEDIATION

Prakash Dhakal

Permission is granted to Auburn University to make copies of this thesis at its discretion, upon the request of individuals or institutions and at their expense. The author reserves all publication rights.

Signature of Author

December 19, 2008
Date of Graduation

VITA

Prakash Dhakal, son of Mr. Devi Prasad Dhakal and Mrs. Indira Devi Dhakal, was born in 1975 in Bhojpur, Nepal. He completed his Secondary Education in 1992 from Juddha Secondary School, Rautahat, Nepal. He received his Intermediate in Science (I.Sc) and Bachelor in Science (B.Sc) in 1996 and 1999, respectively from Tri-Chandra Multiple Campus, Tribhuvan University (TU), Kathmandu, Nepal. His first Master's degree was in "Engineering and Geological Techniques" from Central Department of Geology (CDG), TU in 2002. After working two years as an assistant lecturer at the CDG-TU, he entered Graduate School at Auburn University in fall 2006. Upon completion of his Master of Science degree, he will continue his studies towards a Ph.D. in Environmental Engineering at Vanderbilt University, Nashville, Tennessee, USA.

THESIS ABSTRACT

SORPTION OF ARSENIC BY IRON SULFIDE MADE BY SULFATE-REDUCING BACTERIA: IMPLICATIONS FOR BIOREMEDIATION

Prakash Dhakal

Master of Science, December 19, 2008
(Master of Science, Tribhuvan University, Nepal, 2002)
(Bachelor of Science, Tribhuvan University, Nepal, 1999)

135 Typed pages

Directed by James Saunders

In this study, data from field bioremediation experiments, geochemical modeling, and laboratory batch experiments were integrated with published data on arsenic (As) sorption and coprecipitation onto growing iron (Fe)-sulfide phases [e.g., iron monosulfide, FeS, pyrite, FeS₂, and arsenian pyrite, Fe(S, As)₂] to characterize geochemical processes during *in situ* bioremediation of natural As-contaminated groundwater. Field bioremediation experiments conducted in the past on groundwater in Holocene alluvial aquifers in Bangladesh and the United States (US) have shown that As was incorporated into Fe-sulfide phases in reducing groundwater, and that this process can be fast as well as efficient. This study shows that As can be removed in a matter of weeks after the injection of water-soluble labile organic carbon and sulfate that stimulate metabolism of indigenous sulfate-reducing bacteria (SRB) in Fe-bearing, low-temperature, reduced, As-contaminated groundwater.

A new set of thermodynamic data for thioarsenite species, amorphous arsenic and Fe-sulfide phases, and solid solution of arsenian pyrite ($\text{FeS}_{1.99}\text{As}_{0.01}$ – $\text{FeS}_{1.90}\text{As}_{0.10}$) were compiled into a revised Geochemist's Workbench (GWB) database, *Thermo08-As*, to model the principal geochemical behavior of As in aerobic and anaerobic groundwaters. Compared to the most widely used geochemical modeling programs, which lack thermodynamic data for solid solutions of arsenian pyrite, this new thermodynamic database is more realistic in characterizing and predicting As behavior in changing redox conditions. Under Fe-rich geochemical conditions, the stability field of arsenian pyrite (containing 1 to 10 wt.% As) solid solution completely dominates in reducing Eh-pH space and “displaces” other As-sulfides (orpiment, realgar) that have been implied to be important in previous modeling and field studies.

Sorption of dissolved As in synthetic Fe-sulfide and natural pyrite as a function of total As concentration, sulfide ratio, Eh-pH, time, and grain size of pyrite, were investigated in the laboratory. Arsenic is strongly partitioned on both FeS and FeS₂ under a range of conditions, such as pH and As concentration. In the sulfide-limited (S:Fe=1:1) experiment that produced synthetic FeS, 91% of the initial dissolved As, was sorbed. In contrast, in the excess-sulfide (S:Fe=2:1 and 3:1) experiment, 55% of the initial As concentration was sorbed, but yielded pyrite as a solid phase. Amount of As sorbed onto pyrite is dependent on grain size, but conformed to a Langmuir isotherm at circumneutral pH. Field data, geochemical modeling, and laboratory results clearly indicate that As is mobile under Fe-reducing conditions, but immobile under anaerobic and sulfate-reducing conditions. Fe-oxyhydroxides and arsenian pyrite are the likely stable mineral phases that serve as major sink for As under aerobic and sulfate-reducing conditions, respectively.

ACKNOWLEDGMENTS

It is an immense pleasure to thank my thesis advisor, Dr. James A. Saunders, for bringing me to Auburn University for a master's degree in Geology, and for his active involvement in my research to get the best out of me in my work with constant support and inspirations. I also highly value the guidance received from my committee members, Drs. Ming-Kuo Lee and Lorraine W. Wolf for their support and contribution to complete this study. Special thanks goes to Dr. Ming-Kuo Lee for his guidance in geochemical modeling techniques without which it would almost be impossible to bring this research into conclusion. I would like to thank the faculty, staff, and fellow students of the Auburn University Geology Department for their support and friendship.

I am deeply obliged to Drs. Mark Barnett and Prabhakar Clement of Auburn University's Department of Civil Engineering for providing me access to their laboratory facility. Personal thanks go to Dr. Suhil Raj Kanel, post-doctoral fellow, and other fellow graduate students at the Department of Civil Engineering, Auburn University, for their generous help during laboratory experiments, analytical techniques, and AAS analysis. I cannot forget the help offered by Dr. Thomas Albrecht-Schmitt, Department of Chemistry and Biochemistry, Auburn University, for XRD analysis.

I would I like to express my sincere gratitude to Dr. Kaye Savage of Vanderbilt University's Department of Earth and Environmental Geosciences for LA-ICPMS, and providing me with an opportunity to carry out Ph.D. study under her supervision.

This research was made possible through the financial support from the U.S. National Science Foundation (EAR-0352936 and EAR-0445250), and Auburn University. I thank the Department of Geology and Geography of Auburn University for providing me support through graduate teaching and research assistantships. It is important for me not to forget Mohammad Shamsudduha, Jamey P. Turner, and Tareq Chaudary for prior work in Manikganj and the use of their hard-earned field data.

I feel proud to dedicate this thesis to my family, parents Devi P. Dhakal and Indira D. Dhakal, my beloved sisters Prava and Anusha, and my wife Saraswati Bhetwal for their inspiration, energy, and endless patience and love for me.

Style manual or journal used

Applied Geochemistry

Computer software used

Adobe Acrobat 6 Professional

Adobe Illustrator 9.0

Adobe Photoshop 7

ArcGIS 9.1

EndNote X.0.2

Geochemist's Workbench 2001

Golden Software Grapher 2.0

Golden Software Surfer 8.0

Microsoft Excel 2007

Microsoft Word 2007

TABLE OF CONTENTS

LIST OF FIGURES	xiii
LIST OF TABLES	xvii
CHAPTER 1: INTRODUCTION	1
1.1. Global arsenic groundwater pollution.....	1
1.2. Source and occurrence of arsenic	6
1.3. Research objectives.....	12
1.4. Location for field bioremediation experiment.....	14
1.5. Thesis outline	17
CHAPTER 2: BACKGROUND AND PREVIOUS STUDY	18
2.1. Arsenic speciation in natural waters	18
2.2. Groundwater arsenic geochemistry.....	22
2.3. Transport and sorption chemistry of arsenic in groundwater	23
2.4. Subsurface Microbiology.....	27
2.4.1. Subsurface microbial iron reduction	27
2.4.2. Subsurface microbial sulfate reduction	31
2.5. Formation of microbial and sedimentary iron sulfate.....	32
2.6. Precipitation of arsenic under sulfate reducing conditions.....	34
2.7. <i>In situ</i> bioremediation of arsenic-contaminated aquifer	40

CHAPTER 3: MATERIALS AND EXPERIMENTAL METHODS.....	44
3.1. Field bioremediation experiment.....	44
3.2. Geochemical modeling.....	47
3.3. Laboratory arsenic sorption experiment.....	51
3.3.1. Batch experiment: arsenic sorption onto iron sulfide.....	53
3.3.2. Batch experiment: arsenic sorption onto pyrite.....	55
3.4. Analytical methods.....	58
CHAPTER 4: RESULTS AND DISSUSSION.....	60
4.1. Field bioremediation experiments.....	60
4.2. Geochemical modeling.....	66
4.2.1. Arsenic speciation.....	66
4.2.2. Arsenic precipitation under sulfate-reducing conditions.....	68
4.3. Arsenic sorption experiment.....	73
4.3.1. Sorption of arsenic onto iron sulfide.....	74
4.3.2. Pyrite adsorption experiment.....	84
4.3.2.1. Adsorption kinetics.....	84
4.3.2.2. Adsorption isotherm.....	86
4.3.2.3. Adsorption envelopes.....	89
4.4. Role of arsenic-bearing pyrite in arsenic removal: discussion.....	92
CHAPTER 5: CONCLUSIONS.....	98
5.1. Specific research conclusions.....	99
5.2. Recommendation for future studies.....	102
REFERENCES.....	104

APPENDIX 1: Laboratory results from batch experiments conducted to investigate sorption of arsenic onto synthetic iron-sulfide	114
APPENDIX 2: Tabulated data from laboratory experiments carried out to find the most suitable chemical solution to wash pyrite crystals that can maximize the adsorption of As with minimum changes in pH	115
APPENDIX 3: Laboratory data obtained from the adsorption kinetic experiment on pyrite	116
APPENDIX 4: Data derived from the adsorption isotherm experiment.....	117
APPENDIX 5: Tabulated data from laboratory experiments conducted to investigate changes in As concentration as a function of pH and grain size	118

LIST OF FIGURES

<p>Figure 1.1 Map showing major As-affected natural groundwater aquifers around the world. Location of As-affected groundwater from mining related work and geothermal sources are also marked in the map (modified after Smedley and Kinniburgh, 2002).....</p>	2
<p>Figure 1.2 Location map showing major deltaic region in southeast Asia with elevated groundwater As-contamination. Region marked in numbers are: (1) Indus delta, Pakistan; (2) Terai alluvial plain, Nepal; (3) Ganges-Brahmaputra delta, West Bengal, Nepal; (4) Meghna delta, Bangladesh; (5) Irrawaddy river delta, Myanmar; (6) Red river delta, Ha Noi, Vietnam; (7) Mae-Klong and Chao-Phraya, Thailand; (8) Mekong delta, Vietnam.....</p>	4
<p>Figure 1.3 Map showing the location of bioremediation site at Blackwell, Oklahoma (Source: Saunders et al., 2008)</p>	15
<p>Figure 1.4 Map showing tube well locations in the bioremediation site in the Manikganj district of Bangladesh and their relative dissolved arsenic concentrations. Location of injection well (IW-2) for the Bangladesh bioremediation experiment is also shown (modified after Shamsudduha, 2007).....</p>	16
<p>Figure 2.1 Eh-pH diagram of arsenic species in As-O-S-H₂O system.</p>	19
<p>Figure 2.2 (a) Plot showing speciation of arsenite [As (III)] and (b) arsenate [As (V)] as a function of pH (at different ionic concentration) (modified after Smedley and Kinniburgh, 2002; and Wolthers et al., 2005c).....</p>	21
<p>Figure 2.3 Double-layer adsorption-desorption model calculated using GWB representing the sorption of As(OH)₄⁻ [As (III)] and AsO₄³⁻ [As (V)] at different pH condition. Sorbed percentage (a), and dissolved arsenic concentration against pH calculated by HFO desorption simulations with pH ascending from 2 to 7 (b) and 7 to 12(c) (modified after Lee et al., 2005, and Turner, 2006)</p>	25
<p>Figure 2.4 Schematic model for the biogeochemical cycling of arsenic and iron in the subsurface. (a) sediment deposition; (b) burial; (c) dissolution; (d) diffusion; (e) coprecipitation; (f) diffusion and reaction with sulfide (modified after Cullen and Reimer, 1989 and references therein)</p>	29

Figure 2.5 Sequence of microbial TEAP process in subsurface pristine aquifers (modified after Lovley, 2001; personal commun, Saunders et al., 2008).....	30
Figure 2.6 The proposed reaction pathways for pyrite formation in anoxic sedimentary environment (modified after Morse et al., 1987 and reference therein).....	33
Figure 2.7 Image on the top is a photomicrograph (reflected light) of arsenic-rich biogenic pyrite from Holocene alluvial aquifer in Alabama, USA. Chemical analysis of this sample show up to 1 wt.% of As in pyrite. Arsenic content substantially increases towards core (source, Saunders et al., 1997). Picture on the bottom is a result of a laser ablation inductively coupled plasma mass spectrometry, LA-ICM-MS conducted on the As rich pyrite sample shown above. LA-ICP-MS micro-beam probed onto the sample along the line (3 mm) show coexistence of As-Fe-S in the sample (source, Savage et al., 2000).....	37
Figure 2.8 Schematic of existing and proposed arsenic-removal techniques (modified after Driehaus, 2005)	42
Figure 3.1 Photograph of the single-well field bioremediation experiment carried out in Manikganj, Bangladesh. (a) Photograph showing injected well (IW-2), and (b) water supply-tube well used for water sampling before and after the bioremediation experiment (photo source Shamshudduha, 2007).....	46
Figure 3.2 Photograph of Batron™ anaerobic chamber used for studying arsenic sorption on laboratory prepared Fe-sulfide and hand crushed pyrite crystals	52
Figure 3.3 Plot showing arsenic adsorption with concurrent changes in pH observed in pyrite crystals washed using 5 different approaches: ethanol (C ₂ H ₆ O, 10%) only, nitric acid (0.5M HNO ₃) only, ethanol followed by DIW, nitric acid followed by DIW, and with DIW separately before treating with arsenic concentration.....	56
Figure 4.1 Plot showing changes in As, Fe, and SO ₄ ²⁻ concentration recorded after a single-well bioremediation experiment carried out at Blackwell, Oklahoma (a) and Manikganj, Bangladesh (b).Changes in soluble Fe, As and SO ₄ ²⁻ were recorded after the injection of molasses, Epsom’s salt (MgSO ₄ ·7H ₂ O). Molasses was used as a source of carbon to enhance iron reduction, and the sulfate salts was used as source for sulfate to enhance metabolism in indigenous SRB for sulfate reduction.....	62
Figure 4.2 Eh-pH diagram for As drawn at 25°C with fixed arsenic and SO ₄ ²⁻ activities of 10 ⁻² and Fe ²⁺ activity of 10 ⁻⁸ . Eh value for the system was fixed at 0.75V. Modeling conducted in GWB that included new thermodynamic data for arsenian pyrite solid solution	67

Figure 4.3 Fe-As-S-H₂O composite Eh-pH diagram showing results of geochemical reaction flow-path modeling. Analogous to field bioremediation FeSO₄ was added in the initial system to immobilize As. The simulation was fixed at 25 °C, and 1 bar pressure. Reaction trace (pink solid line) represents the predictive sequence of mineral precipitated as Eh drops during simulation. Chemical precipitation of the minerals in both the geochemical condition, without (a) and with (b) thermodynamic data for arsenian pyrite solid solution (FeS_{1.99}As_{0.01}.FeS_{1.90}As_{0.10}), initiated from top green square at the center of the figure. Reaction came to an end after the precipitation of siderite in the first model (a) but, mineral precipitation continues until arsenian pyrite is precipitated at the final stage in the second model (b) Pink cross marks in center of both the figure shows Eh-pH scatter plot of the water samples from Bangladesh. Model was created using *Act2* module of GWB69

Figure 4.4 Plots showing predictive cumulative sequence of mineral precipitated as Eh decreases as a result of bacterial sulfate reduction. Geochemical reaction-path modeling carried out in a simulation that includes thermodynamic data for arsenian pyrite solid solutions precipitates arsenian pyrite (b) as a most dominant mineral species whereas, such mineral phase is absence in the model that lacks thermodynamic database for arsenian pyrite solid solution (a) Model was created using *React* module of GWB71

Figure 4.5 Plot of the effect of pH values on mineral solubility recorded from GWB simulation that included thermodynamic data for arsenian pyrite solid solution. Solubility diagrams versus aH₂S for Fe-sulfide minerals at 25 °C computed for total dissolved arsenic species activity = 10⁻². Fe-sulfide minerals and aqueous species are separated by solid (red) line. Dashed lines show metastable boundaries for intermediate phases mackinawite (FeS)_{am}, pyrite, and arsenian pyrite at pH=5 (a) and at pH=7 (b).....72

Figure 4.6 Plot showing changes in pH (a) and Eh (b) recorded from the batch experiment. Sulfide-limited experiment with 0.1 mg/L of As concentration shows slight drop in pH and slight increase in Eh. Excess-sulfide samples recorded increase in pH and a drop in Eh compared to the beginning of the experiment (pH 7 and Eh= ~+55 mV).....75

Figure 4.7 Plot showing percentage of As sorbed onto Fe-sulfide in the laboratory batch experiment. Number after the letter in the sample number indicate the ratio of sulfur to iron (e.g., 1=1:1, 2 indicate=2:1, and 3=3:1, sulfur to iron ratio, respectively)..78

Figure 4.8 Images of marcasite (a, and b), and pyrite (c, d, e, and f) taken under reflected light microscope that are formed in the batch experiment. Pyrite observed in figure c, d and f are cubic where as framboidal structure is observed in the sample shown in figure e (unidentified). Black (a, b, and c) and dark brown to light yellow (d, e and f) precipitate seen in the background is mackinawite and HFO respectively. Mineral identification is based on XRD results80

Figure 4.9 Images of different Fe-sulfide minerals formed in the batch experiment. Limited batch samples produced well developed crystallographic minerals, especially those prepared in sulfide-excess condition. Such minerals were not observed in sulfide-limited experiment. (a) marcasite; (b, and c) Fe-sulfide (unidentified); (d) euhedral grain of synthetic troilite; (e) framboidal pyrite (?), and (f) pyrite. Unless indicated, identification of these minerals is based on XRD results.....81

Figure 4.10 Plots of XRD spectra observed at the same arbitrary scale for the end products of the batch reacted with various As concentrations in sulfide-limited and excess-sulfide experiments. Almost all samples aged below 72 hr, regardless of As concentration and sulfide ratio, indicate mackinawite and marcasite were the most dominant Fe-sulfide phases. (similar to 2WC-1_01, and 1WB-2_01 samples). Few samples (matured for 1 to 2 weeks) prepared in excess-sulfide condition indicate the presence of various Fe-sulfide phases (mackinawite, marcasite, pyrite, and troilite)82

Figure 4.11 Graphical plot prepared from the test experiment conducted to calibrate equilibrium adsorption time for fine-(a), intermediate-(b), and coarse-(c) grained pyrite crystals as a function of time. Batch experiments was prepared with different arsenic concentration (0.1 mg/L, 1 mg/L, and 10 mg/L) at solid/solution ratio=6 gm/L. Equilibrium adsorption was reached at about 24 hr87

Figure 4.12 Plots of adsorption isotherm of As on 6 gm/L of pyrite at neutral pH. The lines are the Langmuir isotherm fits for the entire data set. Coefficient of determination, r^2 for the best logarithmic fit on the dataset presented here are 0.9468, 0.9838, and 0.9861 for fine-, intermediate-, and coarse-grained samples, respectively....88

Figure 4.13 Plot showing As adsorption per unit mass adsorbent as a function of pH for fine, intermediate, and coarse grained pyrite crystals for different amounts of added arsenic concentration (0.1 mg/L, 1 mg/L, 10 mg/L). Concentration of pyrite is 6gm/L and equilibrium time is 36 hr91

LIST OF TABLES

Table 1.1 Arsenic concentration ranges in rocks, sediments, and soils (Source: Smedley and Kinniburgh, 2002 and references therein).....	7
Table 1.2 Typical arsenic concentrations in common rock-forming minerals (Source: Smedley and Kinniburgh, 2002 and references therein).....	9
Table 1.3 Summary of naturally-occurring arsenic in groundwater around the world. (Source: except where mentioned, Smedley and Kinniburgh, 2002 and references therein)	11
Table 2.1 Summary of the data acquired from various published sources on arsenic concentration range in various Fe-sulfide phases	39
Table 3.1 Table showing the details for calculating Gibb's free energy ΔG° for various composition of Fe-As-S solid solution ($\text{FeS}_{1.99}\text{As}_{0.01} - \text{FeS}_{1.90}\text{As}_{0.10}$). ΔG° values of two end-member pure phases FeS_2 and FeSAs are also shown. The values of equilibrium constant $\log K$ were calculated for the reaction: $\text{FeS}_x\text{As}_y + X \text{H}_2\text{O} + Y \text{O}_2(\text{aq}) \rightarrow \text{Fe}^{2+} + x \text{SO}_4^{2-} + y \text{As}(\text{OH})_4^- + Z \text{H}^+$ Values X, Y and Z are the stoichimetric coefficients of H_2O , $\text{O}_2(\text{aq})$, and H^+ in the reaction; x and y are the molar ratio of sulfur and arsenic in the Fe-As-S solid solution.....	49

CHAPTER 1

INTRODUCTION

1. Introduction

1.1. Global arsenic groundwater pollution

Natural groundwater arsenic (As) contamination occurs by a variety of geochemical processes (e.g., Welch et al., 2000; Smedley and Kinniburgh, 2002; and Saunders et al., 2005b) and poses a serious threat to human health in many parts of the world, especially in areas where drinking water is derived from young Holocene river flood-plain aquifers (Acharyya et al., 2000; Smedley and Kinniburgh, 2002; Saunders et al., 2005a, b; Acharyya and Shah, 2007, and Saunders et al., 2008). In recent years, natural groundwater As-contamination has been reported from many countries around the world, namely Argentina, Australia, Bangladesh, China, Chile, Cambodia, Pakistan, Taiwan, Thailand, Mexico, Nepal, Vietnam and many parts of the United States (Welch et al., 2000; Smedley and Kinniburgh, 2002; Nickson et al., 2000; Saunders et al., 2005 a,b,d; Tandukar et al., 2005; Bhattacharya et al., 2005; Cole et al., 2005; and Papacostas et al., 2006). Arsenic contamination in water from mining-related activity is reported from other countries, including Ghana, South Africa, Thailand and the US, and natural As linked to geothermal water has been reported from numerous countries such as Argentina, Japan, New Zealand, Chile, Iceland, France, Dominica and parts of the US (Smedley and Kinniburgh, 2002) (Fig. 1.1). Considering the human health effects of

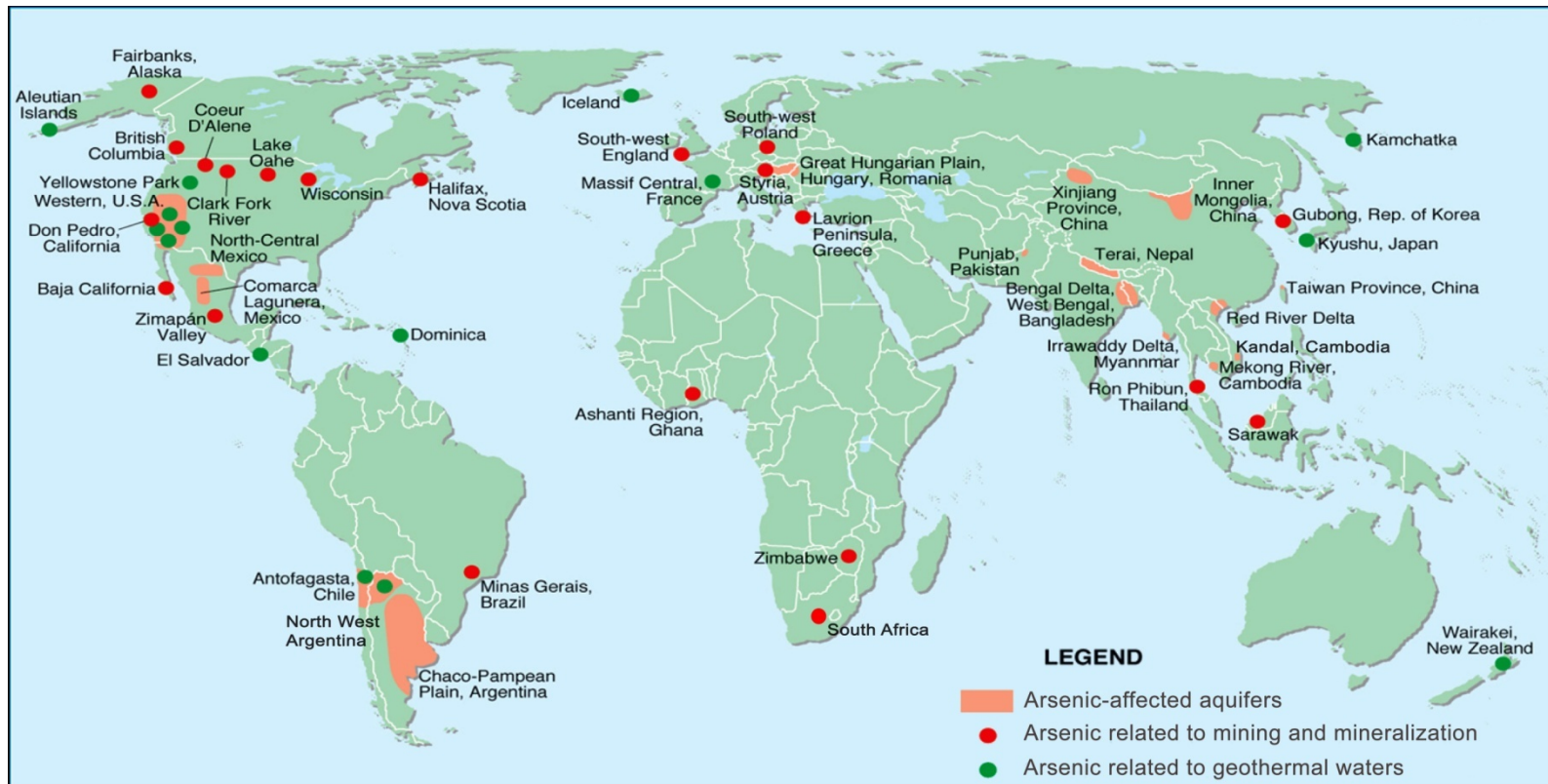


Fig. 1.1 Map showing major As-affected natural groundwater aquifers around the world. Location of As-affected groundwater from mining related work and geothermal sources are also marked in the map (modified after Smedley and Kinniburgh, 2002).

elevated As concentration ($>50 \mu\text{g/L}$), As is a major problem. Developing countries such as Argentina, Bangladesh, Cambodia, Ghana, India and Nepal, where people drink water derived from groundwater that has relatively higher As concentration than drinking water standard ($<5 \mu\text{g/L}$), large populations are exposed to high As concentrations in groundwater, making one of the most serious environmental problems of the twenty-first century (BGS and DPHE, 2001).

Published data on aquifers around the world with locally elevated As concentration indicate that similar groundwater geochemistry and microbiologic process (Saunders et al., 2005d; Bostick et al., 2006) may have operated to produce As-contamination. Local geology and hydrogeologic conditions appear to be similar in young (Holocene) alluvial floodplain aquifers in unconsolidated sediments (Ravenscroft et al., 2005; Acharyya and Shah, 2007). This is why most groundwater in the world elevated with As-contamination is directly linked to young (Holocene) alluvial floodplain aquifers. Paleoenvironments involved in the evolution of such aquifers are usually large alluvial or deltaic island (e.g., Bengal delta, Yellow River plain, Irrawaddy delta, Red River delta, Mekong River delta) (Fig. 1.2) or large inland closed basin in arid and semi-arid geological settings, e.g., Argentina, Mexico, and southwest United States (Smedley and Kinniburgh, 2002).

Today, not only south Asia (e.g., Bangladesh, India, Nepal), but also the South American continent (e.g., Argentina, Chile), North American continent (e.g., parts of the US, Mexico), northern Asia (e.g., China and Taiwan), and even European countries (e.g., Hungary and Romania) have millions of people directly affected by groundwater As-contamination. The massive scale of As-contamination has received attention of the

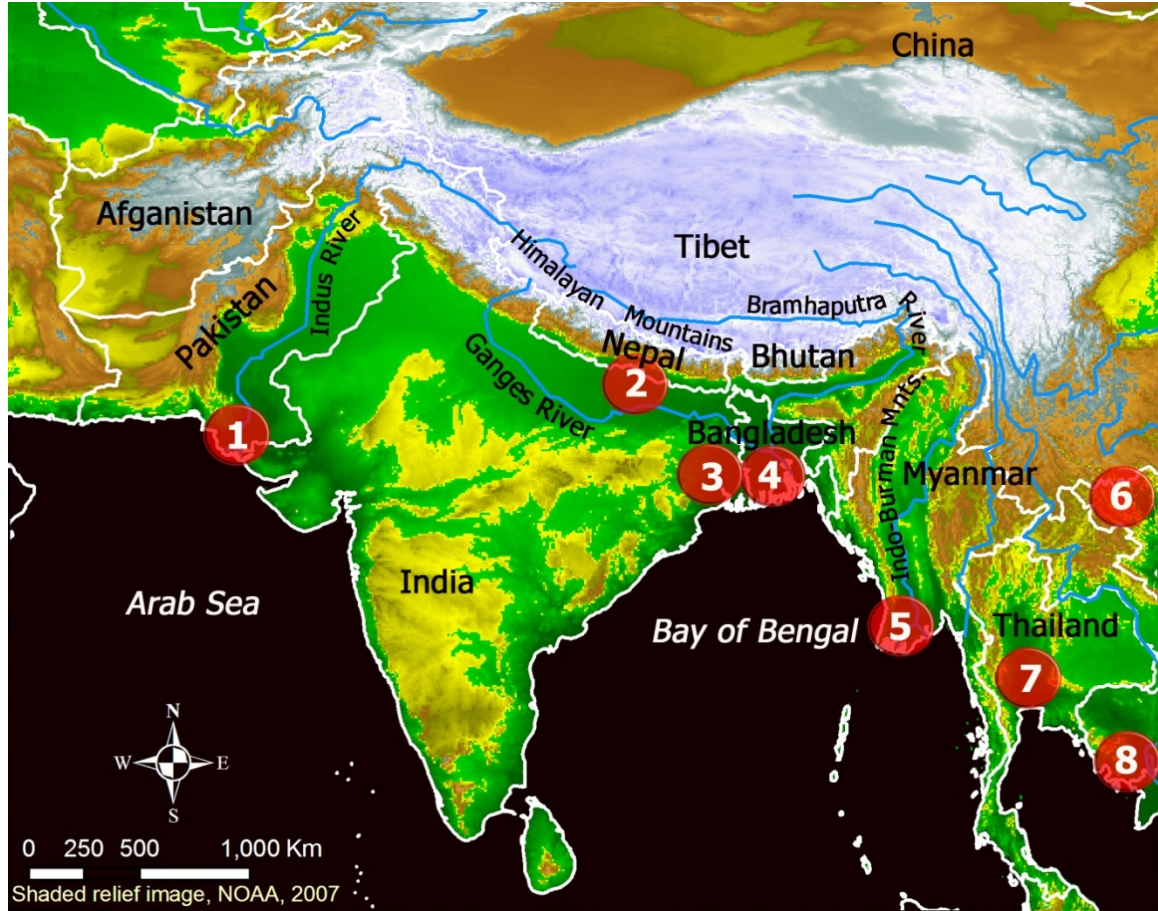


Fig. 1.2 Location map showing major deltaic region in southeast Asia with elevated groundwater As-contamination. Region marked in numbers are: (1) Indus delta, Pakistan; (2) Terai alluvial plain, Nepal; (3) Ganges-Brahmaputra delta, West Bengal, Nepal; (4) Meghna delta, Bangladesh; (5) Irrawaddy river delta, Myanmar; (6) Red river delta, Ha Noi, Vietnam; (7) Mae-Klong and Chao-Phraya, Thailand; (8) Mekong delta, Vietnam.

scientific community around the world, and they are currently working to improve our understanding on the genesis of high As groundwater in order to develop strategies to address this natural catastrophe.

Arsenic contamination of groundwater can be caused by natural and anthropogenic processes. Natural sources responsible for releasing As to the environment include As released from the weathering of As-bearing minerals such as biotite, arsenopyrite, amphibole and ferromagnesian (Fe-Mg) minerals. Arsenic can be released to the atmosphere through inputs from wind erosion, volcanic emissions, low-temperature volatilization from soils, and marine aerosols (Smedley and Kinniburgh, 2002). Atmospheric As, primarily As_2O_3 or volatile organic compounds (WHO, 2001) ultimately become a source of As to natural water system when they return to earth by precipitation or wind. Water-rock interaction in the groundwater containing As-bearing hydrous ferric oxide (HFO) sediments, and As-containing biota are other natural sources of arsenic accountable for natural As-contamination. The anthropogenic sources include mining of As-bearing ore and associated minerals, leaching from the mine tailings, combustion of bio-fuels, a host of pesticides and herbicides, and wood preservatives. While As-contamination from anthropogenic sources is local and does not cause regional effects (Smedley and Kinniburgh, 2002), natural As release to reducing groundwater is a regional phenomenon in Holocene flood plain aquifers around the world (Korte, 1991; Smedley and Kinniburgh, 2002, Saunders et al., 2005a).

In 1993, the maximum admissible concentration (MAC) of As in drinking water was provisionally reduced from 50 to 10 $\mu\text{g/L}$ by World Health Organization (WHO) (WHO, 1996). This reduction MAC was the result of an increasing awareness of

arsenic's toxicity to humans. After WHO's review on MAC of As in drinking water for international community, US-EPA also reduced MAC of As in drinking water to 10 µg/L from 50 in 2001 (Environmental Protection Agency: EPA, 2003). European Union (EU) has set their standard equivalent to WHO and US-EPA. However, most countries have their own MAC limits for As in drinking water. In view of the toxicity for humans, it would be ideal to limit the MAC to zero in drinking water. But it seems almost impossible due to crustal abundance of As and the cost of removing it (Welch et al., 2000).

At the present, treating, and/or removing As from the drinking groundwater involves several processes. Pump and treat (Lee and Saunders, 2003), coagulation, softening, iron and manganese oxidation, ion exchange, activated alumina, membrane processes, or electrodialysis are common approaches in As treatment (Chen et al., 1999). Their reliability and economic feasibility is still a major question in the scientific arena. However, it would appear that adsorption and coprecipitation of As onto preexisting mineral surfaces (e.g., HFO, Fe-sulfide, pyrite) (Farquhar et al., 2002; Bostick and Fendorf, 2003; Wolthers et al., 2007; Lowers et al., 2007) might be the most practical, cost effective *in situ* bioremediation approach for As immobilization (Chen, et al., 1999; Lee and Saunders, 2003; Saunders et al., 2005a, Saunders et al., 2008).

1.2. Source and occurrence of arsenic

In the crust As occurs in a variety of rocks and minerals. Arsenic can be very abundant in igneous rocks, coal and shale and its concentration varies widely depending on rock type (Table 1.1).

Table 1.1 Arsenic concentration ranges in rocks, sediments, and soils (Source: Smedley and Kinniburgh, 2002 and references therein).

Classification	Rock/sediment type	Range of Arsenic concentration (mg/kg)
Igneous rocks	Ultrabasic rocks	0.03–16
	Basic rocks	1.5–110
	Intermediate	0.09–13
	Acidic rocks	0.2–15
Metamorphic rocks	Quartzite	2.2–7.6
	Hornfels	0.7–11
	Phyllite/slate	0.5–140
	Schist/gneiss	< 0.1–19
	Amphibolite/greenstone	0.4–45
Sedimentary rocks	Shale/mudstone	3–490
	Sandstone	0.6–120
	Limestone	0.1–20
	Phosphorite	0.4–190
	Iron formations and iron-rich sediment	1–2,900
	Evaporite deposits	0.1–10
	Coal	0.3–35,000
	Bituminous shale	100–900
Unconsolidated sediments and soils	Sediments	0.5–50
	Soils	0.1–55
	Soils and near sulfide deposits	2–8,000

Natural As occurs as a major constituent in more than 200 mineral species, of which approximately 60% are arsenates, 20% sulfides and sulfosalts, and the remaining 20% include arsenides, arsenites, oxides, silicates and elemental arsenic (Onishi, 1969; Smedley and Kinniburgh, 2002). The most common sulfide minerals containing As are pyrite (FeS_2) or its polymorph marcasite, arsenopyrite (FeAsS), orpiment (As_2S_3), realgar (AsS), and arsenides such as löllingite (FeAs_2) are major hosts for As in geologic environment (Savage et al., 2000; O'Day, 2006).

The common sources of anthropogenic As in the environment are mining and smelting of As-rich sulfide deposits and chemical compounds such as pesticides, herbicides, and wood preservatives used in agriculture and various industries. Groundwater As-contamination from anthropogenic sources typically occurs at a limited scale. In contrast, As-contamination in natural groundwater that occurs at a regional scale in different parts of the world is mostly due to natural processes. Affinity of As to bond with sulfur (S) and iron (Fe) makes arsenopyrite (FeAsS), an ore mineral associated with igneous rocks and hydrothermal ores, a common As mineral. Arsenic-rich pyrite (arsenian pyrite) [$\text{Fe}(\text{S}, \text{As})_2$] is more abundant in sedimentary rocks than arsenopyrite and is probably the most important source of As in nature (Nordstrom, 2000). Most common ore minerals associated with variable amounts of As are chalcopyrite (CuFeS_2), galena (PbS), and marcasite (FeS_2) (Table 1.2). Considerable amounts of As can be easily incorporated into low-temperature authigenic pyrite, mostly formed in sedimentary environments (Huerta-Diaz and Morse, 1992; Neumann et al., 2005; Reich and Becker, 2006; Blanchard et al., 2007).

Table 1.2 Typical arsenic concentrations in common rock-forming minerals (Source: Smedley and Kinniburgh, 2002 and references therein).

Mineral group and name	Range of Arsenic concentration (mg/kg)
Sulfide minerals:	
Pyrite	100–77,000
Pyrrhotite	5–100
Marcasite	20–126,000
Galena	5–10,000
Sphalerite	5–17,000
Chalcopyrite	10–5,000
Oxide minerals:	
Hematite	Max. up to 160
Fe oxide (undifferentiated)	Max. up to 2,000
Fe(III) oxyhydroxide	Max. up to 76,000
Magnetite	2.7–41
Ilmenite	< 1.0
Silicate minerals:	
Quartz	0.4–1.3
Feldspar	< 0.1–2.1
Biotite	1.4
Amphibole	1.1–2.3
Olivine	0.08–0.17
Pyroxene	0.05–0.8
Carbonate minerals:	
Calcite	1–8
Dolomite	< 3.0
Siderite	< 3.0
Sulfate minerals:	
Gypsum/anhydrite	< 1–6
Barite	< 1–12
Jarosite	34–1,000
Other minerals:	
Apatite	< 1–1,000
Halite	< 3–30
Fluorite	< 2.0

Oxide (e.g, zero valent (Fe^0), and ferric (Fe^{3+}) iron oxide) minerals and hydrous metal oxides either incorporate As in the mineral structure or adsorb it onto their surfaces, and they occur in sedimentary environments (Table 1.2).

Significant adsorption of As onto mineral surfaces with positive surface charges is common, and particularly, arsenate [As (V)] is strongly adsorbed in hydrous iron-oxides or HFO and hydrous aluminum and manganese oxides (Nickson et al., 1998; Smedley and Kinniburgh, 2002). Therefore, geological environments that contain HFO, such as alluvial floodplain aquifers, are believed to be the main source for naturally elevated As concentrations in groundwater throughout the world (Korte, 1991; Nickson et al., 1998; Smedley and Kinniburgh, 2002; Sengupta et al., 2004; Turner, 2006) (Table 1.3).

Table 1.3 Summary of naturally-occurring arsenic in groundwater around the world. (Source: except where mentioned, Smedley and Kinniburgh, 2002 and references therein).

Country/region	Aquifer/Sediment type	Population Exposed (millions)	Area (Km ²)	Range of Arsenic Concentration Range (µg/L)
Argentina (Chaco-Pampean Plain)	Holocene and earlier loess with rhyolitic volcanic ash	2	1x10 ⁵	<1-5300 (7500 in some porewater)
Bangladesh	Holocene alluvial/deltaic sediments. Abundance solid organic matter.	30	1.5x10 ⁵	<0.5-2500
Cambodia (Kandal province)	Holocene alluvial aquifers	-	-	<1-768
Northern Chile (Antofagasta)	Quaternary volcanogenic sediments	0.5	1.25x10 ⁵	100-1000
China (Xinjiang province)	Holocene alluvial aquifers	5x10 ⁻⁴	38000	4-750
China: Taiwan	Sediments including black Shale			10-1820
Ghana, West Africa	Quaternary alluvial aquifer and some mining area	-	-	<5-2000 ^a
Hungary, Romania (Danube Basin)	Quaternary alluvial plains	0.029	1.1x10 ⁵	<2-176
West Bengal, India	Holocene alluvial aquifers	6	23000	<10-3200
Inner Mangolia (Huhhot Basin)	Holocene alluvial and lacustrine sediments	0.1	~30000	<1-2400
Mexico	Volcanic sediments	0.4	32000	8-620
Nepal (Tarai region)	Holocene alluvial sediments	0.46-0.75	30000	up to 600 (2620 in one case) ^b
Thailand	Dredged quaternary alluvial	?0.015	100	1 to 5000
USA	Basin and Range, Arizona, USA		2x10 ⁵	up to 1300
	Tulare basin, San Joaquin Valley, California	0.35	5000	<1-2600
	Southern Carson Desert, Nevada		1300	up to 2600
	Southern Iowa and Western Missouri	?	-	34-7020 ^c
	Red River, Ha Noi delta, Vietnam	Holocene alluvial aquifers	>1	1200

^a Norman et al., 2001; ^b Panthi et al., 2006 and references therein; ^c Korte, 1991

1.3. Research objectives

The goal of this research was to integrate and compare the results of field and laboratory experiments to better understand the geochemical behavior of As under reducing groundwater conditions. Field bioremediation experiments from the USA, Bangladesh, new laboratory investigations, and geochemical modeling were employed to that end. Geochemical modeling was carried out to examine the principal geochemical behavior of As in aerobic and anaerobic groundwaters using Geochemist's Workbench (GWB, Bethke, 1996), and laboratory batch experiments were carried out to investigate sorption of As onto Fe-sulfide. In particular, new sorption batch experiments conducted as part of this research are expected to better quantify and characterize sorption of As in Fe-sulfides.

More specifically, the research objectives for this study can be categorized as follows:

1. Field study:

- (a) Investigate the mobility of As in natural groundwater condition after the injection of molasses as a source of carbon into the groundwater that stimulates the metabolic activities of indigenous sulfate-reducing bacteria (SRB) followed by injection of Epsom's salt ($\text{MgSO}_4 \cdot 7\text{H}_2\text{O}$) and/or iron sulfate ($\text{FeSO}_4 \cdot 7\text{H}_2\text{O}$) as a source of sulfate that enhances biogenic sulfate reduction.
- (b) Document the geochemical behavior of Fe, As, and S before and after the *in situ* bioremediation experiment.

2. Geochemical modeling:

- (a) Compile thermodynamic data for thioarsenite species, amorphous As, Fe-sulfide phases, and solid solution of arsenian pyrite ($\text{FeS}_{1.99}\text{As}_{0.01} - \text{FeS}_{1.90}\text{As}_{0.10}$) into GWB database and predict the arsenic behavior in changing redox conditions.
- (b) Carry out geochemical reaction-path modeling to examine As speciation, adsorption/desorption, precipitation under sulfate-reducing condition.

3. Laboratory batch experiment:

- (a) Quantify and characterize the sorption of As onto Fe-sulfides (e.g, mackinawite, $\text{FeS}_{(\text{am})}$, and pyrite).
- (b) Improve understanding of parameters affecting As mobility during the laboratory batch experiment and investigate parameters such as:

- pH
- Eh
- Arsenic concentration
- Quantify sorption of As on different grain size of pyrite

- (b) Evaluate the time required for FeS to convert to pyrite (FeS_2) in reducing ambient temperature, and examine As behavior during that conversion.

The overall objective of this thesis was to test the hypothesis that arsenian pyrite controls As geochemistry under sulfate-reducing condition in groundwater. Previous studies have suggested that realgar and orpiment are important As-sulfide mineral phases involved in As removal mechanism.

This study hypothesizes that Fe-sulfide (e.g., arsenian pyrite) is the likely stable mineral phase that serves as major sink for As under low temperature, iron-bearing, anaerobic, and sulfate-reducing conditions.

1.4. Location for field bioremediation experiment

Two field bioremediation experiments conducted in the past are taken as a part of this study. One field site is in Blackwell, Oklahoma, USA, and the other is in Manikganj, Bangladesh (detailed in Shamsudduha, 2007, and Saunders et al., 2008). These sites were selected with a two-fold intent; the first is to select sites that have implications for As geochemistry under reducing/anaerobic conditions in alluvial aquifers, and the other was aimed to test the hypothesis that indigenous SRB might be simulated to remove As.

The first experiment conducted at a site in Blackwell, Oklahoma where shallow oxidizing groundwater is contaminated by Cd, Zn, As, and SO_4^{2-} from an old zinc smelter (Fig. 1.3). Naturally As-contaminated groundwater aquifer located at Manikganj, Bangladesh, was chosen as a field site for the ongoing bioremediation experiment (Fig. 1.4). In Bangladesh, existing water-supply tube wells were used to inject the supply to groundwater and characterize changes in groundwater geochemistry in the Manikganj region. Water samples for major cations and trace elements were filtered and acidified using U.S. EPA standard procedures at both sites. Details of the geology and geochemistry at the bioremediation site at Manikganj, sampling techniques, and analytical procedures are detailed in Shamsudduha (2007).

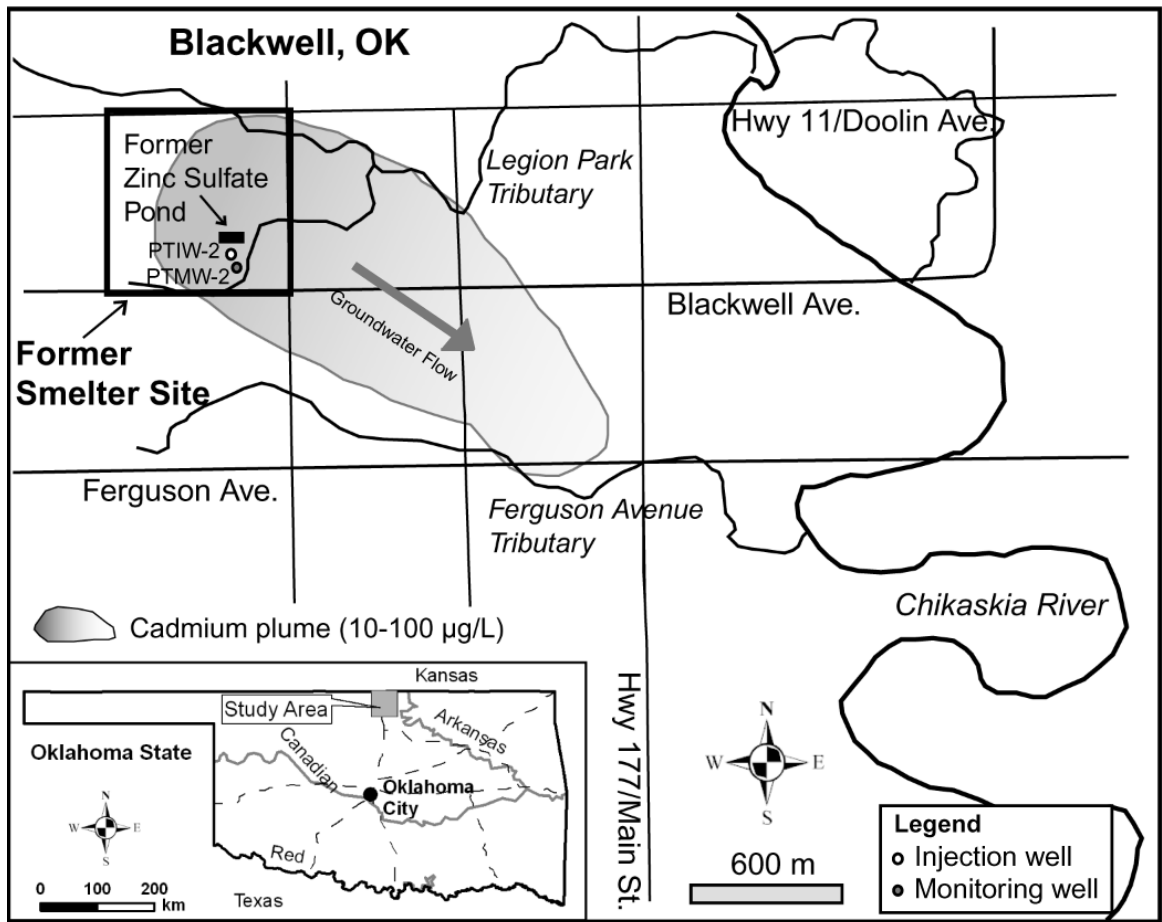


Fig. 1.3 Map showing the location of bioremediation site at Blackwell, Oklahoma (Source: Saunders et al., 2008).

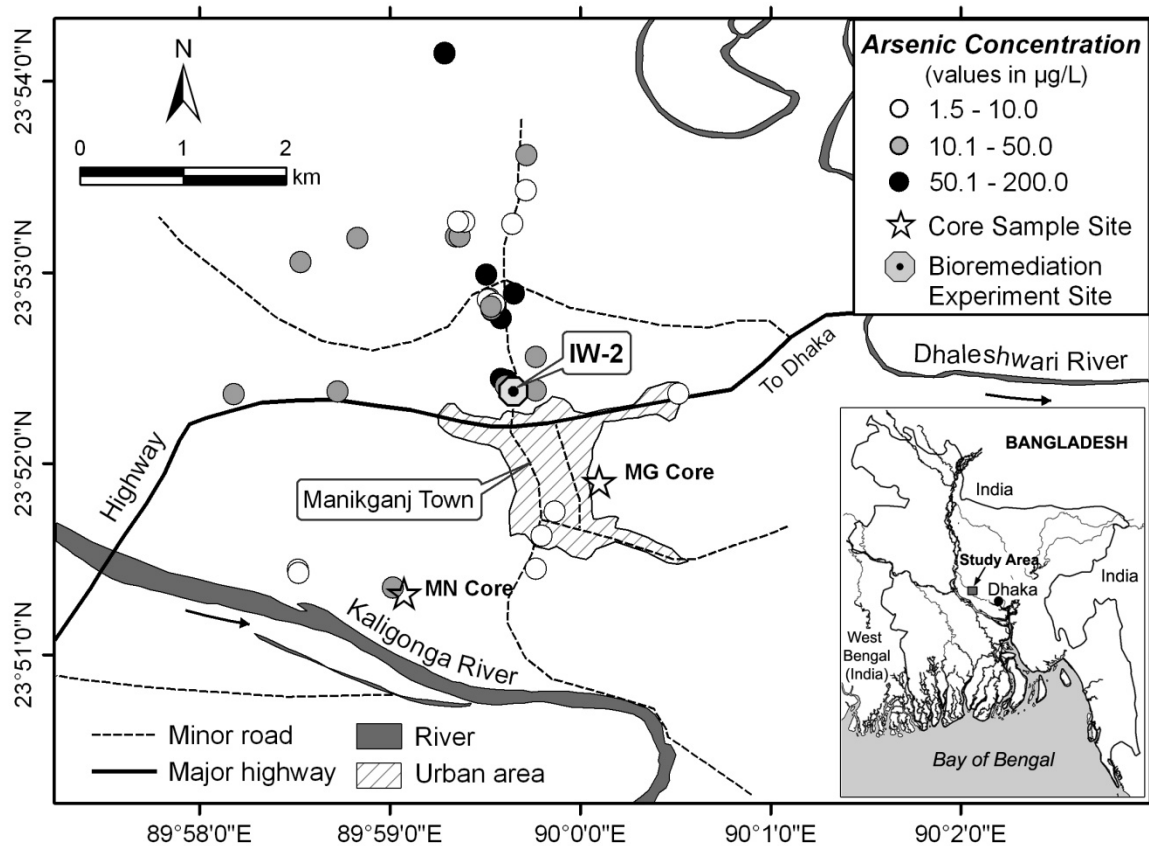


Fig. 1.4 Map showing tube well locations in the bioremediation site in the Manikganj district of Bangladesh and their relative dissolved arsenic concentrations. Location of injection well (IW-2) for the Bangladesh bioremediation experiment is also shown (modified after Shamsudduha, 2007).

1.5. Thesis outline

This study integrates three research methods - field bioremediation, geochemical modeling, and laboratory batch experiments carried out to investigate the sorption of As in Fe-sulfide as an implication for the bioremediation of As-contaminated aquifer. This thesis includes a total of five chapters. A general introduction on global As-contamination of groundwater comprises the first chapter. In addition, research objectives, location of field sites and thesis outline are also discussed in this chapter. Chapter two describes background information related to this study and discusses implications of studies made in the past that provide framework to carry out this thesis research. Chapter two also discusses subsurface microbiology and various methods used in the groundwater remediation. Chapter three outlines all the methods used during this study. The three different methods and the corresponding methodology used (field bioremediation, geochemical modeling, and laboratory batch experiments) in this study is discussed in detail in chapter three. Chapter four elaborates on the results obtained in various phases of this study and finally, chapter five concludes the thesis with the summary of the major findings of the present research.

CHAPTER 2

BACKGROUND AND PREVIOUS STUDY

2. Background and previous study

2.1. Arsenic speciation in natural water

The As geochemical cycle in natural waters, both surface and groundwater, has an unusually complex with oxidation-reduction, ligand exchange, precipitation, adsorption, and desorption reactions all taking place. The most common inorganic As species in water are the trivalent arsenite, As (III), which is more toxic form of As, or pentavalent arsenate, As (V). In contrast, organic As species, perhaps formed by detoxification biologic processes, typically are found in surface waters (Smedley and Kinniburgh, 2002).

The fate of inorganic As in nature is typically controlled by the pH and Eh conditions; it is relatively soluble between pH 5.5 to 8.5 and mobile over a wide range of redox condition (Smedley and Kinniburgh, 2002). Regardless of the specific Eh, it is apparent that in oxic environments, arsenate [As (V)] species including H_3AsO_4 , H_2AsO_4^- , HASO_4^{2-} , and AsO_4^{3-} are stable (Fig. 2.1). Under slightly reducing conditions, at relatively low and neutral pH analogous to most of the groundwater and geothermal hot spring conditions, arsenite [As (III)] dominates the system, mainly as the neutral species $\text{As}(\text{OH})_3$. In absence of iron, As mostly exists as aqueous phases over a wide range of pH-Eh conditions; that explains why it caused widespread groundwater contamination.

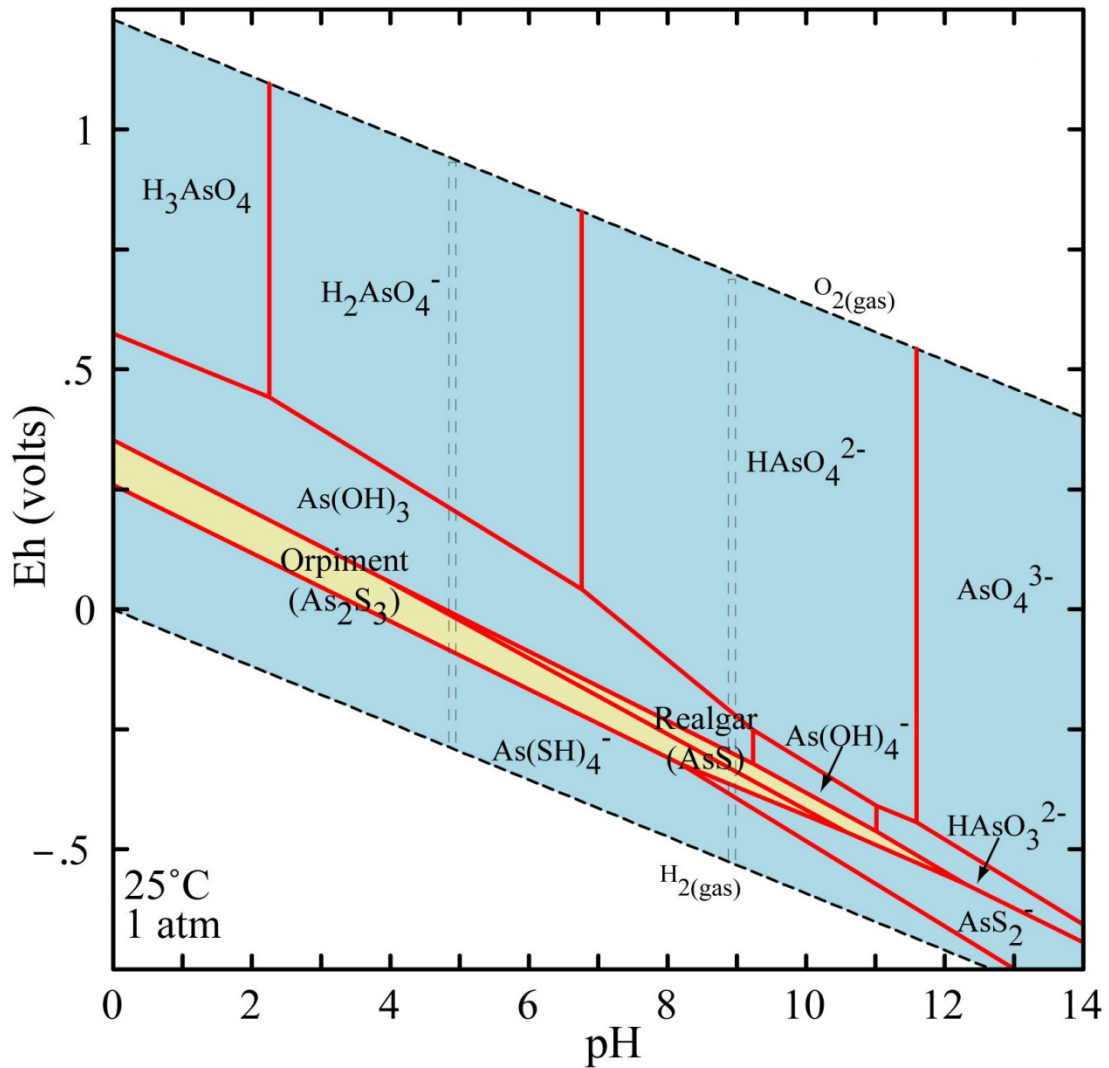


Fig. 2.1 Eh-pH diagram of arsenic species in As-O-S-H₂O system. Activities of arsenic and SO₄²⁻ are fixed at 10⁻² at 25°C. Aqueous As(V) species (H₃AsO₄, H₂AsO₄⁻, HAsO₄²⁻, AsO₄³⁻) are stable in oxidizing conditions (Eh > 0), whereas more toxic As(III) aqueous species [As(OH)₃, HAsO₃²⁻] are mobilized in moderately reducing conditions (Eh < 0). Species in yellow areas represent where solid species predominate. Realgar (AsS) and orpiment (As₂S₃) are redox-controlled precipitates. The area within the vertical dashed bars represents the common Eh-pH domains for natural water. Dashed lines show stability limits of water in 1 atm pressure. Model was created using GWB.

Solid As-sulfides like orpiment (As_2S_3), Realgar (AsS), and thioarsenite [$\text{As}(\text{SH})_4^-$, AsS_2^-] seem more stable in highly reducing groundwater conditions (Fig. 2.1). The range of As species is more restricted, however, when the pH domain of natural waters is considered (Fig. 2.1).

Freshwater systems rarely exceed a pH range of 5-9 (Crecelius et al., 1986) and the maximum pH distribution in seawater is even narrower (7.5-8.3) (Broecker and Peng, 1982). Additionally, As (V) at high pH strongly dominates over As (III) in oxic conditions based on thermodynamic stability relationship (Fig. 2.1 and Fig. 2.2). It therefore appears that the range of water-soluble inorganic As compounds is quite limited and that pH is the major factor controlling the differences in aqueous As speciation in the freshwater (Wilkin et al., 2003) and the marine environment (Huerta-Diaz and Morse, 1992).

Generally, arsenic species are referred to as either As (III) or As (V) without regard to the degree of protonation. Distribution of the As species as a function of pH is shown in Fig. 2.2. Characteristically, oxic natural water in contact with atmosphere is dominated by As (V) due to the fact that As (III) readily oxidizes to As (V). Concentration and relative proportion of As (V) and As (III) in natural waters are not limited to any degree of order, but varies according to input sources, redox condition, biological activity, redox-active solids (especially organic carbon), and geochemical condition of the aquifer (Smedley and Kinniburgh, 2002; Saunders et al., 2005b).

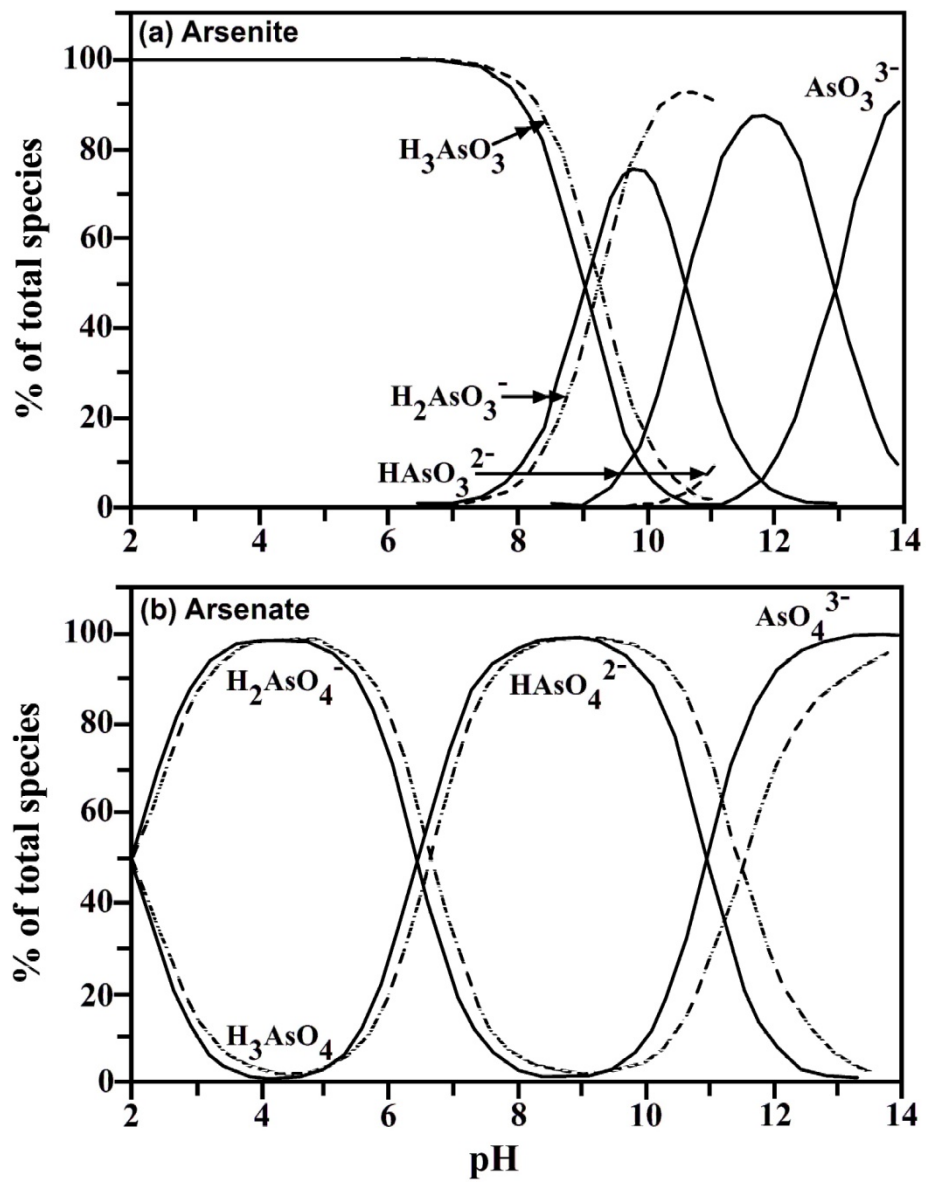


Fig. 2.2 (a) Plot showing speciation of arsenite [As (III)] and (b) arsenate [As (V)] as a function of pH (ionic strength is 0.05M). Dashed lines represent the reaction in 0.01 M ionic strength (modified after Smedley and Kinniburgh, 2002; and Wolthers et al., 2005c).

2.2. Groundwater arsenic geochemistry

Groundwaters, as opposed to surface waters, are the sources of most naturally As-contaminated drinking water in the world. A number of groundwater settings and geochemical processes have been identified that cause elevated As contamination. These include (1) weathering of volcanic rocks (Welch et al., 2000; Smedley and Kinniburgh, 2002); (2) increase in pH due to evapotranspiration like many parts of Argentina and western United States (Bhattacharya et al., 2005; Welch et al., 2000); (3) weathering (oxidation) of As-bearing sulfides as in Nevada, USA (Welch et al., 2000; Smedley and Kinniburgh, 2002); (4) arsenic release from hydrous ferric oxides (HFO) in alluvial aquifers (Acharyya et al., 2000; Nickson et al., 2000; Smedley and Kinniburgh 2002; Saunders et al., 2005a, b, and c; Turner, 2006); and (5) anthropogenic activities (Acharyya et al., 2000). However, one specific geologic setting exposes the most number of people to As contamination in the world. This setting occurs in Holocene alluvial aquifers where As is released to groundwater by the microbial-mediated reductive dissolution of HFO. Because locally elevated concentration of As is specially related to groundwater associated with Holocene flood-plain aquifers, and most of the population affected by As-contamination drink groundwater derived from such aquifers, it becomes apparently important to understand the mechanism of As adsorption and desorption in the subsurface so that we can develop effective remediation methods to address the natural groundwater As-contamination and improve groundwater quality.

Adsorption is a chemical process where a solute particle gets affixed to the surface of the solid or, more generally, the accumulation of solutes in the vicinity of a solid-solution interface (Drever, 1997). Adsorption at the solid-solution interface is essentially

an electrostatic process, where ions in a solution are attracted by a surface of opposite electrical charge (Drever, 1997) or chemical adsorption. The latter is also known as chemisorption, which involves processes like surface complexation, ion exchange, and hydrogen bonding (Stumm, 1992). There are two modes in forming precipitates onto the solid surface from a solute one involves ‘adsorption’, an electrostatic interactions in conjunction with chemisorptions, the other involves ‘sorption’ which includes absorption and adsorption (Stumm, 1992). Depending on the available surface, arsenic in some cases is adsorbed and sometimes absorbed. However, the term sorption is used to combine both adsorption and absorption processes. Sorption is an important process when relatively insoluble Fe-S-As precipitates form in almost all natural groundwater under anoxic and sulfate-reducing conditions (Bostick and Fendorf, 2003; Wolthers et al., 2005c; Gallegos et al., 2007).

2.3. Transport and sorption chemistry of arsenic in groundwater

It is important to understand the mobility and behavior of As and other solutes in groundwater to assess the possible environmental impacts. As arsenic mobilization in the subsurface could cause serious environmental problems, immobilization of As by removal onto solid phases can improve the water quality of such environments. HFO containing sorbed As and natural organic matter in river flood-plain alluvium was suggested as major source of natural As-contamination in groundwater in alluvial aquifers (Korte, 1991). Arsenic released during chemical weathering of As-bearing minerals (Dowling et al., 2002) and sediment with major concentration of As have increased the As load of Holocene alluvial sediments in the form of HFO that coat the

grain surface (Saunders et al., 1997; Saunders et al., 2005c; Acharyya and Shah, 2007; Lowers et al., 2007). After long-term burial and subsidence, fine-grained As-bearing HFO colloids in sediments are deposited in low energy environments near the sea-water/freshwater interface (Dowling et al., 2002), and become a part of the present-day aquifer. HFOs are oxidized iron particles that have very large surface area to volume ratios and are ubiquitous in oxidized coastal plain aquifers. Typically, these ferruginous coatings are found in major Quaternary aquifers in Bangladesh, Nepal, Ghana, Cambodia, China, and are also formed on sand grains and altered biotite micas (Welch et al., 2000; Ahmed et al., 2004; Tandukar et al., 2005; Saunders et al., 2005b, and 2008; Acharyya and Shah, 2007; Lowers et al., 2007).

Under oxic conditions, adsorption of As onto HFOs is pH dependent interaction. Increasing pH (7 to 10) causes significant desorption of As (V) and minor desorption of As (III) (Fig. 2.3 a). As (V) desorbs more than As (III) because it is negatively charged and expelled by the host HFO with negative surface charge at high pH. Moreover, the substantial amount of As sorbed onto HFO would decrease if it competes with other ions for the sorbing sites (Smedley and Kinniburgh, 2002). At lower pH the dominant form of dissolved As in oxidizing environments is H_3AsO_4 , but increasing pH favors the formation of As species such as H_2AsO_4^- , HAsO_4^{2-} , and AsO_4^{3-} (Drever, 1997). An alkaline pH, or the reduction of As(V) to As(III), released substantial proportions of As into solution (Masscheleyn et al., 1991). When As sorption onto HFO is considered, adsorption is low at higher pH (>11), and essentially complete at lower pH (<10) values (Dzombak and Morel, 1990), which is also observed in Fig. 2.3. Arsenic desorption from HFO is also significant below pH 3 (Lee et al., 2005; Turner, 2006).

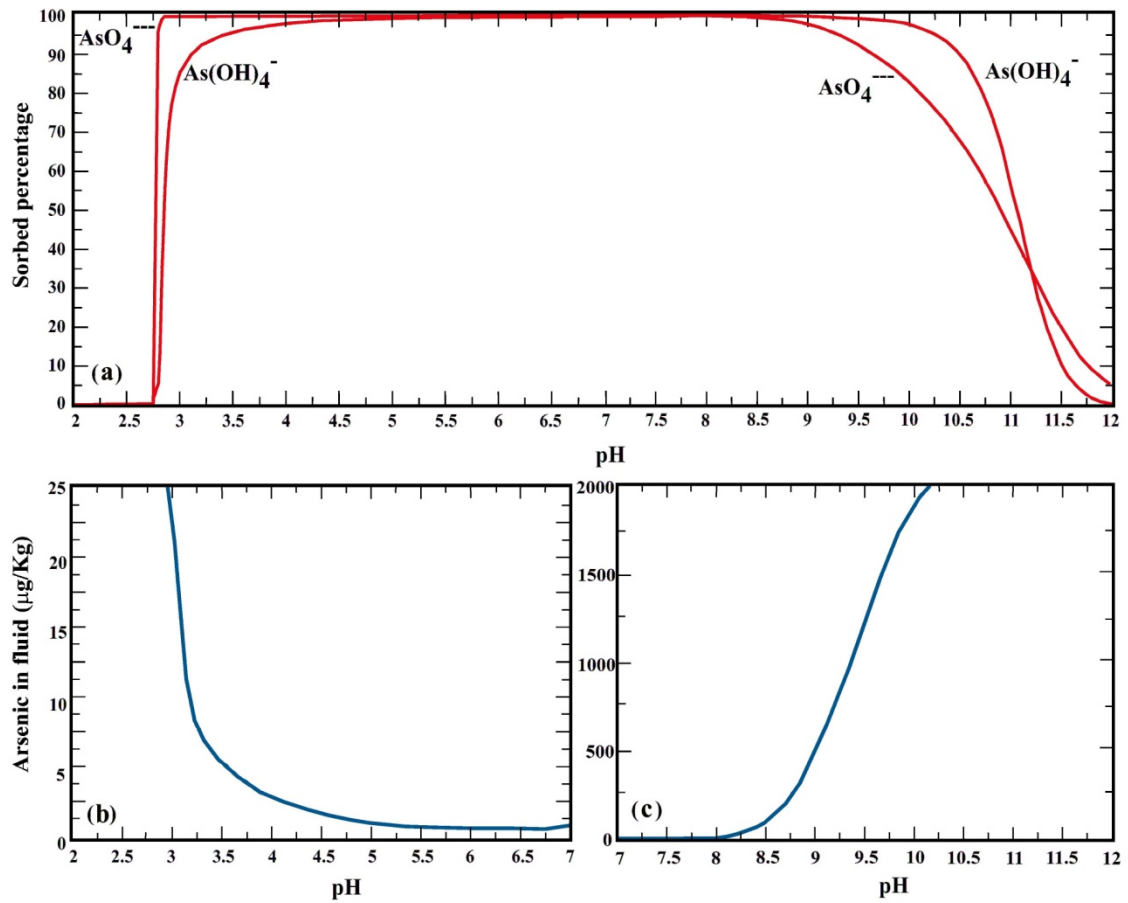


Fig.2.3 Double-layer adsorption-desorption model calculated using GWB representing the sorption of As(OH)_4^- [As (III)] and AsO_4^{3-} [As (V)] at different pH condition. Sorbed percentage (a), and dissolved arsenic concentration against pH calculated by HFO desorption simulations with pH ascending from 2 to 7 (b) and 7 to 12(c). Initial system contains 1 Kg of water at pH 7 with 1 gm of Fe(OH)_3 . Ionic strength of the system was balanced at 0.05M of NaCl with concentration of $1\mu\text{g/Kg}$ of As (III) and As (V) separately (modified after Lee et al., 2005, and Turner, 2006).

Also, an inverse relationship is observed between aqueous As concentration and amount of As sorbed onto HFO (Fig. 2.3 b and c). An increase in dissolved As concentration at lower pH (7 to 3) is a result of lower sorption affinity of As (III) in acidic condition (Fig 2.3b). Similarly, at higher pH (>8.5), a sharp increase in aqueous As concentration occurs with significant decrease in As concentration sorbed onto HFO (Fig. 2.3c).

Groundwater associated with high As concentrations in Bangladesh and the US has near-neutral pH (Smedley and Kinniburgh, 2002; Saunders et al., 2005a, and b; Shamsudduha, 2007). Modeling studies carried out to investigate the effect of bacterial Fe-reduction at near-neutral pH and decreasing Eh showed that if HFO is present in a groundwater system that contain ions such as SO_4^{2-} and Ca, then an Eh drop would result in the release of a large amount of As (Lee et al., 2005). This release of As is far more than that predicted in the system free of competitive ions (Lee et al., 2005). This result implies, large amount of As in the groundwater of Holocene alluvial aquifers is derived not only from desorption but also from bacterial dissolution of HFO. Hence, Lee et al. (2005) concluded that As release mechanisms in reducing groundwater conditions are far more complex than that predicted only by surface complexation model. Arsenic sorbed onto the HFOs will remain stable in oxidizing conditions or more specifically in positive values of Eh. These conditions are typically possible in rivers, the shallow subsurface, and the vadose zone of aquifers. In reducing environments with near-neutral pH, As (V), which is more strongly adsorbed onto HFO, is replaced by less strongly adsorbed As (III). Therefore, decreasing redox potential (ORP) would result in release of a significant amount of As that was sorbed onto HFO into solution.

2.4. Subsurface microbiology

It has long been recognized that redox reactions mediated by microorganisms control the geochemistry and water quality of the subsurface environment (Lovley and Chapelle, 1995; Lovley, 2001). Redox speciation of metals (Fe, Mn, Zn), trace metals (Se, Cd, Ni), and metalloids like As in sedimentary environment are in large part controlled by enzymatic processes in microbial physiology. Many redox reactions occur because microbes are capable of catalyzing redox reactions and promoting thermodynamically favorable chemical reactions in nature (Hem, 1985; Lovley, 2001).

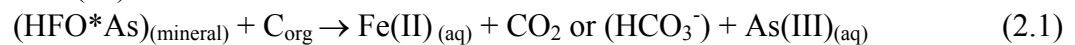
The organic and inorganic geochemistry of the groundwater can be significantly influenced by the presence of iron-and sulfate-reducing microbes. Competitive exclusion of iron-reducing bacteria (FeRB) by SRB in reducing environments (Chapelle and Lovley, 1992) limits As mobility and favors precipitation of As in groundwater (Rittle et al., 1995; Kirk et al., 2004; Chatain et al., 2005). Of special interest for this study are the twofold predominant microbial roles of FeRB and SRB: (i) reduction of As(V), and Fe (III) (Dowdle et al., 1996) by FeRB, which promotes As solubilization and enhances its mobility, and (ii) reduction of sulfate by SRB, which promotes the precipitation of variety of metals and metalloids into sulfide species (Lee et al., 2003, Kirk et al., 2004; Lee et al., 2005, Saunders et al., 2005b; Dhakal et al., 2007).

2.4.1. Subsurface microbial iron reduction

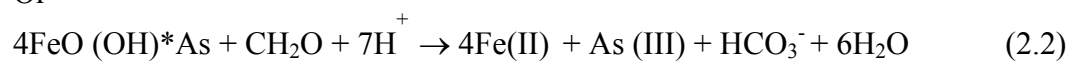
The terminal electron-accepting phase (TEAP) is a solid or aqueous-phase compound that accepts electrons released by the bacterial oxidation of organic matter. Mn (IV), Fe (III), and oxygen are most common TEAP for this organic matter oxidation.

Fe (III) in the form of HFOs acts as TEAP and aids the metabolic activity in microbes. Anaerobic subsurface environments with abundant organic matter are considered favorable for Fe (III) reduction. Least-crystalline Fe (III) phases including HFOs are generally preferred by dissimilatory FeRB as the TEAP as compared to purely crystalline minerals like goethite and hematite. With decreasing ORP in the groundwater, anaerobic iron-[Fe (III)] or manganese-[Mn(IV)] reducing bacteria [FeRB or MnRB, respectively] strip electrons from locally available organic carbon (becomes oxidized) and transfer electrons to HFOs (becomes reduced) (eq. 2.1, and 2.2). *Geobacter* sp. is commonly found FeRB in the groundwater, recorded by Shahnewaz (2003) and Saunders et al. (2005d) in the groundwater filtered from the Kansas City Plant site. In the process of bacterial Fe-reduction, microbes not only reduce HFO for their metabolic activity (Lovley and Chapelle, 1995), but also advance the release of Fe, Mn, and As from As-bearing HFOs into solution (Nickson et al., 2000; Smedley and Kinniburgh, 2002; Lee and Saunders, 2003; Lee et al., 2005; Saunders et al., 2008) (eq. 2.1, and 2.2) (Fig 2.4).

Iron (Fe)-Reducers:



Or



The primary way in which microorganism gain energy at the near-surface portion of the subsurface, for example a pristine aquifer in contact with atmospheric oxygen is by aerobic respiration. Aerobic respiration in such case is achieved by coupling the oxidation of organic matter and reduction of oxygen (Lovley and Chapelle, 1995).

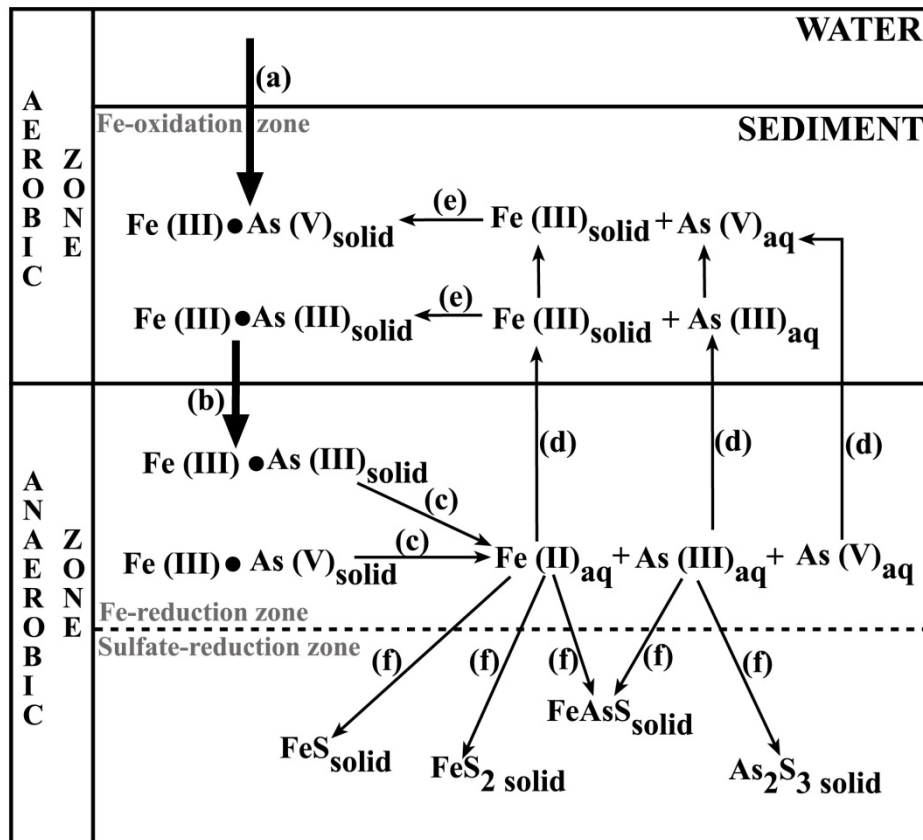


Fig. 2.4 Schematic model for the biogeochemical cycling of arsenic and iron in the subsurface. (a) sediment deposition; (b) burial; (c) dissolution; (d) diffusion; (e) coprecipitation; (f) diffusion and reaction with sulfide. Dashed line represents sediments below which free sulfide favors the formation of Fe-sulfides. Oxide and hydroxide groups are dominant solid iron species above the solid line (modified after Cullen and Reimer, 1989 and references therein).

In absence of oxygen, microbial respiration requires some other TEAP such as nitrate (NO_3^-), manganese (Mn^{+4}), iron (Fe^{+3}), and sulfate (SO_4^{2-}). The order that TEAPs are used depends on their availability and amount of energy to be derived, but typically follows the sequence: nitrate reduction \rightarrow manganese reduction \rightarrow iron reduction \rightarrow sulfate reduction and then methanogenesis (Lovley and Chapelle, 1995, Lovley, 2001). Apparently, this sequence is controlled by thermodynamics consideration involving energy released by the ongoing redox reactions as the condition becomes reducing. Microbes such as FeRB and MnRB compete with SRB for the organic substrates in most of the anoxic sedimentary environment (Chapelle and Lovley, 1992, Lovley, 2001). Distinct zones developed in course of microbial contest for organic substrate is responsible for the commonly observed subsurface geochemical zonation of groundwater aquifers (Fig. 2.5).

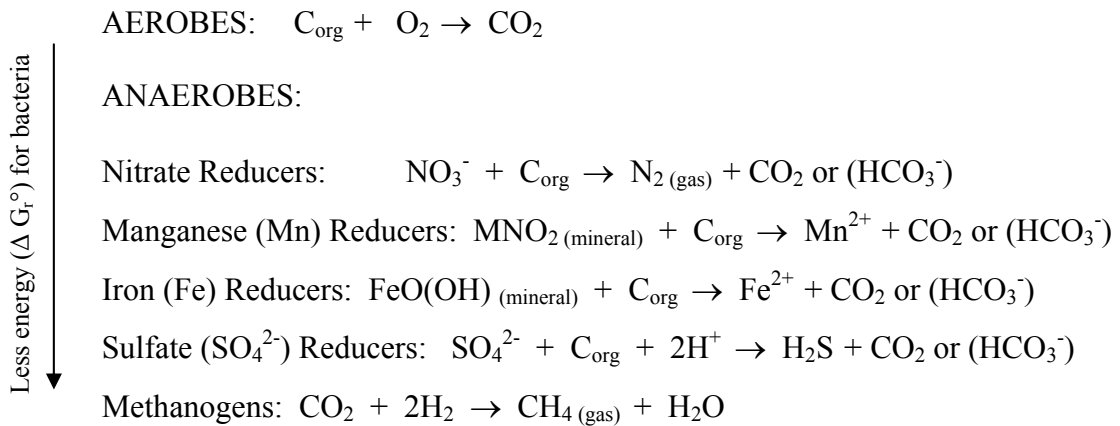


Fig.2.5 Sequence of microbial TEAP process in subsurface pristine aquifers (modified after Lovley, 2001; personal commun, Saunders et al., 2008).

2.4.2. Subsurface microbial sulfate reduction

As shown in Fig. 2.5, bacterial Fe (III)-reduction and SO_4^{2-} -reduction are common processes in anaerobic groundwater. Chapelle and Lovley (1992) showed that these groups of bacteria compete for organic carbon and the competition is influenced by the relative availability of the TEAP's such as reducible Fe-minerals and SO_4^{2-} . Sources of SO_4^{2-} in natural groundwaters include oxidation of sulfide minerals, remnant seawater, or dissolution of SO_4^{2-} -bearing minerals such as gypsum and anhydrite. Large amount of dissolved iron present in the groundwater essentially excludes SRB activity, but biogenic sulfate reduction (by SRB) prevails in the presence of sufficient dissolved SO_4^{2-} concomitantly resulting in decrease iron concentration (Chapelle and Lovley, 1992; Kirk et al., 2004).

It is long been understood that the metabolic activity of SRB, such as *Desulfovibrio desulfuricans* (Shahnewaz, 2003, and Saunders et al., 2005a) in groundwater will convert sulfate to hydrogen sulfide (H_2S) (eq. 2.3). A generic reaction for bacterially-mediated sulfate reduction is as follows:

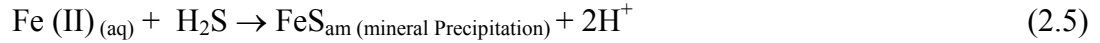
Sulfate (SO_4^{2-}) Reducers:



This bacteria-driven process yield H_2S causing H^+ proton to react with SO_4^{2-} and organic carbon. Anoxic marine and terrestrial sediments are likely natural setting where “rotten egg” smell experienced in the field at low ORP normally indicate active SRB metabolism that produces H_2S . Hydrogen sulfide formed this way at near-neutral pH reacts with metals to form insoluble metal sulfides (eq. 2.4).



Likewise, presence of dissolved Fe (II) in the groundwater particularly, allows formation of relatively insoluble amorphous iron monosulfide (FeS_{am}) (eq. 2.5).



Thus formed FeS_{am} is a thermodynamically metastable Fe-sulfide solid phase (Farquhar et al., 2002; Wolthers et al., 2005b; Wolthers et al., 2007). In the literature, iron monosulfide is often called mackinawite, although stoichiometric mackinawite is a FeS_{1-x} with 0 < x < 0.07.

2.5. Formation of microbial and sedimentary iron sulfide

Under reducing groundwater conditions, sulfate reducers can easily oxidize viable sedimentary organic matter and reduce dissolved SO₄²⁻ to sulfide for their metabolism. Hydrogen sulfide released during dissimilatory microbial reduction of sulfate readily precipitates sulfide from solution with iron (Berner, 1984) (Fig. 2.6). In presence of indigenous SRB, dissolved SO₄²⁻ and dissolved Fe (II) act together and form amorphous Fe-sulfide, which along with a constant supply of H₂S or possibly elemental sulfur eventually transforms into pyrite (Berner, 1972; Rickard, 1975; Rittle et al., 1995; Wilkin and Barnes, 1996). The first report of the formation of biogenic pyrite formed by SRB was by Issatchenko (1912) (as mentioned in Morse et al., 1987). Formation of mackinawite, greigite (Fe₃S₄), pyrrhotite (Fe_{1-x}S), marcasite (FeS₂, orthorhombic), and pyrite (FeS₂, cubic) were also reported from the batch cultures made to investigate the details of Fe-sulfide formation by bacteria (e.g., *Desulfovibrio desulfuricans*) (Rickard, 1968 and 1969).

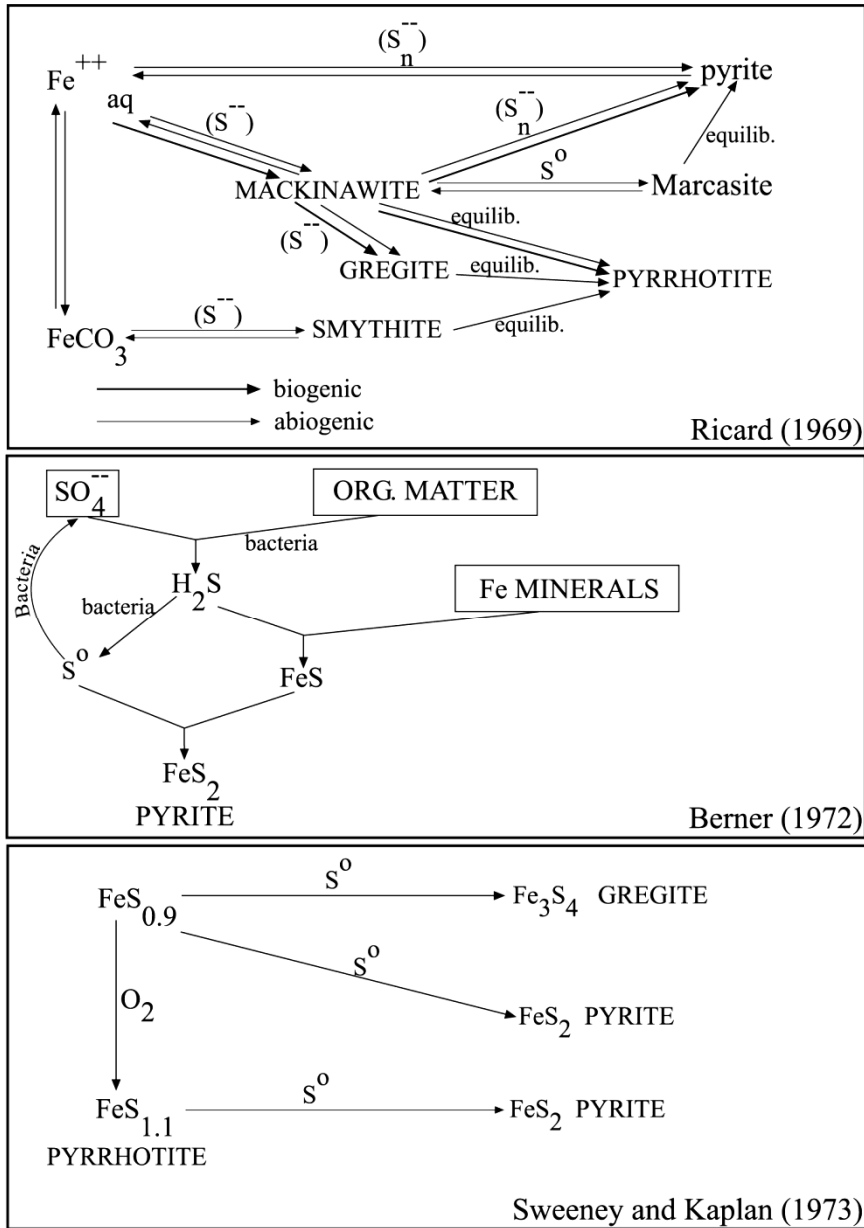


Fig. 2.6 The proposed reaction pathways for pyrite formation in anoxic sedimentary environment (modified after Morse et al., 1987 and references therein).

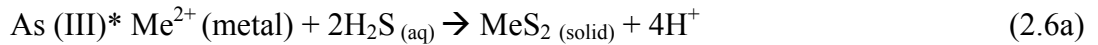
Authigenic Fe-sulfide minerals are viewed as common phases formed in recent as well as ancient marine and terrestrial sediments. Aqueous iron precipitates as ‘amorphous Fe-sulfide’ in anoxic environment in the presence of dissolved sulfide species (Berner, 1984; Rickard and Luther, 1997; Wolthers et al., 2005a). The most common phases of ‘amorphous Fe-sulfide’ upon aging and burial transform into mackinawite, greigite, pyrrhotite, marcasite, and pyrite (Rickard, 1969; Schoonen and Barnes, 1991; Mullet et al., 2002) (Fig. 2.6). Mackinawite, also referred to as tetragonal sulfide, forms nanoparticle with high surface area and is precipitated as early phase in anoxic Fe-S systems (Wolthers et al., 2005b). The formation of intermediate products, such as greigite and pyrrhotite is rarely reported (Schoonen and Barnes, 1991). In the presence of intermediate sulfur species (e.g., polysulfide and thiosulfate), conversion of amorphous Fe-sulfide to pyrite proceeds rapidly along with an increase of oxidation state (Schoonen and Barnes, 1991).

When compared to purely abiotic processes, bacterially mediated transformation of Fe-sulfide into pyrite was found to be more efficient (Donald and Southam, 1999). Biogenic pyrite formed by purely inorganic process and those formed by SRB are distinguished by the isotopic composition of the mineral. Depletion of ^{34}S (with $\delta^{34}\text{S}$ values as low as -50 ‰) in biogenic pyrite is characteristic fingerprint of kinetic isotope fractionation of sulfur by SRB (Saunders et al., 2005d; Lowers et al., 2007).

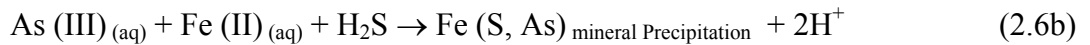
2.6. Precipitation of arsenic under sulfate reducing conditions

Typically, under sulfate reducing conditions, authigenic precipitation of biogenic Fe-sulfides removes As and Fe from solution due to the metabolism of SRB. Arsenic has

a strong affinity to be sorbed and subsequently substitute into bacterially formed ‘amorphous Fe-sulfide’ in early diagenetic processes. This process is a commonly suggested mechanism for As removal from solution in fresh-water and marine sediments (Huerta-Diaz and Morse, 1992; Saunders et al., 1997; Huerta-Diaz et al., 1998; Saunders et al., 2005c; Lowers et al., 2007, Saunders et al., 2008) (eq. 2.6 a and b).



or



As discussed in section 2.4.2., the concentration of dissolved SO_4^{2-} is an important factor in controlling As mobility during sulfate reduction in groundwater. Alluvial aquifers around the world and especially in southeast Asia, typically have low levels of dissolved SO_4^{2-} which limits the chemical reactions expressed in eq. 2.3, and eq. 2.6 a and b for As precipitation. However, local natural attenuation of As and Fe concentration groundwater by active indigenous SRB has been reported (Kirk et al., 2004; Ahmed et al., 2004). Saunders et al. (1997, 2005a, 2008) and Lee et al. (2005) proposed an *in situ* bioremediation approach for As immobilization in sulfate-limited groundwater systems such as are common in southeast Asia. Based on their pilot study, *in situ* bioremediation for As immobilization may be achieved by supplying labile organic carbon (molasses) and iron sulfate (FeSO_4) or magnesium sulfate (MgSO_4) necessary to simulate metabolic activity of SRB in the groundwater.

Amorphous Fe-sulfide formed by both microbial and non-microbial processes has strong affinity to sorb As and other metals from the solution and precipitate with Fe-sulfide (Wilkin et al., 2003; Gallegos et al., 2007) (eq. 2.6 a and b). Wolther et al. (2005b) showed that increasing pH reduces Fe-sulfide solubility and this favors As sorption and subsequent precipitation in sulfate-reducing environment. However, the formation of soluble thioarsenite species at high H₂S/Fe ratios would enhance As mobility (Wilkin et al., 2003). Moreover, arsenic concentrations would remain high in Fe-free solutions when the precipitation of As sulfide solids such as orpiment (As₂S₃) or realgar (AsS) is kinetically prohibited or when their amorphous precursors are formed (Lee et al., 2005).

Microbially derived amorphous Fe-sulfide, in presence of intermediate sulfate species is believed to transform eventually into pyrite which is a ubiquitous, stable Fe-sulfide phase (Schoonen and Barnes, 1991). Field data from a study carried out by Huerta-Diaz and Morse. (1992) and Saunders et al. (1997) also support association between As and Fe-sulfide phases. Additionally, more conclusive data show the occurrence of As in pyrite [‘arsenic rich pyrite’ or arsenian pyrite, Fe (S As)]. As-bearing biogenic pyrite containing significant amount of arsenic (~1wt. %) have been reported from Holocene alluvial aquifers from Bangladesh (Lowers et al., 2007; Acharyya and Shah, 2007), Cambodia (Bostick et al., 2005), and parts of US (Saunders et al., 2005a) (Fig. 2.7). These observations support the hypothesis that natural sorption and coprecipitation of As onto Fe-sulfide phases occurs in iron-rich, sulfate-reducing groundwaters mediated by SRB. There is a wide range of variations in the amount of As that can be incorporated into Fe-sulfide, pyrite, and arsenopyrite (Table 2.1).

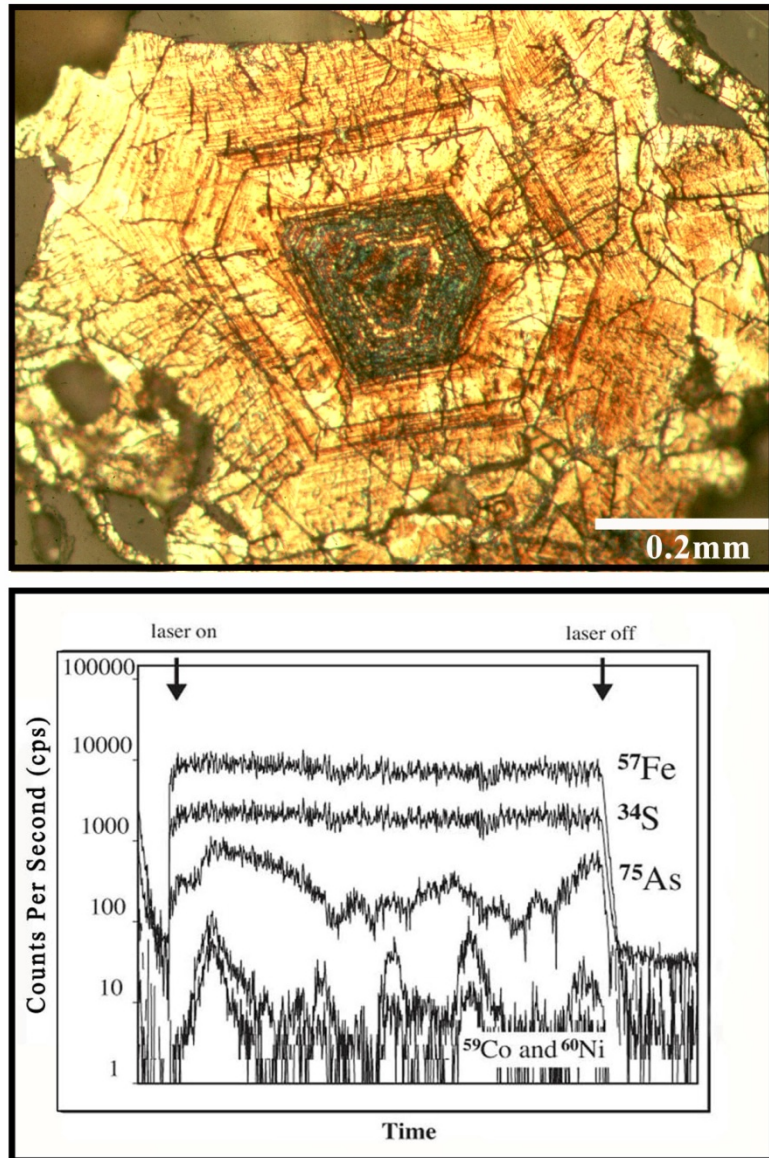


Fig. 2.7 Image on the top is a photomicrograph (reflected light) of arsenic-rich biogenic pyrite from Holocene alluvial aquifer in Alabama, USA. Chemical analysis of this sample show up to 1 wt.% of As in pyrite. Arsenic content substantially increases towards core (source, Saunders et al., 1997). Picture on the bottom is a result of a laser ablation inductively coupled plasma mass spectrometry, LA-ICP-MS conducted on the As rich pyrite sample shown above. LA-ICP-MS micro-beam probed onto the sample along the line (3 mm) show coexistence of As-Fe-S in the sample. X-axis represents the time line when the laser beam was turned on. Background counts are indicated on the left and right side at the top the figure (source, Savage et al., 2000).

However, generally noted range of As incorporation into pyrite is between 0.5 to 1 wt. %, but much higher is expected in metastable Fe-sulfide such as mackinawite (Wolthers et al., 2005c) (Table 2.1).

Based on an X-ray absorption near-edge structure (XANES) study, Bostick and Fendorf (2003) suggested As, preferably As (III) is sorbed onto pyrite to form ‘arsenopyrite-like’ arsenian pyrite. Recent molecular studies indicate that As substitutes for sulfur in growing pyrite or arsenopyrite [Fe (S As)], forming a solid solution (Savage et al., 2000). Thus As adsorption on the surfaces of Fe-sulfide phases and/or co-precipitation may be the most important processes causing scavenging of trace metals and metalloids [e.g., As, Selenium (Se)] in reducing environments (Farquhar et al., 2002; Bostick and Fendorf, 2003; Wolthers et al., 2007). Although not documented in natural groundwater conditions, arsenopyrite (FeAsS) was synthesized in the laboratory, by the interaction of iron with arsenic in presence of SRB (Morimoto and Clark, 1961; Rittle et al., 1995).

Most As-bearing is formed during early diagenetic phases of sedimentary Fe-sulfide formation and their subsequent transformation to pyrite (Lowers et al., 2007). It is also possible that aqueous As is sorbed onto existing pyrite, as coating in pyrite rich sediments to produce arsenian pyrite during microbial sulfate reduction (Saunders et al., 2005b; Dhakal et al., 2008). Assuming Fe-sulfide phases form as a consequence of biogenic sulfate reduction and that pyrite is the thermodynamically favored phases under most situations (Morse et al., 1987), the question of how As is incorporated into these Fe-sulfide phases to make arsenian pyrite remains unanswered.

Table 2.1 Summary of the data acquired from various published sources on arsenic concentration range in various Fe-sulfide phases.

Arsenic in pyrite (FeS ₂) by wt. %	0.03-0.5	Lowers et al., 2007*
	~0.8	Nickson et al., 2000*
	0.93 (in marine sedimentary pyrite)	Huerta-Diaz and Morse, 1992*
	~1	Saunders et al., 2005a*
	1.5-3.2	Lowers et al., 2007*
	3-4.5	Goldhaber et al., 2003**
	Max. up to 4	Thomas and Saunders, 1998*
	>6	Reich and Becker, 2006 **
	~7	Kolker et al., 2003*
	~8	Fleet et al., 1989 *
	~10	Abraitis et al., 2004*
	~10	Blanchard et al., 2007**
	~9.3-16.5 (above 300°C)	Fleet and Mumin, 1997 and reference therein *&***
	~19 (below 300°C)	Reich and Becker, 2006 and reference therein *
Arsenic in arsenian pyrite (Fe-S-As) by wt. %	Avg. 1.2	Savage et al., 2000***
	1(optimum)	Results of geochemical modeling in this study
	0-5	Wolthers et al., 2007***
	>8	Reich and Becker, 2006**
	~9	Reich and Becker, 2006 and reference therein *
	9.3 in arsenian pyrite 16.5 in arsenian marcasite	Fleet and Mumin, 1997* &***
Arsenic in mackinawite (FeS _{am}) by wt. %	>6	Reich and Becker, 2006**
	23 of total As(III)	Wolthers et al, 2005c ***
* Field sample		** Modeling data
		*** Laboratory data

Although orpiment (As_2S_3) and realgar (AsS) have been reported at some arsenic-contaminated sites, their x-ray diffraction (XRD) confirmation in natural systems is lacking. The abundance of iron in natural aquifer sediments and groundwaters makes it unlikely that pure As-S phases will form in nature. Alternatively, arsenian pyrite appears to be thermodynamically favored phase in groundwater where SRB are active (Rickard and Luther, 1997; Thomas and Saunders, 1998).

The most widely used geochemical modeling programs contain thermodynamic data for crystalline As-S phases, and perhaps some amorphous As-S phases and thioarsenite aqueous complex. The lack of thermodynamic data for low-temperature As-Fe-S solid solutions limits the utility of these programs in predicting the behavior of As under reducing conditions. By excluding arsenian pyrite from consideration in geochemical modeling effectively assumes that the phase is not stable, which runs counter to published data on its importance in reducing groundwater.

2.7. *In situ* bioremediation of arsenic-contaminated groundwater

In-situ bioremediation may be a reliable natural long term cleanup method for many of our subsurface contaminated sites. Engineered bioremediation such as biostimulation (addition of organic and inorganic compounds to cause indigenous organism to effect the remediation of the environment) and bioaugmentation (addition of organism to effect remediation of the environment) is becoming an inexpensive and an environmentally friendly process to clean up widespread natural As-contamination. Recognition of the “arsenic calamity” in many parts of the world led to the invention of numerous techniques based either on conventional or state-of-the-art techniques for treating

As- contaminated groundwater. A number of treatment options have been successfully demonstrated since early 90's, and the research in this area is still ongoing. Fig. 2.8 represents an overview of the various As removal techniques commonly undergoing evaluation or being used recently. Most common As removal techniques have been demonstrated in the laboratory ("bench scale"), and a few of them are *ex situ*, such as pump and treat, and filtration processes.

Very few, but promising studies involve field-based, *in situ* remediation techniques that use natural groundwater conditions, indigenous bacterial communities, and include injection of nutrients (Harvey et al., 2002; Lee and Saunders, 2003; Saunders et al., 2005c; Keimowitz et al., 2005, and 2007). Based on the geochemistry of As sorption onto Fe-sulfide, Lee and Saunders (2003) and Saunders et al. (2005c) proposed a method which involves stimulation of indigenous SRB in sulfate-limited, As-contaminated groundwater by adding ample supplies of necessary electron donors and acceptors to immobilize As.

In their pilot bioremediation field experiment, a blend of organic carbon mixed with water was injected into groundwater to simulate bacterial activity, and initially that was primarily biogenic iron reduction. Later, when geochemical conditions of groundwater became more reducing, a source of sulfate was supplied to simulate indigenous SRB. During metabolism that takes place in SRB, sulfate is reduced to sulfide which then reacts with dissolved metal in the groundwater to produce metal sulfide. Formation of sulfide due to indigenous SRB produces two basic chemical effects in a reducing groundwater. First, it forms amorphous nano-scale Fe-sulfide with high surface area. Second, aqueous As in the solution is sorbed and coprecipitated onto amorphous

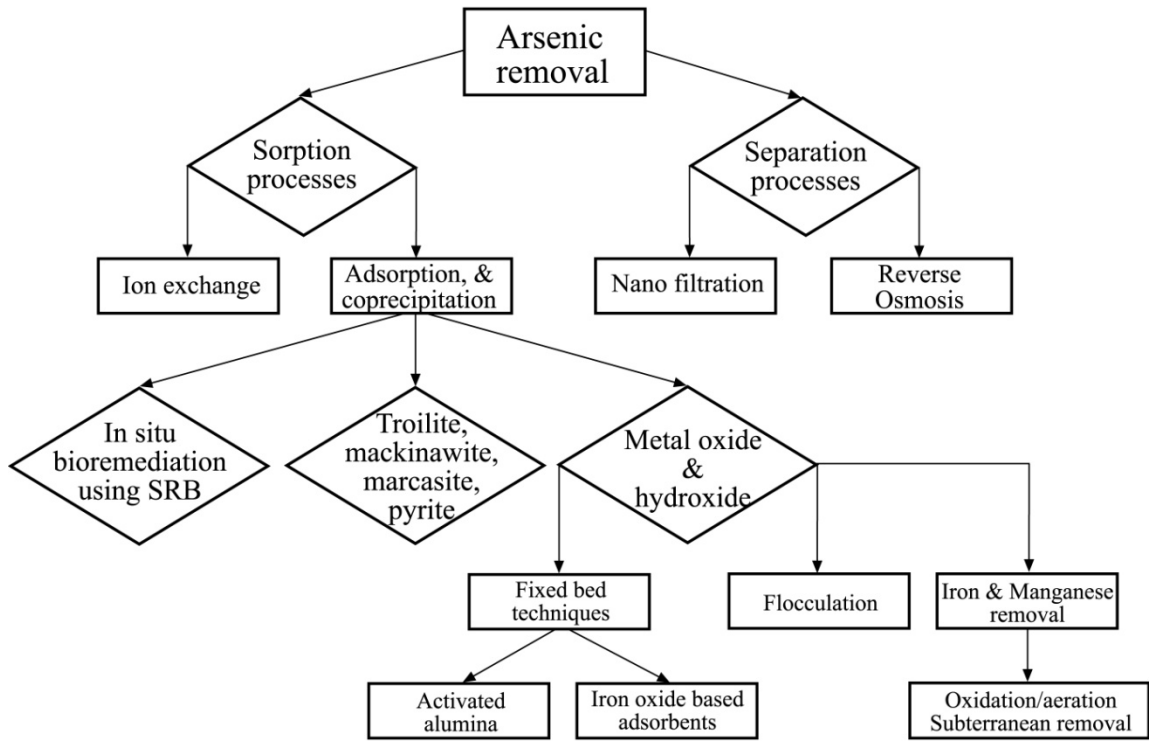


Fig. 2.8 Schematic of existing and proposed arsenic-removal techniques (modified after Driehaus, 2005).

Fe-sulfide formed during biogenic sulfate reduction. Bioremediation experiments conducted by Lee and Saunders (2003) and Saunders et al., (2005c) found that metalloids As and Se (along with other metals) in solution decreased substantially for some time after the stimulating SRB, although those groundwaters were not particularly As-enriched.

The purpose of this thesis is to provide more data on how engineering SRB as an *in situ* bioremediation approach (proposed by Saunders et al., 2005a, 2008) for As might be accomplished. It appears that As can be immobilized by adding a reactive source of carbon (such as molasses) and a sulfate source to stimulate the metabolic activities of SRB in groundwater. This study is based on a hypothesis that arsenian pyrite is the most important solid As phase that can be formed by stimulating indigenous SRB under sulfate-reducing conditions in As-contaminated natural and anthropogenic groundwater system, and that it can effectively remove As from contaminated groundwater.

CHAPTER 3

MATERIALS AND EXPERIMENTAL METHODS

3. Materials and experimental methods

3.1. Field bioremediation experiment

Two field bioremediation experiments were designed and conducted to evaluate if indigenous SRB present in the subsurface could effectively remove As. One field bioremediation experiment, began and briefly described by Saunders et al. (2008), is still ongoing and will be discussed here as a part of this study.

One site investigated is in Blackwell, Oklahoma, USA where tests were conducted on shallow oxidizing groundwater contaminated by Cd, Zn, As, and SO_4^{2-} from an old zinc smelter (Fig. 1.3) (Saunders et al., 2008). A pilot test was performed using indigenous SRB to remediate metals-contaminated (but no arsenic, initially) groundwater. A mixture of methanol (84 mg/L) and sucrose (108 mg/L) were pumped into injection well PTIW-2 (Fig. 1.3) at a rate of 114 L/min for 2 days in the approximate center of the contaminated groundwater plume. Bromide was also added as a tracer to the injected solution (Saunders et al., 2008). Seven multiport wells were established and used as monitoring wells to intercept a portion of the “remediated” groundwater plume along the flow path. Water samples were collected using a peristaltic pump were attached to Teflon tubes that connected to the various multiports of the monitoring wells. Water samples were collected from the monitoring wells for approximately 6 months

after injection and analyzed for Cd, Zn, Fe, As, and sulfate. Only data from the middle multiport (depth=5.2 m) of monitoring well PTMW-2 (see location, Fig. 1.3) is discussed in this study. We selected this monitoring well so a more complete test of the geochemical process could be observed, as this monitoring was closer to the injection well.

A second study area in Manikganj, Bangladesh, was used for another bioremediation experiment (Fig. 1.4). There, an abandoned well (IW-2) with the highest concentration of arsenic (As and Fe were $\sim 105 \mu\text{g/L}$ and $\sim 40 \text{ mg/L}$, respectively) was targeted for study. Groundwaters at Manikganj, Bangladesh are typically Ca-Na- HCO_3 type, with total dissolved solids $< 500 \text{ mg/L}$, are moderately reducing, and have pH values in the range of 6.5 to 7.5 (Shamsudduha, 2007). Twelve kg of molasses was used as a source of organic carbon and was mixed thoroughly with 200 L of water and injected (from well IW-2) into the aquifer on December 2005 (Fig. 3.1). About 30 days later, in January of 2006, 1.5 kg of Epsom's salt ($\text{MgSO}_4 \cdot 7\text{H}_2\text{O}$), which provided a source of sulfate for SRB, was mixed with 30 L of water and injected into the same injection well. In Manikganj, the injection well was also used as the monitoring well to characterize groundwater geochemistry and monitor the progress of the bioremediation experiment at the study site. Both of the alluvial aquifers selected for the experiments were believed to have had similar aquifer mineralogy, but groundwater in Bangladesh was reducing whereas the groundwater condition at Blackwell, Oklahoma, was initially oxidizing but rapidly became reducing after injection of the organic carbon.

From both the sites, water samples for major cations and trace elements were filtered and acidified using U.S. EPA standard procedures. Water samples collected



Fig. 3.1 Photograph of the single-well field bioremediation experiment carried out in Manikganj, Bangladesh. (a) Molasses injected at well (IW-2) as a source of carbon. Thirty days later, Epsom's salt, as a source of sulfate was injected from the same well. (b) Water supply-tube well used for water sampling before and after the bioremediation experiment. (photo source Shamshudduha, 2007)

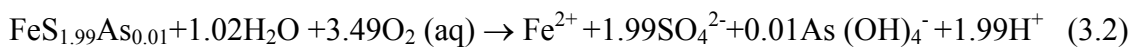
before and after the nutrient injection were analyzed using ICP-OES and ICP-MS, and parameters like Eh, pH were recorded in the field. Water sampling and analytical procedures for Bangladesh and USA are detailed in Shamsudduha (2007) and Saunders et al. (2008).

3.2. Geochemical Modeling

In a given geochemical system, a reaction path model can establish the evolution of a fluid's chemistry, and can account for precipitation and dissolution of minerals over the course of the modeled geochemical process. In the past, the absence of thermodynamic data for arsenian pyrite made it difficult to approximate natural minerals formed in As-Fe-S bearing groundwater systems using any available geochemical modeling thermodynamic data bases. Geochemical models constructed for this study integrate new thermodynamic data developed for arsenian pyrite ($\text{FeS}_{1.99}\text{As}_{0.01}$ – $\text{FeS}_{1.90}\text{As}_{0.10}$) in As-Fe-S solid solution in order to investigate As mobility and reactivity under sulfate reducing conditions. The equilibrium constant for chemical reactions can be calculated directly from the standard free energy change by

$$\log K = \frac{-\Delta G_R^0}{2.303RT_K}, \quad (3.1)$$

where R is the gas constant and T_K is absolute temperature. The composition of pyrite, in the eq. 3.2, is replaced by various compositions of As-Fe-S solid solutions ($\text{FeS}_{1.99}\text{As}_{0.01}$ – $\text{FeS}_{1.90}\text{As}_{0.10}$) in order to calculate the molar concentration of the reaction components in arsenian pyrite.



The Gibbs free energy ΔG_R of the reaction was calculated using the expression

$\Delta G_R^\circ = \Delta G_f^\circ \text{ product} - \Delta G_f^\circ \text{ reactants}$. Experimentally extrapolated Gibb's free energy for

FeAsS [$\Delta G^\circ (\text{FeAsS}) = -141.6 \pm 6 \text{ kJ/mol}$], and Gibb's free energy for arsenite [ΔG_f°

{As(OH)₃} = -639.77 kJ/mol] at 25°C and 1bar (Pokrovski et al., 2002) were used to

calculate Gibb's free energy for various composition of arsenic and sulfur in Fe-As-S

solid solution using coefficient of concentration in reaction with arsenic and sulfur in

above equation (3.2). Similarly, established Gibb's free energy values

$\Delta G_f^\circ (\text{FeS}_2) = -166.9 \text{ kJ/mol}$, $\Delta G_f^\circ (\text{H}_2\text{O}) = -243.14 \text{ kJ/mol}$, $\Delta G_f^\circ (\text{SO}_4^{2-}) = -744 \text{ kJ/mol}$, and

$\Delta G_f^\circ (\text{Fe}^{2+}) = -82.88 \text{ kJ/mol}$ (Drever, 1997), and $\Delta G_f^\circ [\text{As}(\text{OH})_3] = -639.77 \text{ kJ/mol}$

(Pokrovski et al., 2002) were used to obtain Gibb's free energy for [As(OH)₄⁻], and log K

value for the reaction:



Using the mass action equation, Gibb's free energy and log K values for [As(OH)₄⁻] for

the reaction (eg. 3.3) were calculated as -859.87 kJ/mol, -9.2329, respectively. Finally,

free energy for arsenian pyrite solid solution FeS_xAs_y was calculated from that of FeSAs

by an equation (eq. 3.3) presented by Pokrovski et al. (2002):

$$\Delta G^0 (\text{FeS}_x\text{As}_y) = \Delta G^0 (\text{FeSAs}) + 2.303RT(\log x + \log y) \quad (3.4)$$

Calculated ΔG_f° and log K values for various arsenian pyrite solid solution containing 1 to

10 mol % of arsenic (i.e., FeS_{1.99}As_{0.01} – FeS_{1.90}As_{0.10}) are summarized in table 3.1.

Thermodynamic data for arsenian pyrite, thioarsenite species, and amorphous As and Fe

sulfide phases were compiled into a revised GWB database *Thermo08-As*.

Table 3.1 Table showing the details for calculating Gibb's free energy ΔG° for various composition of Fe-As-S solid solution ($\text{FeS}_{1.99}\text{As}_{0.01}$ – $\text{FeS}_{1.90}\text{As}_{0.10}$). ΔG° values of two end-member pure phases FeS_2 and FeSAs are also shown. The values of equilibrium constant $\log K$ were calculated for the reaction:

$\text{FeS}_x\text{As}_y + X \text{H}_2\text{O} + Y \text{O}_2(\text{aq}) \rightarrow \text{Fe}^{2+} + x \text{SO}_4^{2-} + y \text{As}(\text{OH})_4^- + Z \text{H}^+$
 Values X, Y and Z are the stoichiometric coefficients of H_2O , $\text{O}_2(\text{aq})$, and H^+ in the reaction; x and y are the molar ratio of sulfur and arsenic in the Fe-S-As solid solution.

Sulfur (S) and Arsenic (As) fraction	S	As	Molecular Weight	$\Delta G^\circ_f(\text{FeAsS})$	S(x)	As(y)	$2.303RT(\log x + \log y)$	$\Delta G^\circ_f(\text{FeS}_x\text{As}_y)$	Fe-As-S Solid Solution	ΔG° for the Reaction	Log K
				-141.6	2.00	0.00	-25.29	-166.89			
$\text{S}_{1.99}\text{As}_{0.01}$	1.99	0.01	120.396	-141.6	1.99	0.01	-5.62	-147.22	Fe-As-S Solid Solution	-1147.58	199.78
$\text{S}_{1.98}\text{As}_{0.02}$	1.98	0.02	120.824	-141.6	1.98	0.02	-4.63	-146.23		-1145.63	199.44
$\text{S}_{1.97}\text{As}_{0.03}$	1.97	0.03	121.253	-141.6	1.97	0.03	-4.06	-145.66		-1143.27	199.02
$\text{S}_{1.96}\text{As}_{0.04}$	1.96	0.04	121.681	-141.6	1.96	0.04	-3.65	-145.25		-1140.74	198.58
$\text{S}_{1.95}\text{As}_{0.05}$	1.95	0.05	122.110	-141.6	1.95	0.05	-3.34	-144.94		-1138.12	198.13
$\text{S}_{1.94}\text{As}_{0.06}$	1.94	0.06	122.539	-141.6	1.94	0.06	-3.08	-144.68		-1135.44	197.66
$\text{S}_{1.93}\text{As}_{0.07}$	1.93	0.07	122.967	-141.6	1.93	0.07	-2.87	-144.47		-1132.72	197.19
$\text{S}_{1.92}\text{As}_{0.08}$	1.92	0.08	123.396	-141.6	1.92	0.08	-2.69	-144.29		-1129.97	196.71
$\text{S}_{1.91}\text{As}_{0.09}$	1.91	0.09	123.825	-141.6	1.91	0.09	-2.53	-144.13		-1127.19	196.23
$\text{S}_{1.90}\text{As}_{0.10}$	1.90	0.10	124.253	-141.6	1.90	0.10	-2.38	-143.98		-1124.4	195.74
				-141.6	1.00	1.00	0.00	-141.60	FeSAs		

Reaction-path modeling was carried out using *React* module of GWB. The general chemical composition of contaminated groundwater from Bangladesh was used as the initial condition in the simulation. Field data for minerals, dissolved species, and gases collected by BGS, at well no 297_00331 (BGS, and DPHE, 2001) [$\text{Na}^+ = 0.10\text{mg/L}$; $\text{Cl}^- = 0.10\text{mg/L}$; $\text{Ca}^{++} = 10\text{ mg/L}$; $\text{HCO}_3^- = 50\text{ mg/L}$; $\text{As(III)} = 2400\text{ }\mu\text{g/L}$; $\text{As(total)} = 2540\text{ }\mu\text{g/L}$; $\text{Fe}^{++} = 0.24\text{ mg/L}$; $\text{SO}_4^{2-} = 1.5\text{ mg/L}$; $\text{Eh} = -0.12\text{ V}$; $\text{pH} = 7.32$] was used to initiate the numerical reaction path modeling.

GWB calculations were carried out using use new thermodynamic data to characterize the speciation of As in Fe-S-As-H₂O systems. Geochemical reaction path modeling was carried out to find As speciation, adsorption/desorption, precipitation under sulfate-reducing conditions. Changes in water chemistry, and Eh/pH were recorded. Results of tracing reaction paths was produced using *Gtplot* subroutine of GWB.

This study compares the results of geochemical modeling between two data sets, one with thermodynamic data for thioarsenite species and amorphous As and Fe-sulfide phase compiled by Lee et al. (2005) in GWB database *Thermo04-As*, and other with *Thermo08-As* developed as part of this research.

3.3. Laboratory arsenic sorption experiments

Batch experiments were conducted to evaluate the amount of sorbed As onto laboratory prepared Fe-sulfide and natural pyrite crystals in an O₂-free (N₂- purged) anaerobic chamber, except where noted (Fig. 3.2). Chemicals used in this study were of analytical grade, unless otherwise stated, and used without further purification. Synthetic laboratory Fe-sulfide was prepared under reducing condition using reagent grade disodium sulfide (Na₂S·9H₂O), and iron sulfate (FeSO₄·7H₂O) (Fisher chemicals). Natural cubic pyrite crystals were purchased from Wards Natural Science, NY, USA. Surface impurities of bulk pyrite hand samples were cleaned using 0.1M HCl and then by deoxygenated doubly deionized distilled water (Milli-Q, 18 MΩ) (DIW), and dried out in a furnace with circulating dry air for 1 hr. Dry pyrite crystals were then ground in a laboratory hand crusher for several hours, and then separated into three different grain size using standard mesh; 63μm -125μm, 180μm-250μm, and 425μm -500μm later named as ‘fine’, ‘intermediate’, and ‘coarse’ grained, respectively. Molecular weight of pyrite crystals used for adsorption experiments was 120.0 grams per mole and is 46.5% iron by weight. To prevent further oxidation, these samples were temporarily stored inside the anaerobic chamber.

All solutions were prepared using DIW. Arsenic stock solution (1000 mg/L) was prepared by dissolution of arsenic trioxide powder (As₂O₃, 99.95%; Fisher chemicals) in DIW inside the anaerobic chamber. It was hypothesized that preparation under reducing conditions would limit the oxidation of arsenite to arsenate.

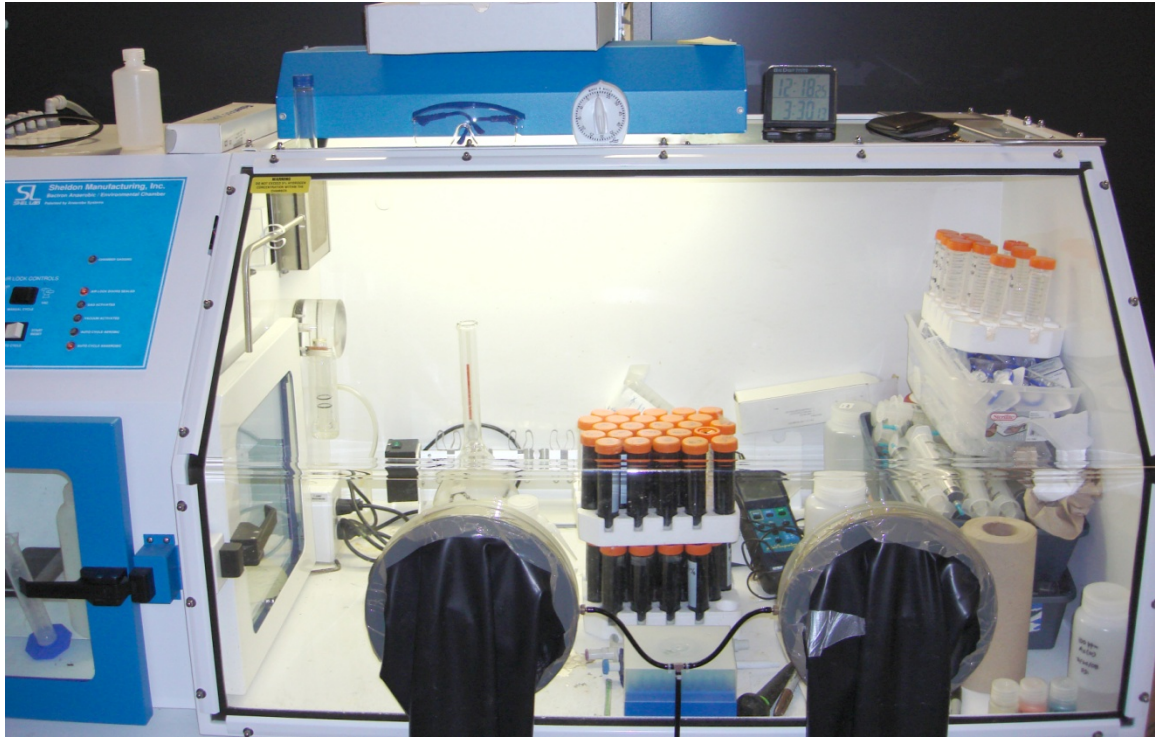


Fig. 3.2 Photograph of Batron™ anaerobic chamber used for studying arsenic sorption on laboratory prepared Fe-sulfide and hand crushed pyrite crystals. All the batch experiments performed for this study were conducted entirely in an O₂-free (N₂-purged) anaerobic chamber.

A minimum quantity of 1M NaOH solution was added until the solid As_2O_3 was completely dissolved in DIW following procedure of Farquhar et al. (2002). Before making the volume of water in a volumetric flask, equal amount of 1M HNO_3 was added to the solution to neutralize the effect of NaOH in the solution. A magnetic stir bar was inserted into the As solution and stirred for 2 days to achieve maximum dissolution following procedure of Perfetti et al. (2008). The stock solution thus prepared was filtered through a 0.45 μm Millipore filter, capped in the air tight flask bottles, and stored in the anaerobic chamber. Different concentrations of arsenic (0.1, 1, 10, 20, 30, 40, 50, and 100 mg/L) in solution were obtained by dilution of the stock solution.

After mixing all the components, samples were further mixed for determined time intervals using an end-over-end rotator inside the anaerobic chamber. Changes in pH and Eh were recorded in almost all batch experiment at determined time intervals. After each experiment the batch solution was filtered through 0.45 μm Millipore filter using a 60 ml syringe. The filtered solution was acidified with 1M HNO_3 solution, and capped in a refrigerator pending As analysis. Measurements for As concentration were carried out using a Perkin Elmer HGA-600 Graphite Furnace and a 3110 Perkin Elmer Atomic Absorption Spectrometry (AAS) in the Department of Civil Engineering, Auburn University.

3.3.1. Batch experiment: arsenic sorption onto iron sulfide

1M stock solution of disodium sulfide ($\text{Na}_2\text{S}\cdot 9\text{H}_2\text{O}$) and 0.5M stock solution of iron sulfate ($\text{FeSO}_4\cdot 7\text{H}_2\text{O}$) were prepared on a separate flask inside the anaerobic chamber by weighing fixed amount of respective chemicals and mixing them with DIW. The stock

solution was stirred for 12 hr using magnetic bar to obtain maximum dissolution. Chemically synthesized fresh amorphous iron monosulfide was prepared by mixing $\text{Na}_2\text{S}\cdot 9\text{H}_2\text{O}$, and $\text{FeSO}_4\cdot 7\text{H}_2\text{O}$ in DIW following the method used by Donald and Southam (1999) but at a different concentration. Sorption of As onto FeS was studied in sulfide-limited (S:Fe=1:1) and excess-sulfide (S:Fe=2:1 and 3:1) batch experiment similar to the study made by Wolthers et al. (2007).

A stock solution of $\text{Na}_2\text{S}\cdot 9\text{H}_2\text{O}$ was diluted to make 0.25, 0.5 and 0.75M solutions, and the stock solution for $\text{FeSO}_4\cdot 7\text{H}_2\text{O}$ was diluted to make a 0.25M solution. The first set of batch experiments with S to Fe ratio of 1:1, are referred to as the *sulfide-limited* experiments. These were carried out using a 50 ml low-density polyethylene tube where 0.25M of $\text{Na}_2\text{S}\cdot 9\text{H}_2\text{O}$ is mixed with 0.25M of $\text{FeSO}_4\cdot 7\text{H}_2\text{O}$ solution. The second set of batch experiment, with S to Fe ratio of 2:1 and 3:1, are referred to as the *excess-sulfide* experiments, was conducted to produce two sets of experiments where 0.25M $\text{FeSO}_4\cdot 7\text{H}_2\text{O}$ solution was mixed separately with 0.5 and 0.75M of $\text{Na}_2\text{S}\cdot 9\text{H}_2\text{O}$ solution separately. In both the sulfide-limited and excess-sulfide experiments, the concentrations of As used were 0.1 mg/L, 1 mg/L and 10 mg/L. Ionic strength of the solution was maintained using 0.01M NaNO_3 solution.

The initial pH of the sulfide-limited and excess-sulfide batch experiments was adjusted to 7. Changes in As concentration, Eh and pH were monitored at the following time interval; 6 hr, 12 hr, 24 hr, 36 hr, 72 hr, 1 week, and 2 week (“Appendix 1”). After each time interval, samples were filtered and stored in a refrigerator pending As analysis. Precipitation obtained during filtering was dried in O_2 -free condition for 2-4 days for XRD to characterize the solid phase produced during the experiment.

3.3.2. Batch experiment: arsenic adsorption onto pyrite

The adsorption studies were run at a room temperature under reducing conditions to investigate As adsorption onto pyrite. A small fraction (0.3 gm) of coarse-grained pyrite crystals was washed using 5 different approaches: ethanol (C_2H_6O , 10%) only, nitric acid (0.5M HNO_3) only, ethanol followed by DIW, nitric acid followed by DIW, and with DIW separately before treating with As concentration of 1 mg/L. The purpose of the initial batch experiments is to find the most suitable solution among the five used which can maximize the adsorption of As onto pyrite and in the same time effect minimum changes in pH of the solution. This chemical solution would be used for washing pyrite crystals in future experiments. Ionic strength of 50 ml experimental solution prepared in low density polyethylene centrifuge tube was balanced using 0.01M $NaNO_3$ solution. The initial pH value of the experimental solution was adjusted to neutral (pH=7) using either 0.1M HNO_3 or 0.1M $NaOH$ solution.

After the samples were prepared, they were mixed for 72 hours using end-over-end rotator inside the anaerobic chamber. Changes in As concentration and pH were monitored at 6 hr, 12 hr, 24 hr, 36 hr, and 72 hr time interval. One batch sample was sacrificed at each time point while it was filtered using 0.45 μ m syringe filter, acidified in 1M HNO_3 , and stored in a refrigerator pending analysis. When least changes in pH from the initial value together with high As adsorption was considered most suitable conditions, results of the batch experiment conducted for 72 hour showed that pyrite first washed with 0.5M HNO_3 and then by DIW adsorbed median As content (0.38 μ M/gm of FeS_2), and with the least fluctuation in pH value (<12%) (Fig. 3.3) (laboratory data in “Appendix 2”).

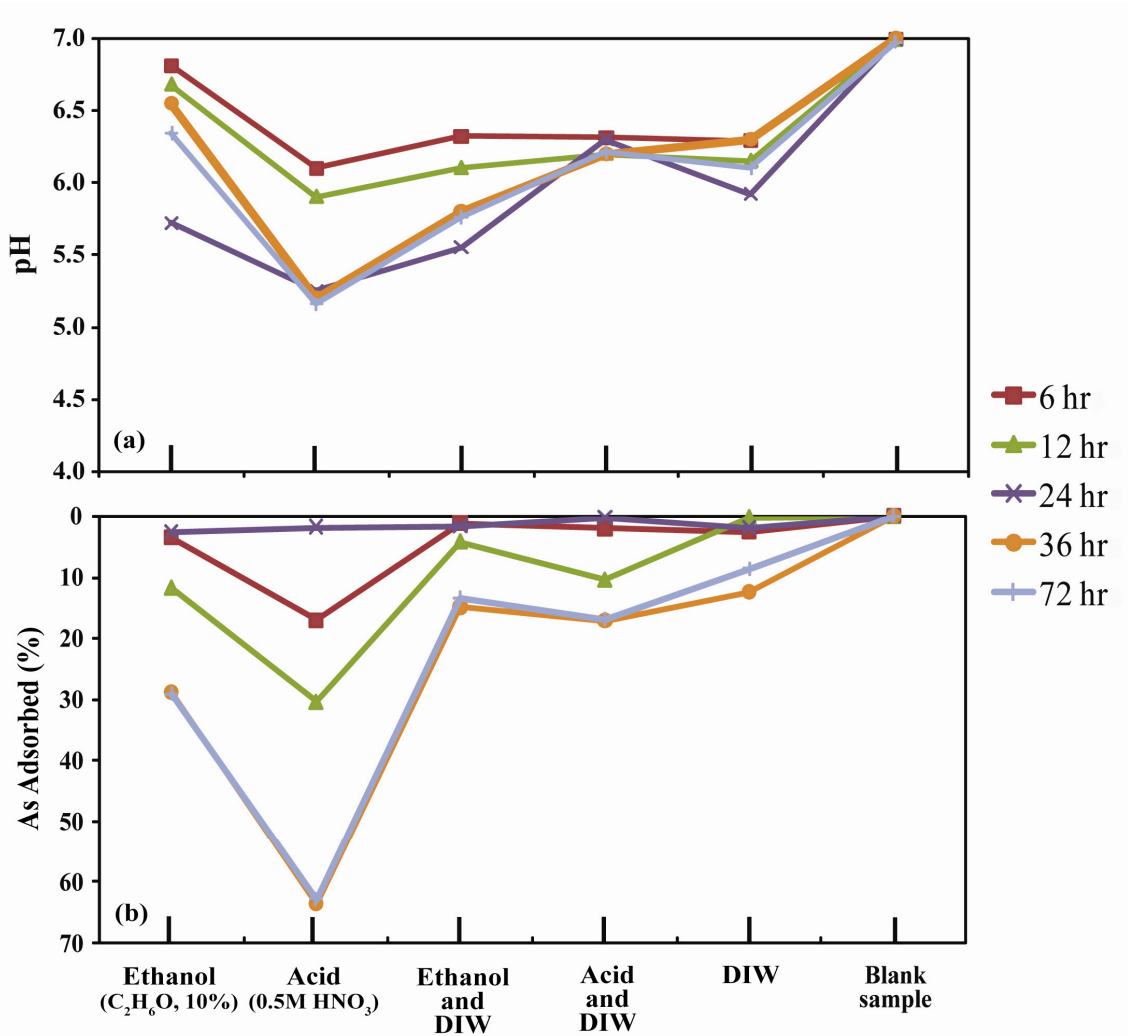


Fig. 3.3 Plot showing arsenic adsorption with concurrent changes in pH observed in pyrite crystals washed with 5 different chemical solutions. Coarse grained pyrite washed first with 0.5M HNO₃, and then by DIW demonstrated more consistent pH(a) value from the beginning of the experiment, and adsorbed median arsenic concentration from the solution (b). Experiment was conducted under reducing condition at the initial pH of 7.

Later, all pyrite crystals used for the further batch experiments were first washed with 0.5M HNO₃ solution and then by DIW.

Adsorption Kinetics

Adsorption kinetic experiments were conducted with 3 different sizes of pyrite (fine, intermediate, and coarse) to determine the time required to reach equilibrium between As and pyrite. Three different As concentrations, 0.1 mg/L, 1mg/L and 10mg/L were used for all three pyrite crystals. In each case, 50 ml of experimental batch solution was prepared by mixing arsenic, 0.3 gm of pyrite crystals (6gm/L), 0.01M NaNO₃, and DIW. A low-density polyethylene centrifuge tube was used for each batch experiment. Initial pH of the solution was balanced at 7 using either 0.1M HNO₃ or 0.1M NaOH solution. The time duration designed for the experiment was 72 hr. Changes in pH and As concentration after the beginning of the test were recorded at different time interval (15 min, 30 min, 1 hr, 3 hr, 6 hr, 12 hr, 24 hr, 36 hr, and 72 hr). After completion of the experiment, samples were collected, filtered, stored, and analyzed in the same manner as described before.

Adsorption Isotherms

Adsorption isotherms were obtained at a pH of 7 and constant ionic strength (0.01M NaNO₃). Samples were prepared in 50 ml low-density centrifuge tubes. Fine-intermediate-and coarse-grain pyrite crystals were treated separately with 8 different As concentrations (0.1, 1, 10, 20, 30, 40, 50, and 100 mg/L). Based on the results of kinetic experiment, a time duration of 36 hours was selected for this experiment. After the completion of the experiment samples were filtered, stored and analyzed in the same manner mentioned previously.

Adsorption envelope

Adsorption envelope (i.e., percent adsorbed as a function of pH at constant arsenic concentration) experiments were performed to measure As sorption as a function of pH. Solutions varied in As concentration (0.1 mg/L, 1 mg/L, and 10 mg/L) and size (fine, intermediate, and coarse) of pyrite crystals used for the experiment was also varied. Ionic balance of the experimental solution was set to a constant using 0.01M NaNO₃ solution. For all experiments, the pH of the batch solution was varied from 4 to 10 using 0.1M NaOH or 0.1M HNO₃ solution to reach the desired pH. DIW was used to fill a 50 ml centrifuge tube with 0.3 gm of pyrite crystals, and desired arsenic concentration. Sample prepared in this manner were allowed to equilibrate for 36 hours, and then were sampled, filtered, preserved and analyzed in the same manner as mentioned previously.

3.4. Analytical methods

Samples from the batch experiments were acidified with 1M HNO₃ equivalent to the matrix match for AAS. Samples obtained after the experiment were diluted to match the upper detection limit of AAS (i.e., 1 mg/L), if necessary, and were injected onto platforms inside a graphite tube in 20 µL increments along with 5 µL of palladium-magnesium nitrate matrix modifier. An AAS instrument was calibrated each time prior to analysis using standard As concentration (20, 40, 60 and 100 µg/L). An equal amount of NaNO₃ and HNO₃ were incorporated in the standard As calibration solutions to match samples being measured. A sample being measured always had a blank and was

analyzed in replicates of two. The calibration curve was judged accurate when the standard was retested and the results yielded concentration within 5% of the actual concentrations.

Throughout the experiment conducted to study the As sorption onto Fe-sulfide and pyrite, Eh and pH was measured using EXTECH 407227 Eh-pH meter that included Eh and pH electrode separately. The pH electrodes were calibrated between two points prior to each use using two of the available three buffers (pH 4.0, 7.0, and 10.0) depending on pH range of the samples requiring analysis. Each time before and after the measurements were taken Eh electrode was rinsed with electrode cleaning solution and then with DIW.

After filtering the batch sample with Fe-sulfide black precipitate, produced initially while studying As sorption on Fe-sulfide, for measuring the As concentration in the solution, residual Fe-sulfide precipitate that remained in the bottom of the experimental tube was laid as thin veneer onto a thin glass slide. Such samples of Fe-sulfide extracted after fixed time interval (6 hr, 12 hr, 24 hr, 36 hr, 72 hr, 1 week and 2 weeks) were left to dry in reducing condition for 2-3 days. Thus prepared samples were studied under reflected light microscopy, and crystallographic Fe-sulfide minerals were later analyzed by XRD to characterize their identity.

CHAPTER 4

RESULTS AND DISCUSSION

4. Results and discussion

4.1. Field bioremediation experiments

At the Manikganj, Bangladesh field site bioremediation experiment included the injection of molasses as a source of carbon, followed by injection of sulfate salt solution as a source for Fe and SO_4^{2-} to stimulate indigenous SRB that cause Fe-sulfide precipitate, and to effect As removal (Lee and Saunders, 2003; Lee et al., 2005; Saunders et al., 2005c). However, injecting sources of carbon, into aquifers at first simulates biogenic Fe-reduction, causing groundwater to become more reducing, and dissolved Fe may increase (and arsenic as well). After reducible Fe in minerals are consumed, indigenous SRB metabolism begins and H_2S is produced. H_2S produced during the sulfate reduction process reacts with Fe (II) and precipitates iron monosulfide (FeS)_{am}, and finally pyrite (Rickard, 1975; Berner, 1984; Schoonen and Barnes, 1991; Wilkin and Barnes, 1996; Rickard and Luther, 1997; Donald and Southam, 1999).

Field data from groundwater geochemical studies and bioremediation experiments indicate that dissolved As and Fe are released under moderately reducing conditions during microbial-mediated reductive dissolution of HFO in Holocene alluvial aquifers. Dissolved Fe and As released by this process react with H_2S produced by SRB to precipitate amorphous Fe-sulfide containing As, which ultimately transforms into more

stable arsenian pyrite. Arsenic can substitute for sulfur in the crystal lattice (Savage et al., 2000) or can be sorbed on solid sulfide surfaces, and both cause As removal from solution (Fig. 2.7).

In the Blackwell, Oklahoma bioremediation experiment, groundwater was initially oxidizing, contained low dissolved Fe, and virtually no As shown as in Fig. 4.1(a). Soon after injecting the organic carbon source, substantial increases in Fe and As concentrations were observed from 14 to 28 days. This increase in Fe and As concentration in the groundwater is interpreted to be the results of the onset of biogenic Fe-reduction and perhaps mirrors the natural process that released As to groundwater in Manikganj, Bangladesh and other countries. Sulfate remains relatively stable about for a month, but then As and Fe concentrations decrease radically after about 4 weeks. Substantial decrease in Fe and As (along with sulfate) after 42 days is apparently due to the onset of biogenic sulfate reduction. With the beginning of biogenic sulfate reduction, formation of Fe-sulfide commences resulting in a drop of SO_4^{2-} concentration as it is turned into H_2S , and solid Fe-sulfide phases. Arsenic concentration drops to below pre-injection levels after 7 weeks until end of the experiment (25 weeks, Fig 4.1a). Most probably, a fall in As concentration is due to the sorption of As onto the “biominerals” (in particular Fe-sulfide phases) produced during biogenic sulfate reduction. Perhaps replacement of the remediated plume by the fresh flowing (oxidized) groundwater may oxidize some Fe-sulfide phases resulting in an upward spike of both Fe and SO_4^{2-} after 9 weeks.

It is hypothesized at the Blackwell, Oklahoma site that oxidation of newly formed Fe-sulfide leads to the release of Fe, and SO_4^{2-} into the groundwater, and perhaps

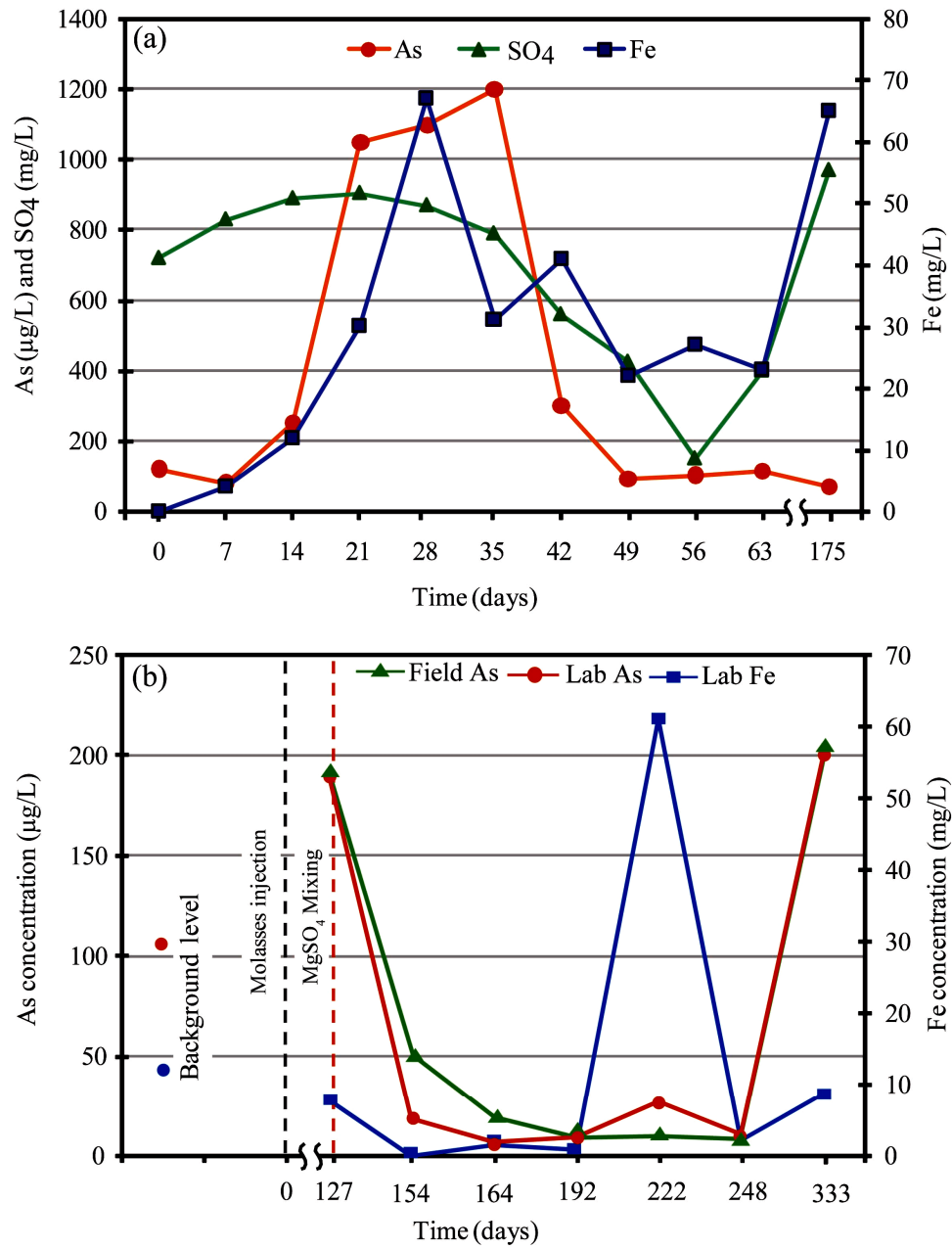


Fig. 4.1 Plot showing changes in As, Fe, and SO_4^{2-} concentration recorded after a single-well bioremediation experiment carried out at Blackwell, Oklahoma (a) and Manikganj, Bangladesh (b). Changes in soluble Fe, As and SO_4^{2-} were recorded after the injection of molasses, Epsom's salt ($\text{MgSO}_4 \cdot 7\text{H}_2\text{O}$). Molasses was used as a source of carbon to enhance iron reduction, and the sulfate salts was used as source for sulfate to enhance metabolism in indigenous SRB for sulfate reduction.

also causing the formation of new HFO mineral phases (e.g., replace sulfides) which would continue to sorb dissolved As onto its surface at the end of remediation experiments. Laboratory experiments conducted by Wharton et al. (2000) showed that pyrite oxidation to HFO could retain previously sulfide-sorbed technetium (Tc), and it is suggested a similar process might have occurred during the Blackwell, Oklahoma bioremediation experiment with respect to As. Thus, the fairly low As concentration observed after 8 weeks of the experiment, almost equal to the pre-injected level of As, may have been caused due to sorption of As onto newly formed HFO. More research should be conducted on retention of trace metals and metalloids on neo-formed HFO from Fe-sulfide oxidation to further characterize natural geochemical processes of trace elements during redox changes.

Results of the initial single-well bioremediation experiment conducted at Manikganj, Bangladesh are presented in Fig. 4.1b. Shallow groundwater exploited in the region is hosted by Holocene sand, silt and clay locally containing organic matter deposited in the flood plain of the Ganges and Brahmaputra Rivers which traverse the region. A 200-m deep semi-continuous core-holes extracted from the study area indicate Holocene deposits are typical alluvial floodplain sediments (Shamshudduha, 2007) similar to those described elsewhere in Bangladesh (Smedley and Kinniburgh, 2002; Ahmed et al., 2004). Groundwater in Manikganj is initially moderately reducing, neutral pH with relatively low sulfate, and is an iron-rich Ca-Mg-HCO₃ type (Shamsudduha, 2007). Holocene alluvial aquifers contaminated with elevated As have shown low sulfate concentration not only in Bangladesh (Nickson et al., 2000; Smedley and Kinniburgh, 2002) but also in other parts of the world (Tandukar et al., 2005; Smedley and

Kinniburgh, 2002; Bostick et al., 2006). Groundwater in the vicinity of the injection well at this study site contained elevated dissolved moderate As concentrations, ranging from 50-200 $\mu\text{g/L}$ (Fig. 1.4). A tube well tapping relatively As-contaminated groundwater ($\sim 100 \mu\text{g/L}$ As from depth of 37 m) in the study area was selected for the bioremediation experiment. Geochemical changes in the groundwater following the injection of nutrients were recorded during the process of the field experiment.

For the initial Bangladesh experiment, 200 L of a carbon-bearing solution was prepared by mixing ~ 11 kg of molasses with groundwater from the site. This solution was then poured into the well by gravity injection (Fig. 3.1a). Water samples over the next 6 months were collected periodically using standard methods suggested by US-EPA. Arsenic concentration of the remediated groundwater was tested in the field using a colorimetric technique and also sampled for laboratory analysis. Injection of molasses initially causes dissolved As to increase, yet dissolved Fe remains relatively constant (Fig. 4.1b). The increase in As concentration at early stage of experiment is believed to be the result of stimulating Fe-reducing conditions, which mobilizes As from HFO. A similar result was also observed at Blackwell bioremediation experiment (Fig. 4.1a) and a field experiment conducted by Harvey et al. (2002) in Bangladesh.

As a source of sulfate, 4 kg of Epsom's salt ($\text{MgSO}_4 \cdot 7\text{H}_2\text{O}$) mixed with water was added into the aquifer about 18 weeks after the injection of molasses in Manikganj bioremediation site. A drop in Eh values and "rotten egg" smell of the water from injection well occurred at about 4 weeks after the injection, suggesting the beginning of biogenic sulfate reduction. Similar to what observed in the Manikganj remediation experiment, sulfate reduction in the Blackwell experiment had also begun at about same

time interval after organic carbon was added, although dissolved SO_4^{2-} was already present in the groundwater there.

At the Manikganj site, the dramatic drop in Fe and As concentration that was observed between 154 and 192 days apparently indicates the beginning of biogenic sulfate reduction in the groundwater (Fig. 4.1b). Dissolved iron reverted to background level about 206 days after the injection of Epsom's salt, and at the same time, the level of As in the solution changed to slightly higher than the pre-injection level. At the end of the experiment in Bangladesh, Fe-reducing conditions apparently had returned again. It seems that enough organic carbon remained after the depletion of injected sulfate (or natural organic matter was still present) to provide sufficient carbon source for FeRB. Artificially induced Fe-reduction process at the latter phase of the experiment appears to have released more As from aquifer HFO.

During Fe-reduction and prior to sulfate reduction, the Blackwell, Oklahoma site had relatively more dissolved iron in the groundwater than in Manikganj, Bangladesh. No doubt reactive HFO present under initial oxidizing conditions at the site led to the high iron levels once Fe-reduction began. This high iron content may have been major criterion that resulted in more effective As removal at Blackwell compared to the results from Manikganj. It appears higher dissolved iron levels may lead to more Fe-sulfide phase product, which is apparently required for efficient As removal. Thus, replacing Epsom's salt by ferrous sulfate ($\text{FeSO}_4 \cdot 7\text{H}_2\text{O}$) for sulfate source can overcome the shortage of dissolved Fe in the solution in Manikganj, Bangladesh, hence making As removal from the solution more effective and perhaps more long lasting. Results of both the bioremediation experiments suggest that SRB metabolism might lead to *in situ*

arsenic removal from As-contaminated groundwater. Moreover, as discussed below, Fe-sulfide precipitation in the vicinity of the well might be an effective As removal process even after the biogenic sulfate reduction has come to an end (e.g., nano particles of Fe-sulfide can sorb As on their surfaces).

4. 2. Geochemical modeling

4.2.1. Arsenic speciation

With the new thermodynamic data for thioarsenite species and arsenian pyrite calculated in this study, a new phase diagram for As speciation in the presence of SO_4^{2-} was computed using *Act2* module of *GWB*. Model simulations conducted under oxic condition reveal that at low $\text{pH} < 7$, the protonated forms of arsenate predominate (H_3AsO_4 , H_2AsO_4^-), whereas arsenite species (HAsO_4^{2-} , AsO_4^{3-}) occurs at higher pH (Fig 2.1). Under reducing conditions and over a wide range of pH values, H_3AsO_3 becomes the most dominant arsenite species. Under even more reducing conditions, affinity of As for sulfur results in the formation of non-ferrous solid As-sulfides as orpiment (As_2S_3) or realgar (AsS) (Fig. 2.1). Interestingly, arsenian pyrite ($\text{FeS}_{1.99}\text{As}_{0.01}$) completely replaces pure As-sulfide and thioarsenite aqueous complex in a system containing a fairly small amount of iron ($\log \text{Fe}^{2+}$ activity = 10^{-8}) (Fig. 4.2). Besides pyrite, As-sulfide phases such as arsenopyrite and arsenides such as löllingite can be considered major As host in Fe-rich reducing geologic environments (Savage et al., 2000). Arsenic atoms may enter the structure of pyrite via an atomic exchange between S and As to yield arsenopyrite (Savage et al., 2000) rather than for iron (Blanchard et al., 2007). Previous research conducted by Morse et al. (1987) and Wolthers et al. (2005b) are consistent with these modeling results that arsenian pyrite or arsenopyrite is thermodynamically more stable

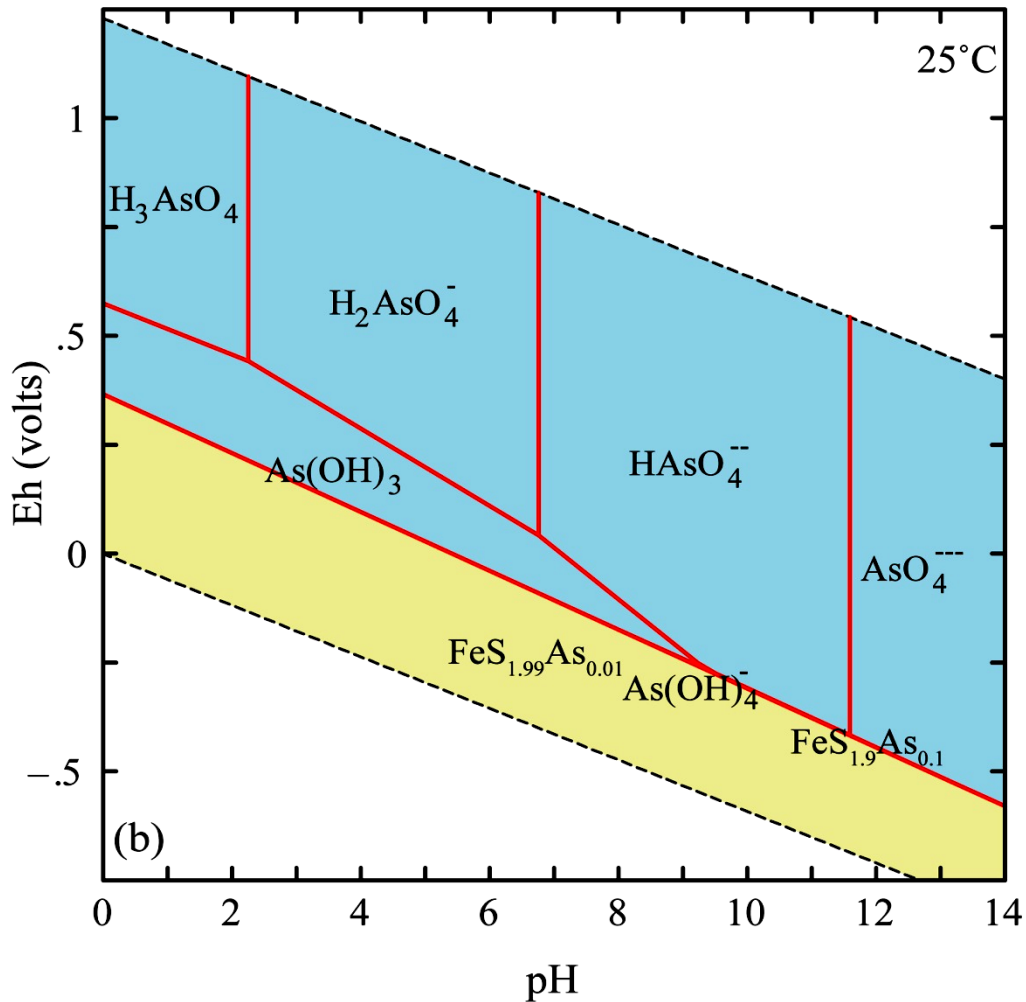


Fig. 4.2 Eh-pH diagram for As drawn at 25°C with fixed arsenic and SO_4^{2-} activities of 10^{-2} and Fe^{2+} activity of 10^{-8} . Eh value for the system was fixed at 0.75 V. Dashed lines show stability limits of water at 1 bar pressure. Species in the blue area are aqueous phases and those in yellow area are solid minerals. Modeling conducted in GWB that included new thermodynamic data for arsenian pyrite solid solution.

than pure As-sulfides under Fe-bearing sulfate-reducing conditions. Further, pure orpiment is rarely found in natural waters because its precipitation is kinetically inhibited at near-neutral pH conditions (Webster, 1990).

4.2.2. Arsenic precipitation under sulfate-reducing conditions

This study investigates how bacterial sulfate reduction can promote the precipitation of metal sulfides and As from an As-contaminated groundwater. Results of reaction flow-path modeling (Fig. 4.3) conducted to examine the predictive sequence of mineral precipitation (Fig. 4.4) which was carried out in two different systems; one that does not include thermodynamic data for arsenian pyrite solid solution ($\text{FeS}_{1.99}\text{As}_{0.01}$ - $\text{FeS}_{1.90}\text{As}_{0.10}$) and the other with it, are discussed here. As an initial geochemical condition for the simulation, the published water chemistry from one typical well in Bangladesh [well no 297_00331, BGS-DPHE (2001)] was used for modeling purpose. This groundwater had an elevated As concentrations of 2540 $\mu\text{g/L}$ and was under near-neutral pH condition. To model the effect of SRB metabolism analogous to the field bioremediation, fluid reactants containing 300 μM of Fe^{2+} and SO_4^{2-} were added into the initial system and the values of Eh slide from +150 mV (oxidizing) to -150 mV (reducing) over the reaction path. In the calculations, SO_4^{2-} is automatically converted to H_2S due to drop in Eh.

Model results show that ferric hydroxide, $\text{Fe}(\text{OH})_3$ is the most dominant iron mineral species in aerobic initial conditions (Fig. 4.3 and Fig. 4.4). During bacterial sulfate reduction, initial $\text{Fe}(\text{OH})_3$ becomes unstable (Fig. 4.4). When Eh values of the system are progressively lowered, in both the models, with and without thermodynamic

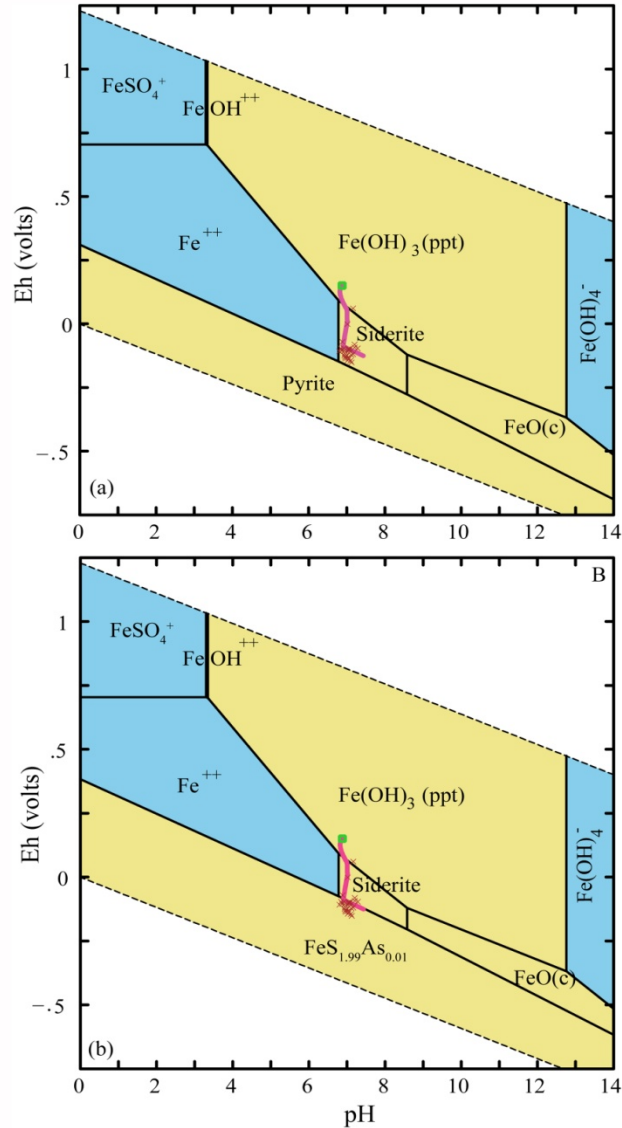


Fig. 4.3 Fe-As-S-H₂O composite Eh-pH diagram showing results of geochemical reaction flow path modeling. Field data for minerals, dissolved species, and gases collected from well no 297_00331 (BGS, and DPHE, 2001) was used to initiate the numerical reaction path modeling. Analogous to field bioremediation FeSO₄ was added in the initial system to immobilize As. The simulation was fixed at 25°C, and 1 bar pressure. Reaction trace (pink solid line) represents the predictive sequence of mineral precipitated as Eh drops during simulation. Chemical precipitation of the minerals in both the geochemical condition, without (a) and with (b) thermodynamic data for arsenian pyrite solid solution (FeS_{1.99}As_{0.01}-FeS_{1.90}As_{0.10}), initiated from top green square at the center of the figure. Reaction came to an end after the precipitation of siderite in the first model (a) but, mineral precipitation continues until arsenian pyrite is precipitated at the final stage in the second model (b). Pink cross marks in center of both the figure shows Eh-pH scatter plot of the water samples from Bangladesh. Model was created using *Act2* module of GWB.

data for arsenian pyrite solid solutions, soluble Fe combines with bicarbonate (HCO_3^-) released from organic sources to form carbonate mineral siderite (FeCO_3) (Fig. 4.3 and Fig. 4.4). This result is consistent with presence of authigenic (biogenic) siderite in alluvial sediments of Manikganj (Shamshuddua, 2007), India and Bangladesh (Nickson et al., 2000; Acharyya and Shah, 2007), and coastal plain sediments in the Mississippi and Alabama (Lee et al., 2007). It is important to note that, in extremely reducing environments, where SO_4^{2-} reduction takes place in the presence of dissolved As, reduced Fe reacts with H_2S to form arsenian pyrite (instead of pure pyrite) (Fig. 4.3b and Fig. 4.4b), which can remove As from groundwater by co-precipitation. Formation of arsenian pyrite is not observed in the model results when thermodynamic data for the arsenian pyrite solid solution is not included, rather the reaction ceases after the formation of mineral siderite (Fig. 4.3a and Fig. 4.4a).

Fig. 4.5 shows the stability fields of various Fe-sulfide phases for the Fe-S-As system at fixed redox ($E_h = -150\text{mV}$) and different pH value [pH=5 (Fig. 4.5a) and pH=7 (Fig. 4.5b)]. In the presence of relatively high concentrations of soluble Fe and H_2S , near-neutral pH (5 to 7), and reducing conditions, model results show that biogenic sulfate reduction favors the formation of mackinawite as the first Fe-sulfide mineral (Fig. 4.5). Mackinawite is generally regarded to be the first mineral to form in reducing conditions at near-neutral pH, and is considered to be the kinetically favored amorphous precursor to pyrite (Schoonen and Barnes, 1991; Wilkin and Barnes, 1996; Wolthers et al., 2005a). This phase can sequester As from the solution by sorption and coprecipitation onto its surface (Benning et al, 2000; Bostick and Fendorf, 2003; Wolthers et al., 2005b; Wolthers et al., 2007). At near-neutral pH, arsenic forms stable arsenian pyrite at low

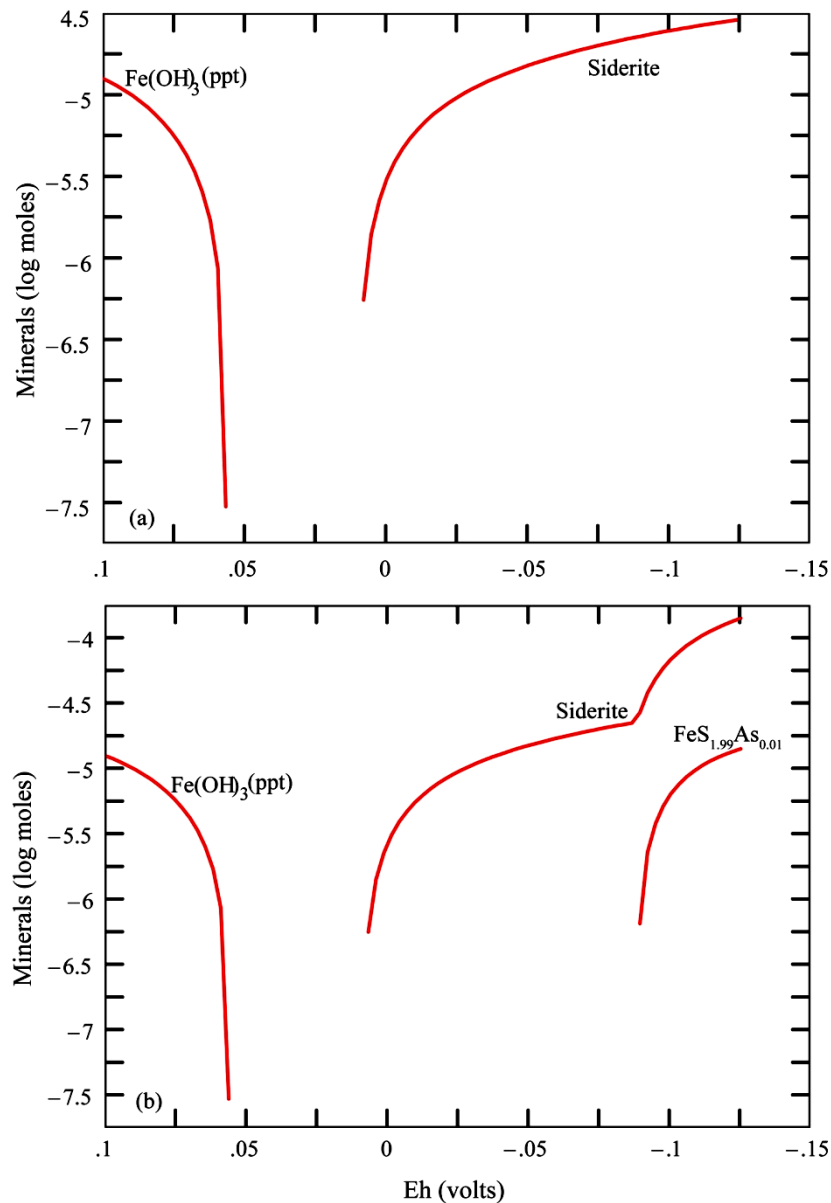


Fig. 4.4 Plots showing predictive cumulative sequence of mineral precipitated as Eh decreases as a result of bacterial sulfate reduction. Geochemical condition considered for the model is identical as mentioned in Fig. 4.3. Geochemical reaction path modeling carried out in a simulation that includes thermodynamic data for arsenian pyrite solid solutions precipitates arsenian pyrite (b) as a most dominant mineral species whereas, such mineral phase is absence in the model that lacks thermodynamic data for arsenian pyrite solid solution (a). Hematite and magnetite are suppressed (not considered in the calculation). Model was created using *React* module of *GWB*.

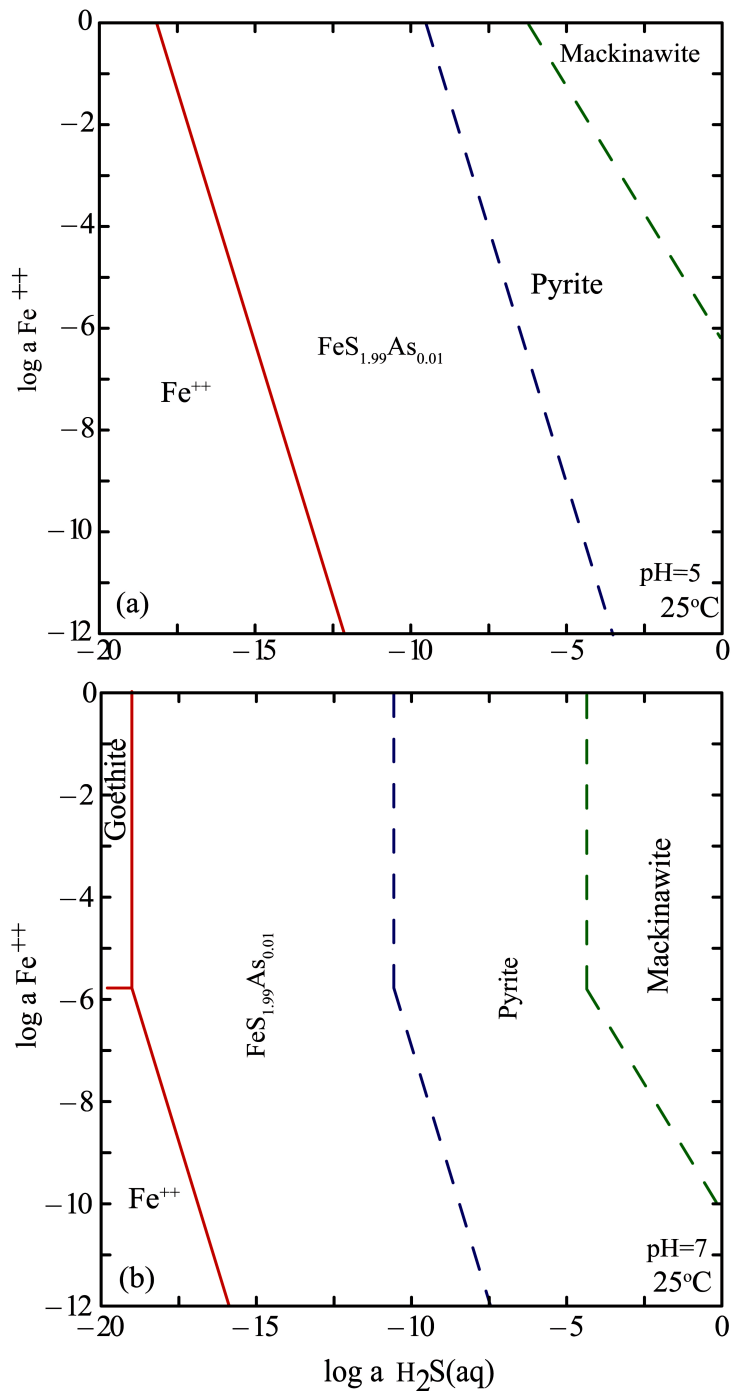


Fig. 4.5 Plot of the effect of pH values on mineral solubility recorded from GWB simulation that included thermodynamic data for arsenian pyrite solid solution. Solubility diagrams versus $a_{\text{H}_2\text{S}}$ for Fe-sulfide minerals at 25°C computed for total dissolved arsenic species activity = 10^{-2} . Fe-sulfide minerals and aqueous species are separated by solid (red) line. Dashed lines show metastable boundaries for intermediate phases mackinawite (FeS_{am}), pyrite, and arsenian pyrite at pH=5 (a) and at pH=7 (b).

activity of H₂S even if the geochemical system comprises low iron concentration (Fig. 4.5). A decrease in Fe-sulfide solubility is observed during increase of pH value (Fig. 4.5 a, and b). As pH increases, arsenic tends to become less strongly sorbed onto adsorbing sites (Dzombak and Morel, 1990) and most likely desorption may also take place (Bostick and Fendorf, 2003; Lee et al., 2005), but bacterial sulfate reduction could promote the precipitation of Fe-sulfide and arsenian pyrite by increasing pH which can enhance As sorption and removal from solution. *In situ* bioremediation is expected to produce a similar geochemical effect involving a precipitation of dissolved As onto biogenic sulfide minerals during biogenic sulfate reduction. Dissolved As can thus be removed by sorption or coprecipitation with amorphous to crystalline Fe-sulfides formed during sulfate reduction. Geochemical modeling conducted by Lee et al. (2005) on similar geochemical condition, but without including thermodynamic data for the arsenian pyrite solid solution, showed that metastable intermediate Fe-sulfide phases like mackinawite, and pyrrhotite are eventually replaced by more stable pyrite. Thus, formation of arsenian pyrite predicted by the geochemical model agrees well with the observed occurrence of As-bearing biogenic pyrite (containing 1 to 6 wt. % As) in As-contaminated groundwaters of Bangladesh and USA under reducing conditions.

4. 3. Arsenic sorption experiments

Batch sorption experiments were conducted to gain an understanding of the As mobility in sulfate reducing conditions, and XRD study of solid reaction products were also conducted. Because results of geochemical processes occurring during bioremediation in the field cannot be directly observed, these experiments were planned

to observe formation of Fe-sulfide phase like arsenian pyrite and pyrite in reducing As-contaminated groundwater during biogenic sulfate reduction. In addition, the field groundwater geochemical conditions were simulated in the laboratory batch experiments to study the hypothesized sorption of As onto Fe-sulfide. A detailed descriptive explanation of experimental approach is found in Chapter 3.

4.3.1. Sorption of arsenic onto iron sulfide

Immediately after mixing desired solution of sodium disulfide and iron sulfate in the batch tube, black iron monosulfide precipitated. Acid decomposition of $\text{Na}_2\text{S}\cdot 9\text{H}_2\text{O}$ generates H_2S (Rickard and Luther, 1997) and thus under reducing conditions H_2S produced reacts with aqueous iron to form iron monosulfide as a black precipitate. This upon aging transforms into mackinawite (Berner, 1964; Benning et al, 2000). A spike in pH and drop in Eh values were observed after the beginning of the experiment in the excess-sulfide batch solution (Fig. 4.6). H_2S produced in the batch from chemical reaction between sulfide (S^{2-}), released during the dissociation of Na_2S , and H^+ in the solution apparently caused the observed pH and Eh values. Laboratory sulfate reduction conducted to investigate As removal mechanism by Keimowitz et al. (2007) also reported similar changes in pH and Eh values. Such striking change in pH and Eh values are not likely to develop in natural groundwater systems. However, over the time of two weeks these values again dropped down to a lower level, yet still do not correspond to the near-neutral pH and moderately reducing natural groundwater conditions.

Sulfide-limited batch solutions exhibited little change in pH and Eh values compared to excess-sulfide experiment. The changes in pH and Eh values in the

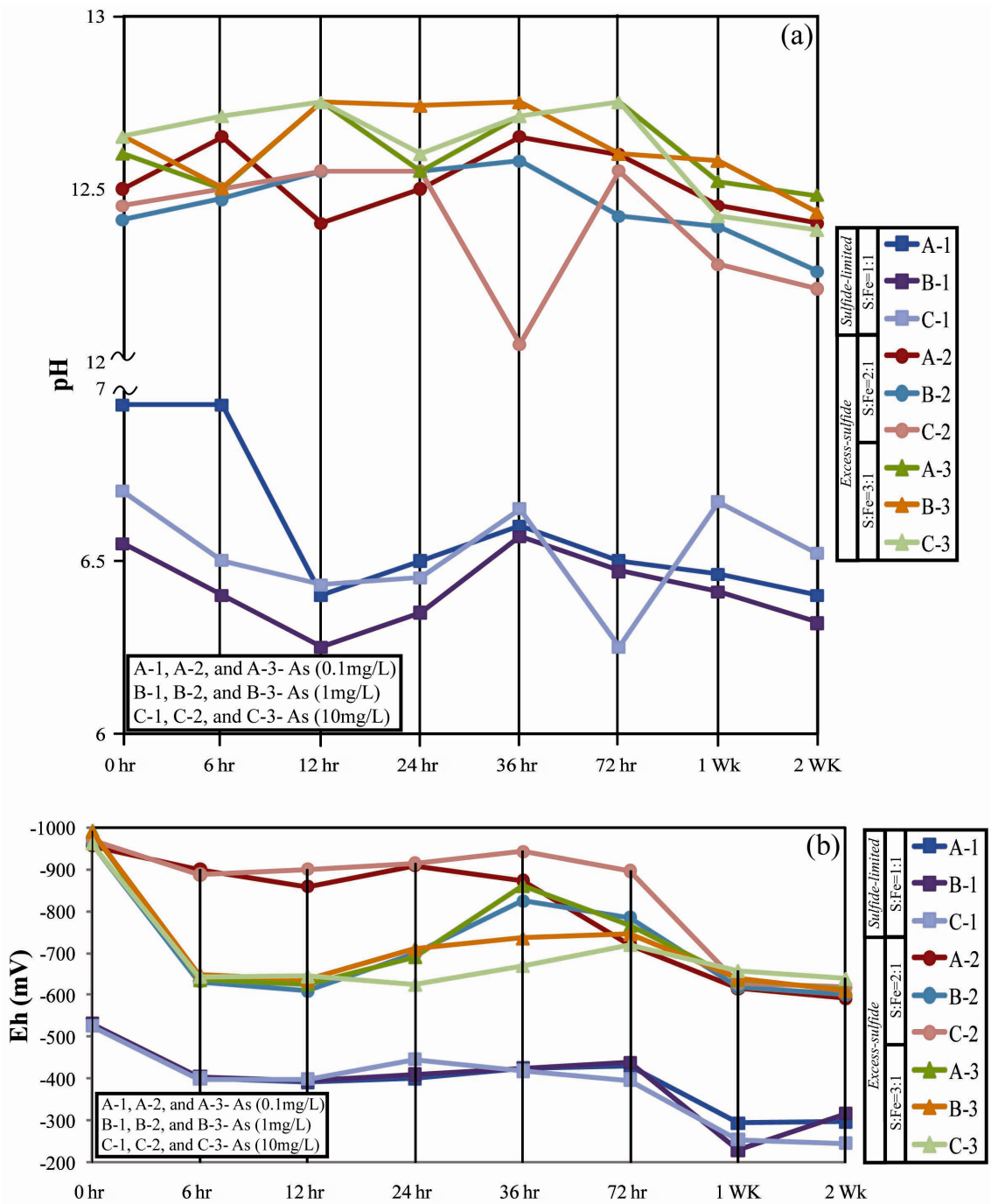


Fig. 4.6 Plot showing changes in pH (a) and Eh (b) recorded from the batch experiment. Sulfide-limited experiment with 0.1 mg/L of As concentration shows slight drop in pH and slight increase in Eh. Excess-sulfide samples recorded increase in pH and a drop in Eh compared to the beginning of the experiment (pH 7 and Eh= ~+55 mV). However, Eh value in the sulfide-excess case drops down substantially at the end of two weeks.

sulfide-limited experiment was from neutral (pH=7) to 6.5 and oxic (Eh=+55) to reducing (-200 to -400mV), respectively (Fig. 4.6). In such reducing environments and circumneutral pH conditions, formation of HS⁻ is not likely and H₂S oxidation pathways dominate the system (Rickard, 1997). However, due to increased ionization in an alkaline environment, as observed in excess-sulfide experiments, H₂S present in the specimen must either be in a dissolved state or HS⁻ dominates the system. In addition, Wilkin and Barnes (1996) proposed that thiosulfate is the dominant sulfate species at neutral to slightly alkaline solution, and is found unreactive with iron monosulfide; hence, formation of pyrite is favored at acidic to neutral pH and gradually tends to decrease towards alkaline pH (Wilkin and Barnes, 1996). In contrast, sulfide-limited experiments were apparently H₂S limited and did not yield much crystalline Fe-sulfide compared to excess-sulfide solutions which occurred at extremely reducing conditions and higher pH.

Possible two mechanisms proposed in the earlier studies that are responsible in the formation of Fe-sulfide crystals are: a) imperfections developed in Fe-sulfide after the sorption of As, perhaps served as direct pyrite nucleating sites (Wolthers et al., 2007), and b) the presence of dissolved H₂S aided in the transformation of amorphous Fe-sulfide formed at the beginning to crystalline Fe-sulfide such as pyrite (Berner, 1964; Rickard, 1975; Wilkin and Barnes, 1996). Alternatively, in the absence of reactive surface sites on Fe-sulfide after they were completely covered by sorbed As, Fe-sulfide probably transforms into marcasite and pyrite on aging (Wolthers et al., 2007). Arsenic sorbed onto Fe-sulfide can be considered stable in the conditions mentioned above.

Still, based on similar studies carried out in the past, simply observing the changes in pH and Eh in the batch experiment conducted in this research does not yield a definitive conclusion on the exact mechanism of As uptake in such extreme conditions.

Irrespective of the dramatic change in pH and Eh of the batch solution, which was believed to reduce the As sorption onto Fe-sulfide, about 91% of the initial As (0.1mg/L) in the solution was sorbed by the solid Fe-sulfide formed in the sulfide- limited experiments. In case of high As concentration (10 mg/L), 55% of initial As was sorbed by Fe-sulfide. In excess-sulfide experiments, about 79% and 48% of the initial As was sorbed from 0.1mg/L and 10mg/L solutions, respectively (Fig. 4.7, and lab data on “Appendix 2”). Amounts of As sorbed onto solid Fe-sulfide phases produced from the sulfide-limited and excess-sulfide conditions in our batch experiments is consistent with the finding from a study conducted by Wothers et al. (2007) in similar S:Fe stipulation to investigate sorption of As and its effect on Fe-sulfide transformation. Sorption of As onto Fe-sulfide increased continuously during the period of two weeks (Fig. 4.7). Results of batch experiments indicate that equilibrium time for As sorption onto fresh prepared Fe-sulfide is less than or equal to 6 hours. At the end of day seven (1 week), a slight drop in As sorption was observed, but As sorption continued again not long after. Constantly decreasing aqueous As from the solution throughout the experimental time frame indicates continual sorption of As by amorphous Fe-sulfide and possibly by pyrite that is formed at the later phase of the experiment (Fig. 4.8).

In almost all batch solutions prepared at lower concentration of As (0.1mg/L) and 1:1 sulfur to iron ratio, crystalline Fe-sulfide phases were not observed. Few samples prepared at higher concentration of As (1 and 10 mg/L) in sulfide-limited conditions and

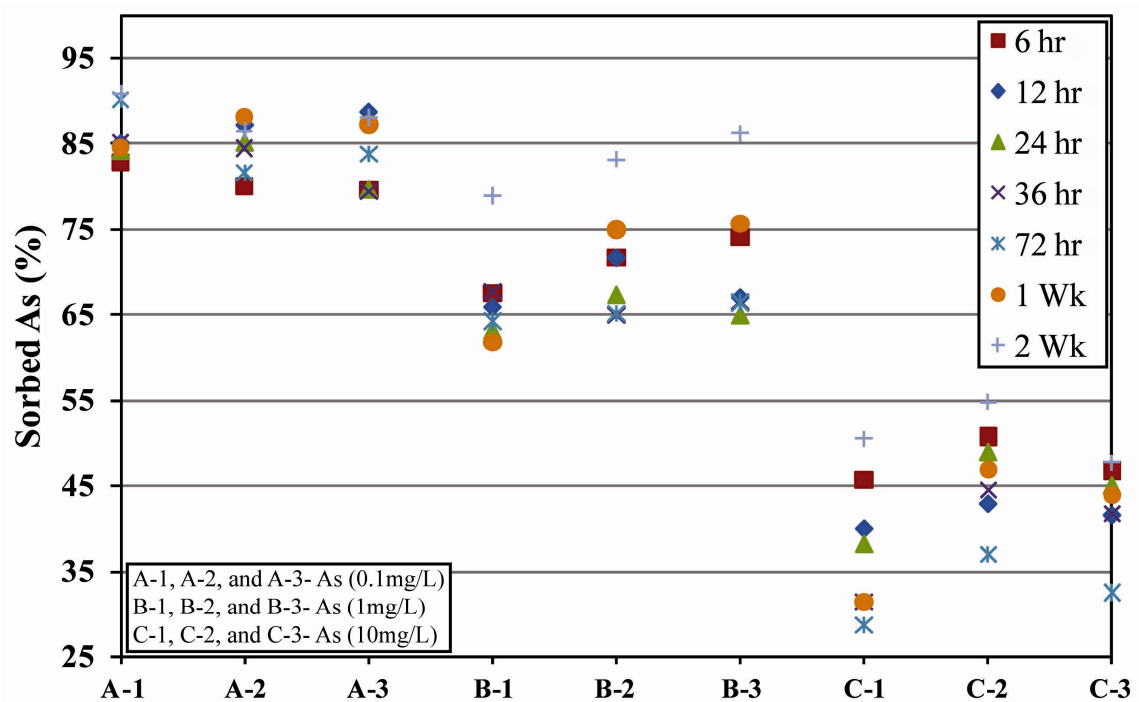


Fig. 4.7 Plot showing percentage of As sorbed onto Fe-sulfide in the laboratory batch experiment. Number after the letter in the sample number indicates the ratio of sulfur to iron (e.g., 1=1:1, 2 indicate=2:1, and 3=3:1, sulfur to iron ratio, respectively).

matured for two weeks yield marcasite and other unidentified crystalline Fe-sulfide (Fig 4.9 b and Fig. 4.10). One sample prepared from sulfide-limited batch solution exhibited framboidal structure that very much resembles authigenic pyrite (Fig. 4.8e). However, XRD could not establish its identity. Excess-sulfide samples prepared with high As concentration (1 mg/L and 10mg/L) showed the presence of a wide range of Fe-sulfides minerals (Fig. 4.8 and Fig.4.9). Generally, all samples extracted before 72 experimental hours showed the presence of mackinawite, but as the sample aged to 1 to 2 weeks, marcasite (Fig. 4.8 a and b), cubic pyrite (Fig. 4.8 c and d), troilite (Fig. 4.9d), and other unidentified Fe-sulfide (?) minerals were observed with minor amounts of mackinawite and HFO. Various forms of Fe-sulfide recorded in this study are shown in Fig. 4.9.

Nearly all of the samples that produced crystalline phases under reflecting microscope were studied by XRD to characterize their mineralogy. XRD results provide evidence of solid phase bulk transformations of Fe-sulfide minerals from amorphous to crystalline phases (Fig. 4.10) that were formed in the batch experiment. Due to time constraints, planned X-ray absorption near-edge structure (XANES) and expanded X-ray absorption fine structure (EXAFS) on these pyrite crystals were not conducted. Thus, interpretation of the exact mechanism of As incorporation into these Fe-sulfide phases should be the basis of future research.

As observed by many researchers, iron monosulfide or mackinawite is the first Fe-sulfide precursor to form in sulfate-bearing reducing groundwater environment (Rickard and Luther, 1997; Benning et al., 2000; Butler and Rickard, 2000; Wolthers et al., 2005 a

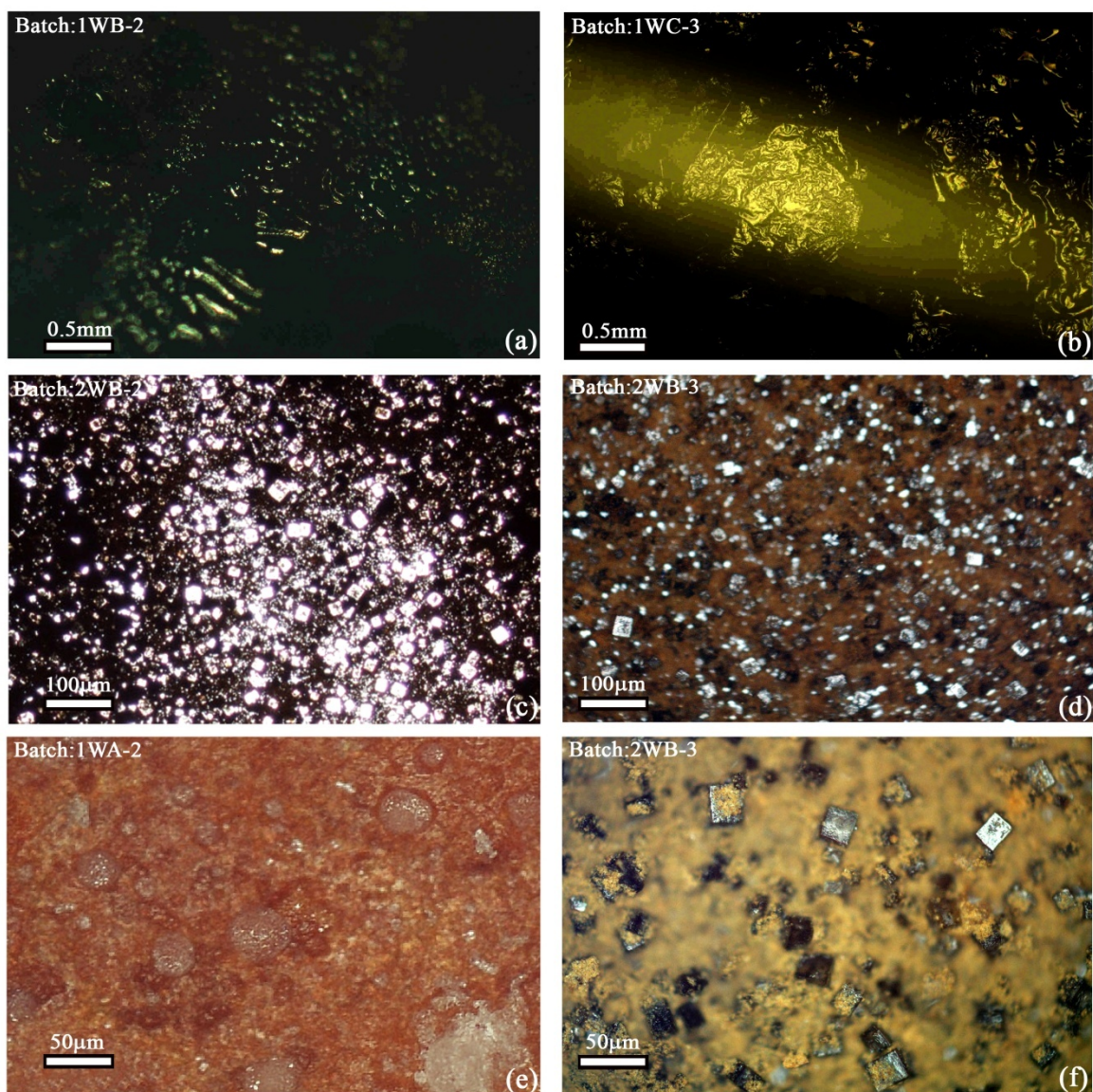


Fig. 4.8 Images of marcasite (a, and b), and pyrite (c, d, e, and f) taken under reflected light microscope that are formed in the batch experiment. Pyrite observed in figure c, d and f are cubic whereas framboidal structure is observed in the sample shown in figure e (unidentified). Black (a, b, and c) and dark brown to light yellow (d, e and f) precipitate seen in the background is mackinawite and HFO respectively. Mineral identification is based on XRD results (Fig. 4.10).

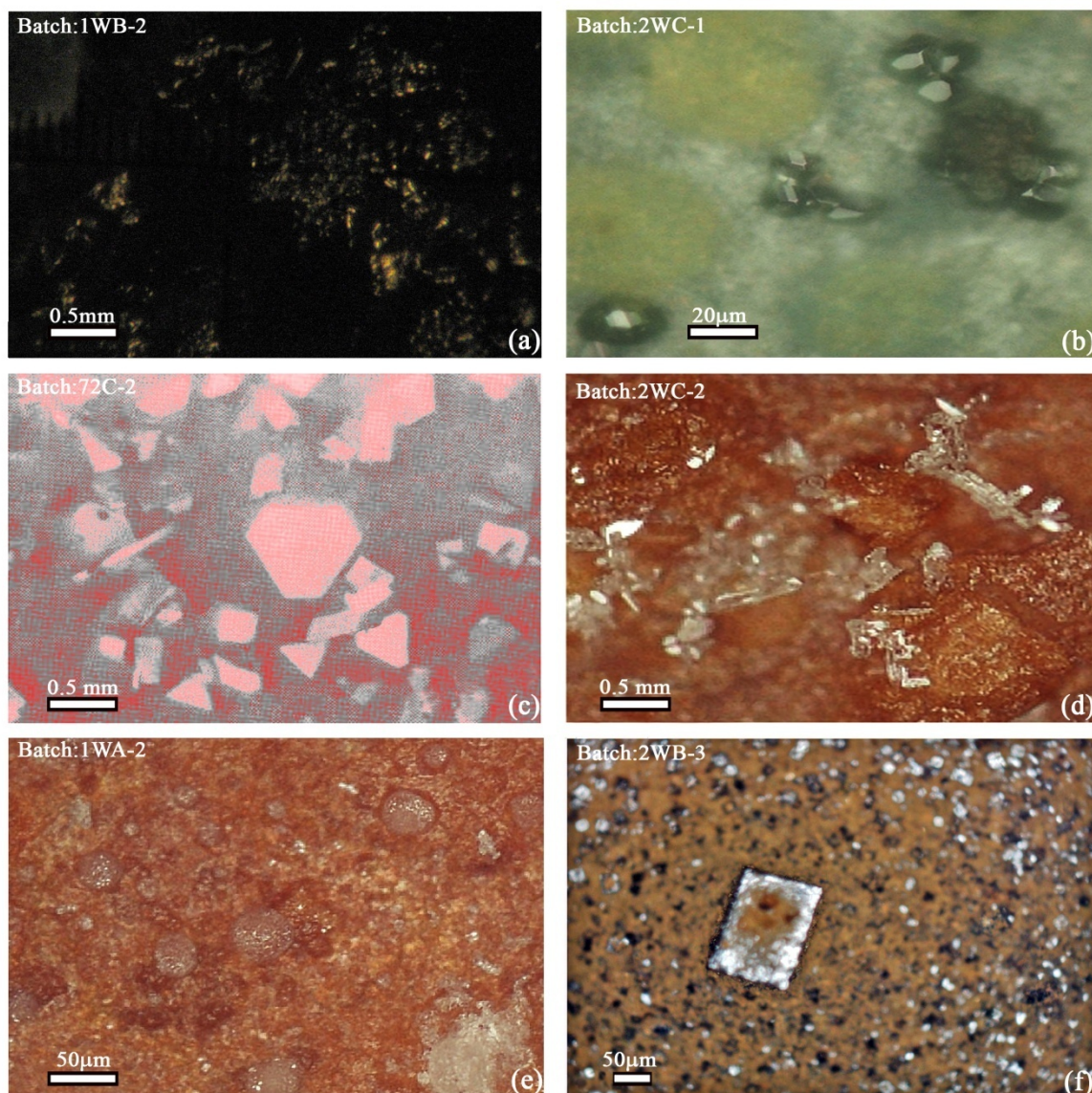


Fig. 4.9 Images of different Fe-sulfide minerals formed in the batch experiment. Limited batch samples produced well developed crystallographic minerals, especially those prepared in sulfide-excess condition. Such minerals were not observed in sulfide-limited experiment. (a) marcasite; (b), and (c) Fe-sulfide (unidentified); (d) euhedral grain of synthetic troilite; (e) framboidal pyrite (?), and (f) pyrite. Unless indicated, identification of these minerals is based on XRD results (Fig. 4.10).

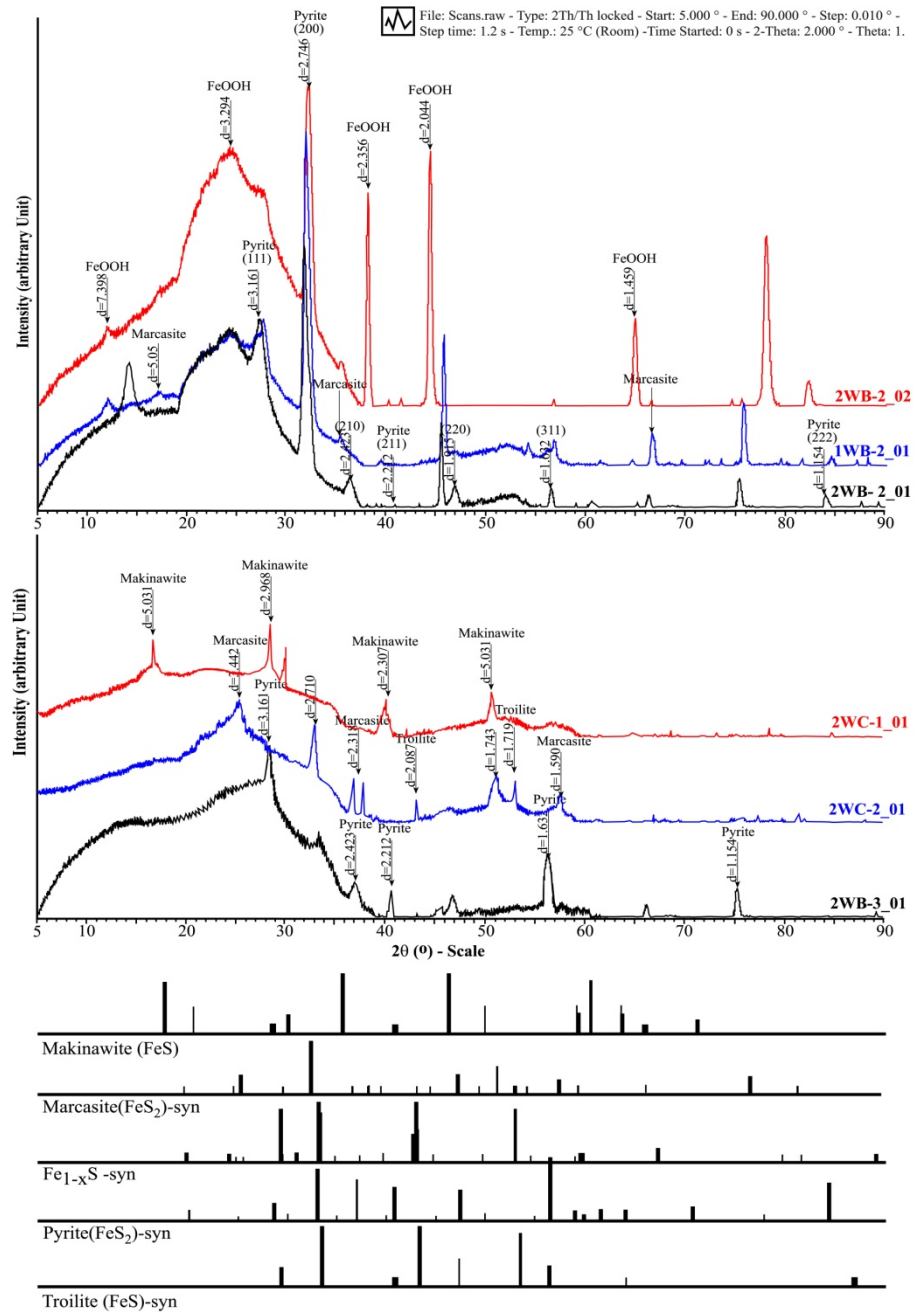


Fig. 4.10 Plots of XRD spectra observed at the same arbitrary scale for the end products of the batch reacted with various As concentrations in sulfide-limited and excess-sulfide experiments. Reference spectra for mackinawite, marcasite, pyrrhotite, pyrite and troilite are shown as solid lines at the bottom of the figure. Almost all samples aged below 72 hr, regardless of As concentration and sulfide ratio, indicate that mackinawite and marcasite were the most dominant Fe-sulfide phases. (similar to 2WC-1_01, and 1WB-2_01 samples). Few samples (matured for 1 to 2 weeks) prepared in excess-sulfide condition indicate the presence of various Fe-sulfide phases (mackinawite, marcasite, pyrite, and troilite) (1WB-2_01, 2WC-1_01, 2WB-2_01, 2WB-2_02, 2WC-2_01, and 2WB-3_01).

and c), which under certain geochemical condition transforms into pyrite (Schoonen and Barnes, 1991; Wilkin and Barnes, 1996; Rickard and Luther, 1997; Bostick and Fendorf, 2003; Wolthers et al., 2005b; Wolthers, et al., 2007). Formation of such Fe-sulfide phases is geologically important because Fe-sulfide is the most abundant sulfide mineral phase in marine as well as freshwater system (Rickard and Morse, 2005) and the transformation of such Fe-sulfide to arsenian pyrite has been interpreted as potential sinks for As in anoxic sediments (Bostick and Fendorf, 2003) (Table 2.1). Although arsenian pyrite and pyrite are commonly observed in the sedimentary geologic setting, laboratory confirmation of their genesis are lacking and often conflicting. In particular, laboratory studies involving Fe-sulfide genesis and aging in As-rich solutions (similar to natural conditions) are lacking.

In the beginning of this study it was assumed that most Holocene alluvial aquifers around the world containing elevated As were formed by the reductive dissolution of As-rich HFO (Nickson et al., 2000; Saunders et al., 2008). Under anoxic sulfate reducing conditions, in the presence of abundant soluble iron, Fe-sulfide may effectively remove As from the solution (Lee and Saunders, 2003; Lee et al., 2005; Keimowitz et al., 2007; Dhakal et al., 2008; Saunders et al., 2008). Enhanced sulfate reduction could offer an *in situ* As removal technique that causes a large proportion of dissolved As in the solution to sorb and coprecipitation with Fe-sulfides. Results of the sulfate reduction experiment conducted in this study in a similar environment to that of natural groundwater conditions provides strong evidence to support the implication.

4.3.2. Pyrite adsorption experiment

Batch experiments were performed to investigate the magnitude of As adsorption onto the surface of pyrite in a controlled environment where certain variables could be controlled or adjusted. The intent of these experiments was to develop a predictive understanding of the uptake of As by pyrite surfaces and quantify the magnitude of the sorption. The processes of As sorption onto pyrite occurs through the formation of outer sphere complexes (Farquhar et al., 2002). Pyrite has been proposed to be the most stable As sink in reducing groundwater conditions, and all the studies carried out in the past have utilized unisize pyrite crystals. Different crystals sizes were used in this study to quantify the amount of As adsorption depending on grain size (and thus surface area).

This study examines the effect of time, concentration, adsorption sites, and pH on As adsorption onto pyrite. The pH is the main factor in controlling the fate of As in solution; most of the natural groundwaters contaminated by As have near-neutral pH (Smedley and Kinniburgh, 2002; Saunders et al., 2005a, and b). Thus, batch experiments conducted for this study were conducted at neutral pH and effect of As concentration on different amount of available adsorption sites were investigated. A kinetic experiment was conducted in the beginning to determine the equilibrium time, and thus establish time limits for subsequent experiments. Finally, an isotherm was measured in order to determine the effect of concentration on As adsorption.

4.3.2.1. Adsorption kinetics

An adsorption rate experiment was carried out on the pyrite crystals to determine the equilibrium time for the As sorption to occur. Three different crystal sizes of pyrite

were used; fine, intermediate and coarse (grain size classification is discussed in detail in Chapter 3) was separately used for the batch experiment. The pyrite was prepared after crushing, sieving, and washing it first with 0.5M HNO₃ and then by DIW, drying them on a hot air, and finally it was stored in the O₂-free N₂ chamber. Batch experiment was conducted using three different pyrite grain sizes, each sample weighted 0.3 gm, and was treated with three different (0.1 mg/L, 1 mg/L and 10 mg/L) As concentration in a 50 ml low-density polyethylene centrifuge tube for 72 hours before the batch solution was filtered for As analysis. Adsorbed concentration of As was measured by subtracting the amount of As in the solution from the initial concentration. Blank solutions were measured in parallel to ensure the reliability as well as quality of the experiment. Maximum changes in pH value after the beginning (pH=7) of the experiment was less than 9%, which was considered insignificant fluctuation in pH to cause major shift in the adsorption value.

Rapid adsorption occurred during the first 6 hours in all the adsorption batch experiments. Experiments that used a solution of 0.1 mg/L As showed 42-82 % As adsorption. Experiments with 1 mg/L and 10 mg/L of As resulted 4-28%, and 1-5% of As adsorption, respectively. Lower As adsorption was observed in the coarse-grained pyrite, which implies adsorption is dependent on surface area and number of adsorption sites. The smaller the crystal size of pyrite, the more adsorption sites are available, and thus more As is adsorbed. Much slower adsorption was observed after 12 hours and aqueous phase As concentration were almost constant after approximately 24 hours (Fig. 4.11).

Regardless of As concentration or size of pyrite used for the experiment, a plateau in As adsorption onto pyrite crystals was established at 24 hr (laboratory results tabulated in “Appendix 3”). As a result, the time span of 24 hour was chosen as an equilibrium time span for As sorption onto pyrite, and all batch experiment conducted to study the adsorption of As on pyrite were then fixed at 36 hr.

4.3.2.2. Adsorption Isotherms

Fig. 4.12 graphically shows the adsorption of As on different grain sizes of pyrite at constant pH. Adsorption of As increased with increasing arsenic concentration rapidly onto the solid pyrite. The initial trend of increase in aqueous phase concentration is proportional to the increase of As in solid phase (Fig. 4.12). With increasing soluble As concentration, adsorption sites are rapidly occupied and adsorption can no longer be sustained.

This non-linear trend indicates that there is not only a decrease in As adsorption capacity of the pyrite with increase in As concentration, but also that pyrite adsorption capacity is dependent on the amount of surface area. Therefore, experimental data approximate the Langmuir isotherm, which is typical of solute adsorption where the total concentration of adsorption sites cannot be completely occupied. Average As adsorption onto fine-grained pyrite crystal is relatively higher (7.12 $\mu\text{M}/\text{gm}$ of pyrite) than adsorption on coarse-grained pyrite crystals (3.4 $\mu\text{M}/\text{gm}$ of pyrite; Fig. 4.12, and laboratory data on “Appendix 4”). However, more As can be adsorbed if pH of the solution is raised, as arsenic adsorption onto pyrite is pH-dependent and would increase if pH is increased (Bostick and Fendorf, 2003).

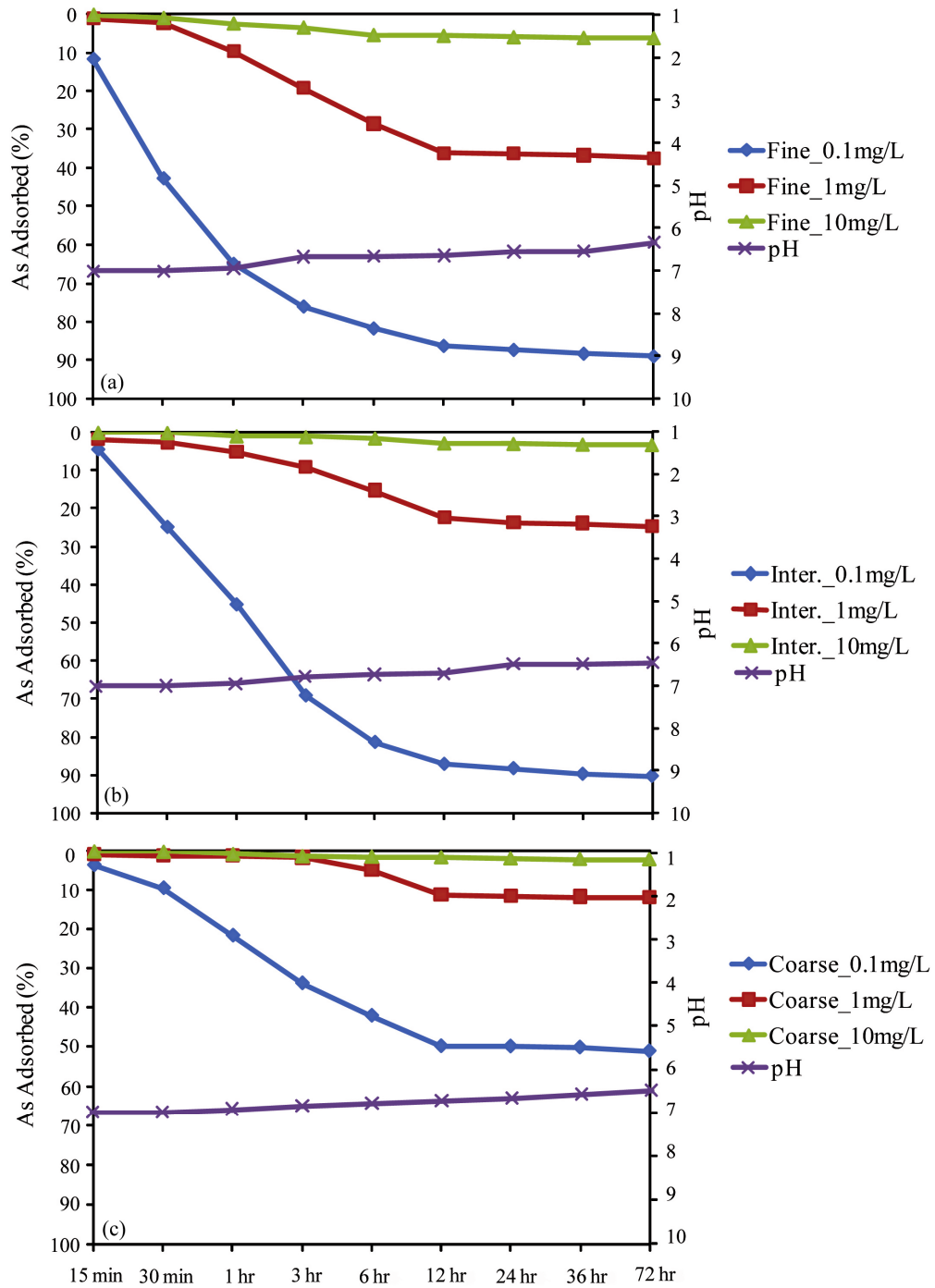


Fig. 4.11 Graphical plot prepared from the test experiments conducted to calibrate equilibrium adsorption time for fine-(a), intermediate-(b), and coarse-(c) grained pyrite crystals as a function of time. Batch experiment was prepared with different arsenic concentration (0.1 mg/L, 1 mg/L, and 10 mg/L) at solid/solution ratio=6 gm/L. At the end of the experiment pH value of the solution dropped about 7 to 9 % compared to the original neutral pH. Equilibrium adsorption was reached at about 24 hours.

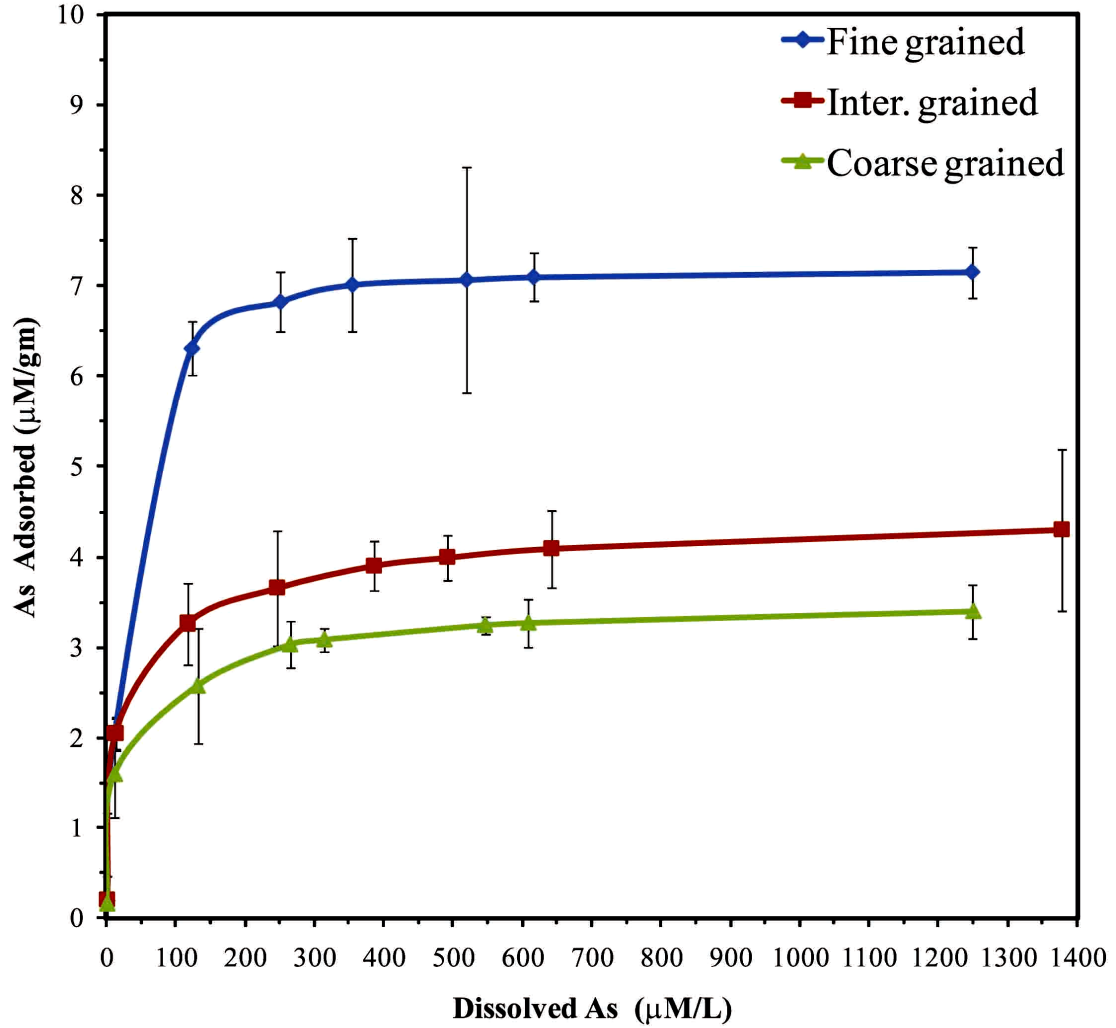


Fig. 4.12 Plots of adsorption isotherm of As on 6 gm/L of pyrite at neutral pH. The lines are the Langmuir isotherm fits for the entire data set. Coefficient of determination, r^2 for the best logarithmic fit on the dataset presented here are 0.9468, 0.9838, and 0.9861 for fine-, intermediate-, and coarse-grained samples, respectively. Vertical bars represent the value of standard deviation in the data.

4.3.2.3. Adsorption envelopes

The adsorption envelopes (% adsorbed versus pH at constant As concentration) graphically show the importance of pH on adsorption potential of an adsorbing media. In this study, adsorption pH envelopes were developed to graphically display the variation observed in As adsorption for the various crystal size of pyrite. The adsorption percentage of As on different grain size of pyrite surfaces plotted against pH for three different As concentrations (0.1 mg/L, 1 mg/L, and 10 mg/L) is shown in Fig. 4.13. In the experiment, 50ml solution was prepared using different arsenic concentration with 0.3gm of pyrite crystals. Ionic strength was balanced using 0.01M NaNO₃, and initial pH was balanced using either 0.1M HNO₃ or 0.1M NaOH. All the samples were then allowed to equilibrate for 36 hours.

The pH effect is clearly depicted in the sorption isotherm for pyrite. At lower pH (less than 6) As adsorption is less than 21%. Dramatic increase in As adsorption (up to 98%) with increasing pH indicates the As adsorption onto pyrite surface is pH dependent. These results are consistent with the results of arsenite [As (III)] adsorption onto pyrite, shown in the study carried out previously by Bostick and Fendorf (2003). It is also observed that with decrease in surface area of pyrite crystal there is simultaneous decrease in As adsorption. This experiment, which was conducted under reducing conditions, probably kept As (III) (that was used as a source of As) from oxidizing to As (V). Arsenic adsorption onto pyrite observed in this study and a study carried out by Bostick and Fendorf (2003) is distinctly different from other studies (Pierce and Moore, 1982; Dzombak and Morel, 1990; Hsia et al., 1994) conducted to study As adsorption onto HFO. Arsenic sorption by a HFO is generally interpreted as a 'double layer' model,

when HFO exhibit maximum adsorption at near-neutral pH and least adsorption at high pH (Pierce and Moore, 1982; Dzombak and Morel, 1990; Hsia et al., 1994).

Anion adsorption onto HFO occurs essentially through ligand exchange of surface hydroxyl groups with an anion in solution (Anderson et al., 1976) similarly, anion adsorption in sulfide mineral surface is proposed through the exchange of surface hydroxyl groups (Balsley et al., 1998). At lower pH (<7), H_2AsO_4^- is dominant aqueous arsenic species (Fig. 2.1 and Fig. 4.2). At higher pH concentration of H^+ in the solution decreases and the HFO surface become increasingly more negative which results in desorption of HAsO_4^- and AsO_4^{3-} that are dominant aqueous arsenic species at $\text{pH}>8$. Observed pH-dependent adsorption of As onto metal sulfides observed in Fig. 4.13 does not follow electrostatic (outer sphere) adsorption (Farquhar et al., 2002). Steep adsorption slope from pH 4 to 6 observed in Fig. 4.13 (data on “Appendix 5”) shows rapid adsorption of As onto pyrite. Adsorption of As onto pyrite is remains constant at higher pH (>6). A study carried out to investigate As desorption from pyrite by Bostick and Fendorf (2003) also depicted similar graph showing deep lag in desorption at similar pH (4 to 6) values, and suggested that a slow process more compatible with the formation of strong, inner sphere complexes. Bostick and Fendorf (2003) suggested from an XANES study that arsenite is adsorbed to pyrite by forming ‘arsenopyrite-like’ surface precipitates.

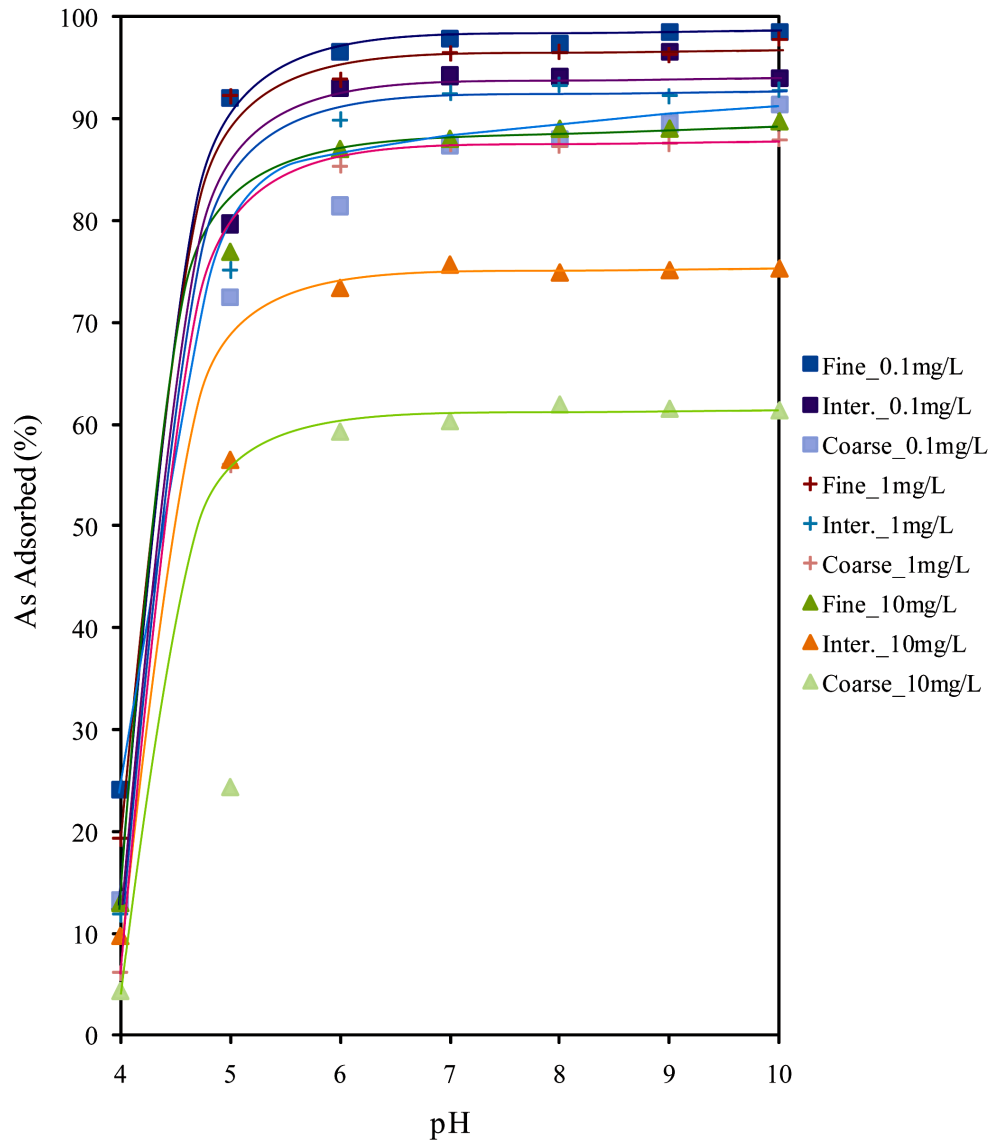


Fig. 4.13 Plot showing As adsorption per unit mass adsorbent as a function of pH for fine, intermediate, and coarse grained pyrite crystals for different amounts of added arsenic concentration (0.1 mg/L, 1 mg/L, 10 mg/L). Concentration of pyrite is 6 gm/L and equilibrium time is 36 hr. Lines connecting the values in the figure represent the best fit curve and standard error in the fit is ignored.

4.4. Role of arsenic-bearing pyrite in arsenic removal: discussion

As described above and shown by Lee and Saunders (2003), and Saunders et al. (2005c), injection of organic carbon into the groundwater as a source of carbon first stimulates biogenic Fe-reduction. When geochemical conditions become more reducing and Fe-reduction ceases, the presence of sulfate in the groundwater allows the initiation of biogenic sulfate reduction (Lee and Saunders, 2003; Saunders et al, 2005c).

Apparently, biogenic sulfate reduction can only proceed after the depletion of ferric hydroxide phases that serve as electron acceptor for anaerobic FeRB. Chapelle and Lovley (1992) and Lovley and Chapelle (1995) showed that there is more energy to be derived from Fe-reduction than sulfate reduction, and that FeRB and SRB compete with each other in anaerobic groundwater for electron donors (e.g., organic carbon).

Conversely, the presence of both viable FeRB and SRB in naturally As-contaminated groundwater is typical (Kirk et al., 2004; Saunders et al., 2005a). Data from the field demonstrate that the indigenous SRB in the As-contaminated aquifer are capable of anaerobically catalyzing sulfate reduction. In batch experiments, the overall trend was towards progressively more reducing conditions with time as indicated by the Eh data, which makes it possible for formation of relatively insoluble Fe-sulfide. Arsenic-rich Fe-sulfides formed as a consequence of sulfate reduction apparently sorb significant amounts of soluble As, which under reducing conditions continues to sorb As and eventually transforms into more stable sulfide minerals like pyrite and arsenian pyrite, these phases can sequester As more firmly than amorphous Fe-sulfide.

Extensive documentation in the literature supports pyrite is a very common authigenic mineral that forms under sulfate-reducing conditions, provided that ample sources of Fe and sulfate are available (Morse et al., 1987). In As-rich environments, the pyrite is kinetically inhibited as a direct precipitation under sulfate-reducing conditions (Wolthers et al., 2007), and typically amorphous Fe-S phases form initially, which in presence of H₂S invert to pyrite (Morse et al., 1987). In anoxic marine sediments of the Gulf of Mexico, Huerta-Diaz and Morse (1992) found that Fe-sulfides (amorphous FeS and pyrite) incorporate trace elements such as As, Co, Ni, and Mo into pyrite and acid volatile sulfide phases (volatize in strong acid). Similarly, Saunders et al. (1997) documented arsenic, and to a lesser extent Co and Ni, were incorporated into authigenic biogenic pyrite in a Holocene alluvial aquifer in central Alabama under sulfate reducing conditions. As-rich pyrite (Fig. 2.7) obtained from a Holocene alluvial aquifer described by Saunders et al. (1997) and Southam and Saunders (2005) was formed during replacement of wood fragments. Sulfur isotopic studies conducted on the As-rich pyrite crystals indicate that SRB were responsible for its formation. Pyrite $\delta^{34}\text{S}$ values are isotopically light as expected as a consequence of bacterial sulfate reduction. Pyrite is also zoned with respect to As content, and electron microprobe analyses show that individual zones contain up to 1 wt. % of As. More recently, ion microprobe analyses confirmed that isotopically lightest sulfur in core of the pyrite grain corresponds with highest As content (Saunders et al., 2005a), and laser ablation ICP-MS study confirms the coexistence of Fe-S-As in the sample (Dhakal et al., 2007).

Discovery of As-bearing pyrite in natural As-contaminated groundwaters in West Bengal, India (Archaryya and Shah, 2007), Bangladesh (Nickson et al., 2000; Lowers et al. 2007), and in a Holocene alluvial aquifer in USA (Saunders et al., 1997; Southam and Saunders, 2005) suggest that arsenian pyrite is a principal authigenic sulfide phase in such identical geologic environments. Yet others have tentatively documented orpiment and realgar as the dominant As-sulfide species at one site where anthropogenic As contamination occurs (O'Day et al., 2004). In absence of XRD data, confirming the presence of realgar (e.g., O'Day et al., 2004) requires further documentation. In addition, some studies carried out to investigate As uptake by various Fe-sulfide minerals have shown the formation of various As solids including orpiment (Farquhar et al., 2002) and realgar-like phase (Gallegos et al., 2007). Laboratory and geochemical modeling data from this study, however, support that arsenian pyrite as an important final As-Fe-S mineral phase in iron-bearing, anoxic groundwater settings, although such As-rich pyrite may have transformed from intermediate Fe-sulfide such as mackinawite, and marcasite that formed initially. In absence of dissolved iron, sorption and coprecipitation of As is apparent in realgar-like phases from pH 5 to pH 9 (Gallegos et al., 2007). Considering the natural abundance of iron in nature, formation of realgar or orpiment in natural groundwater at near-neutral pH appears inconsistent with new thermodynamic data on arsenian pyrite solid solutions determined as part of this study.

Field data observed during this study, along with the data of others cited above, coupled with results of geochemical modeling that includes thermodynamic data for As-bearing pyrite and laboratory studies presented here, show that As-bearing pyrite is the most important solid Fe-sulfide phase that sequester As from solution under

sulfate-reducing condition in natural groundwater. Oxidation of As-bearing sulfides can cause natural As-contamination locally (Welch et al., 2000; Smedley and Kinniburgh, 2002). However, in Holocene alluvial aquifers, As-bearing pyrite is a sink rather than a source of As (Saunders et al., 2005a; Lee et al., 2005). The inverse relationship noticed between As and sulfate in groundwater of Bangladesh (Nickson et al., 2000; Smedley and Kinniburgh, 2002) reflects the fact that a lack of dissolved sulfate in groundwater limits the metabolism of SRB (Chapelle and Lovley, 1992) and thus limits As immobilization (Kirk et al., 2004).

The actual mechanism implicated in removal of As by Fe-sulfides have been studied previously, but results have been inconclusive. Assuming Fe-sulfide phases precipitate first as a consequence of biogenic sulfate reduction and that pyrite is the thermodynamically favored phase under most situations, questions still persist about how As is incorporated into these phases to make arsenic-bearing pyrite. There is a general agreement that arsenic is sorbed to surface of Fe-sulfides phases under reducing conditions where such sulfides are stable (Farquhar et al., 2002; Wolthers et al., 2005c; Wolthers et al., 2007). On aging, initially formed Fe-sulfide may incorporate sorbed As into the growing crystal lattice of pyrite and other Fe-sulfide by replacing sulfur (Savage et al., 2000), and taken together (e.g., sorption, crystal growth), these processes can be called “coprecipitation”. From the present study it appears that pyrite typically forms with ~1 wt. % of As under reducing conditions where there is sufficient dissolved Fe, As, S and an organic carbon source to drive biogenic sulfate reduction. Arsenopyrite was synthesized in the laboratory by Morimoto and Clark (1961), and Rittle et al. (1995) in a biogenic sulfate reduction experiments conducted in a Fe-As-S system using SRB.

Because of the abundance of iron in the crust, it is likely As-Fe-sulfides will be the predominant As phases forming under reducing conditions. Additionally, a study conducted on As replacement of sulfur in pyrite, Reich and Becker (2006) theoretically proved pyrite solid solutions can incorporate up to 6 wt. % of As at room temperature (Table 2.1), whereas beyond this concentration As and Fe-sulfide reacts to form arsenopyrite. Evidence of As-rich pyrite containing up to 8 wt. % of As was reported by Fleet et al. (1989) from a gold mine, and the solution energy that were calculated by density functional theory (DFT) showed prevalence of As-rich pyrite with 10 wt.% of As (Blanchard et al., 2007) (Table 2.1). But optimum amount of As that can be incorporated into pyrite at normal temperature (25°C) that is reported by Reich and Becker (2006) seems more consistent with the results of geochemical modeling in this study. Structural differences between pyrite (cubic) and arsenopyrite (FeAsS, orthorhombic) or löllingite (FeAs₂, orthorhombic) (Lowers et al., 2007) presumably cause a lack of extensive solid solution between the phases (Reich and Becker, 2006). The highest As concentrations in pyrite may represent metastable solid solutions, but in other cases, As is incorporated within the pyrite lattice by atomic substitution (Savage et al., 2000).

Results of field bioremediation experiments (Saunders et al., 2008), and laboratory batch experiments of this study (and recent laboratory investigations by Keimowitz et al., 2007) suggest that As is removed under sulfate-reducing conditions when the SRB are actively metabolizing. However, the exact mechanism of As removal during sulfate reduction and Fe-sulfide formation is still not well documented. Perhaps the formation of an As-Fe-S phase like that observed by Rittle et al. (1995) could explain As removal from solution, but more likely sorption of As on Fe-sulfide phases made during SRB

metabolism occurs. Eventually, at the latter stage of aging of the initial Fe-sulfide phase, As could incorporate into the pyrite crystal lattice. In the Oklahoma experiment, after sulfate-reduction ceased and dissolved sulfate and iron increased late in the experiment (Fig. 4.1a), arsenic did not show a parallel increase in the groundwater. This result suggests Fe-sulfide phases made during biogenic sulfate reduction have some residual capability of removing As by sorption even though biogenic sulfate reduction has ceased. An X-ray absorption spectroscopy study conducted by Wharton et al. (2000) to investigate the behavior of technetium (Tc) and rhenium (Re) during subsequent oxidation of mackinawite coprecipitated with Tc and Re at the onset of reducing conditions, found that HFO evolved during oxidation continues to adsorb these elements even after sulfate-reduction has ceased. Beside residual capability of Fe-sulfide to sorb As even after the completion of biogenic sulfate reduction as discussed before, alternative mechanism responsible for long term As sorption is the adsorption process observed by Wharton et al. (2000) that continues after reoxidation of the host precipitate (Fe-As-sulfide) which not only sorb As in the beginning, but also continues to adsorb As onto HFO that forms by oxidation of biogenic Fe-As sulfide. In Bangladesh, our experiments were designed to first assess the results of adding labile organic carbon and sulfate, and then to investigate the effect of additional dissolved iron. In the beginning, As was not removed during biogenic sulfate reduction in Bangladesh experiment (Fig. 4.1b) as was observed in the Oklahoma experiment, but As levels returned to background levels over time. Problems still need to be addressed, but it is hoped that *in situ* bioremediation can be optimized to become an appropriate, inexpensive, technology for removing As from drinking water that are drawn from Holocene alluvial aquifers in southeast Asia.

CHAPTER 5

CONCLUSIONS

5. Conclusions

It has been postulated that *in situ* bioremediation techniques that involve injection of soluble organic carbon and sulfate into As-contaminated aquifers enhances microbial sulfate reduction leading to Fe-sulfide precipitation that apparently can effectively sorb and coprecipitate soluble As from solution. This approach potentially could be used on anthropogenically contaminated groundwater sites and possibly where As released during microbial-mediated reductive dissolution of HFO in Holocene floodplain alluvial aquifers occurs. It was also assumed that initially formed Fe-sulfide during biogenic sulfate reduction transforms into pyrite over time, and the new phases not only continue to sorb As from the solution, but also may immobilize As more efficiently than just surface sorption. The initial impetus of this work stemmed from the need for understanding whether or not arsenian pyrite is the likely stable mineral phase formed under anoxic, sulfate-reducing groundwater conditions, instead of pure As-S phases, and whether providing both electron donor and electron acceptor to bacteria could effect a practical remediation approach. Field and laboratory investigations conducted here present data supporting the formation of stable Fe-sulfide minerals phase that are responsible for sequestering As, and also demonstrate the details of geochemical process using thermodynamic modeling.

5.1. Specific research conclusions

1. A pilot-scale bioremediation experiment conducted in Blackwell, Oklahoma, showed a significant lowering of dissolved As and Fe after the beginning of biogenic sulfate reduction. Substantial decrease in As concentration compared to the initial levels occurring under Fe-reducing conditions is interpreted to be the result of sorption and coprecipitation of As on Fe-sulfide minerals formed by biogenic sulfate reduction. Results of the bioremediation experiment carried out in Manikganj, Bangladesh showed similar results. However, at the end of the initial Bangladesh experiment, it was found that a Fe-reducing condition returned in the groundwater and As increase back to pre-test levels. The exact explanation for the sudden change in geochemistry at the later phase of the experiment at Bangladesh is not yet fully understood. It is proposed that either depletion of organic matter or complete replacement of treated groundwater plume by fresh groundwater could be possible causes. Groundwater systems with high dissolved H₂S but low Fe content can enhance As mobility by forming thioarsenite aqueous complex (Lee et al., 2005), and thus can be implied as the third plausible explanation for the increase in As concentration at the end of the experiment in Bangladesh. However, that possibility is not likely due to the fact that Fe increased too.
2. Arsenian pyrite (FeS_{1.99}As_{0.01}) appears to be the most predominant Fe-As-S mineral formed in anoxic iron-bearing natural groundwater conditions. Reaction-path modeling conducted to trace As reactivity and precipitation in natural As-rich groundwater under sulfate-reducing condition appears to rule out the possibility that As-sulfide minerals like orpiment and realgar can form in such geological

conditions. However, formation of such species cannot be excluded in very specific conditions when high concentrations of As come from anthropogenic sources.

Geochemical modeling conducted using GWB included newly derived thermodynamic data for arsenian pyrite solid solution ($\text{FeS}_{1.99}\text{As}_{0.01}$ - $\text{FeS}_{1.90}\text{As}_{0.10}$) in this study is useful in characterizing and predicting As behavior in reducing iron-bearing groundwater.

- 3 In both sulfide-limited and excess-sulfide conditions mackinawite is the first precipitated iron monosulfide in batch experiment conducted as part of this research. Marcasite and pyrite were recovered from the batch experiment that ran longer than one week (confirmed by XRD studies). It is believed that such crystalline Fe-sulfide is formed on aging and transformation from the first precipitated Fe-sulfide. A few unidentified Fe-sulfides were also obtained during batch experiments. In low As concentration (0.1 mg/L), about 91% of the initial As concentration was sorbed onto Fe-sulfide, whereas up to 55% of initial As concentration was sorbed onto Fe-sulfide in the batch test prepared with high As concentration (10 mg/L). Continued low aqueous As concentrations observed for two weeks indicate uptake of As by amorphous Fe-sulfide, and more probably, by growing neo-formed pyrite. In absence of XANES and EXAFS studies that are commonly used to characterize surface and atomic structure of laboratory synthesized pyrite and other Fe-sulfide in this study, the exact mechanisms of As incorporation on those Fe-sulfide remains unclear. Thus, XANES and EXAFS studies are a worthy topic for future research.

4. Batch experiments conducted to investigate As adsorption onto pyrite revealed that As is very rapidly adsorbed onto pyrite at the beginning, and adsorption reached equilibrium in about 2 days. The adsorption isotherms indicate a non-linear sorption process. In fine-grained pyrite crystals, adsorption is more rapid compared to coarse-grained pyrite. Also, As adsorption is more complete in experiments with low As concentrations, but at higher concentration, less As is adsorbed. Thus, there is a possibility of desorption of As at higher concentration. Batch experiments that involves fine-grained pyrite crystals adsorbed $\sim 7.12 \mu\text{M/gm}$ of pyrite, which was significantly higher than for coarse-grained pyrite (about $3.4 \mu\text{M/gm}$ of pyrite). Adsorption of As onto pyrite is pH dependent (Bostick and Fendorf, 2003); therefore increase in arsenic adsorption is expected if pH of the solution is raised.
5. Results from the adsorption envelopes clearly depict sharp increases in As adsorption if pH is raised. Sharp adsorption of As is observed at pH above 6. This spike in As adsorption above pH 6 indicates optimum As adsorption onto pyrite at near-neutral pH. Bostick and Fendorf (2003) reported “arsenopyrite-like” surface precipitates when As is adsorbed onto pyrite. Assuming arsenian pyrite is formed during *in situ* bioremediation and biogenic sulfate reduction, arsenopyrite-like surface precipitate can develop if dissolved As is continuously adsorbed onto arsenian pyrite.

Finally, results from this study indicate that a decrease in dissolved As in groundwater during bioremediation is consistent with As sorption onto newly formed Fe-sulfide surfaces. This appears to result in the formation of arsenian pyrite with $\sim 1 \text{ wt. } \%$

of As, which has been observed under some documented field situations. Geochemical modeling conducted on iron-bearing, sulfate-reducing As-rich contaminated groundwater with new thermodynamic data for arsenian pyrite solid solution developed as a part of this study indicates that arsenian pyrite is thermodynamically more stable than pure As-sulfide under sulfate-reducing conditions. In this study, amorphous Fe-sulfide formed at the beginning of the laboratory batch experiment, upon aging, produced pyrite. The observed formation of amorphous Fe-sulfide followed by crystalline Fe-sulfide minerals in progressively reducing conditions strongly support our hypothesis that sorption and possibly coprecipitation of dissolved As onto stable Fe-sulfide minerals under sulfate-reducing conditions might be accomplished using indigenous SRB in groundwater contaminated with As.

5.2. Recommendations for future study

The findings presented in this work provide further support for the concept of simulating indigenous SRB to engineer *in situ* bioremediation, which could be an inexpensive, effective, and efficient As removal technique. Biogenic sulfate reduction is believed to produce nano-scale iron monosulfides with high surface areas that are effective in sorbing and coprecipitating As from solution. If the exact geochemical mechanisms of iron monosulfide inversion to more stable pyrite is better understood, then long term *in situ* As removal might be accomplished. Future work related to sequestering As from As-contaminated natural groundwater system that builds upon these studies could involve the following areas: a) refining the proposed bioremediation technique such for different geological and geochemical conditions by controlling material used

during bioaugmentation and integrating the factors like dynamic flow condition and groundwater geochemistry, and b) understanding exact mechanism on how Fe-sulfide transform into pyrite.

Further research needs to be done in quantifying optimum amount of As that can be removed during bioremediation. Possible desorption of As from the Fe-sulfide during the final phase of bioremediation needs clarification. However, conjecture from the results of the study conducted by Wharton et al. (2000) can possibly address what happens to the sorbed As if pyrite gets oxidized by lowering water tables in the field. Arsenic incorporated onto pyrite upon oxidation most likely does not release As, but incorporates into the HFO formed as a result of Fe-sulfide oxidation caused by lowering water table. However, subsequent reduction of HFO may re-mobilize As again. Additional research should also be undertaken to determine how well this carefully controlled laboratory synthesized pyrite can be formed in natural groundwater system. Further investigation can be conducted to study of the Fe-sulfide prepared in the lab in this study at a molecular level to understand structural bonding and geochemistry of these minerals.

REFERENCES

- Abraitis, P.K., Patraick, R.A.D., Vaughan, D.J., 2004. Variations in the compositional, textural and electrical properties of natural pyrite: a review. *Int. J. of Mineralogical Processes*. 74, 41-59.
- Acharyya, S.K., Lahiri, S., Raymahashay, B.C., Bhowmik, A., 2000. Arsenic toxicity of groundwater of the Bengal Basin in India and Bangladesh: the role of Quaternary stratigraphy and Holocene sea level fluctuation. *Environ. Geol.* 39, 1127–1137.
- Acharyya, S.K., and Shah, B.A., 2007. Arsenic-contaminated groundwater from parts of Damodar fan-delta and west of Bhagirathi River, West Bengal, India: influence of fluvial geomorphology and Quaternary morphostratigraphy. *Environ. Geol.* 52, 489-501.
- Ahmed, K.M., Bhattacharya, P., Hasan, M.A., Akhter, S.H., Alam, S.M.M., Bhuyian, M.A.H., Imam, M.B., Khan, A.A., and Sracek, O., 2004. Arsenic enrichment in groundwater of the alluvial aquifers in Bangladesh: An overview. *Appl. Geochem.* 19, 181–200.
- Anderson, M.A., Ferguson, J.F., Gavis, J., 1976. Arsenate adsorption on amorphous aluminium hydroxide. *J. Colloid Interface Sci.* 54, 391-399.
- Balsley, S.D., Brady, V.P., Krumhansl, J.L., Anderson, H.L., 1998. Anion scavenger for low-level radioactive waste repository back fills. *J. Soil Contam.* 7, 125-141.
- Benning, L.G., Wilkin, R.T., Barnes, H.L., 2000. Reaction pathways in the Fe-S system below 100°C. *Chem. Geol.* 167, 25-51.
- Berner, R.A., 1964. A synthesis of framboidal pyrite. *Eco. Geol.* 64, 383-384.
- Berner, R.A., 1972. Sulfate reduction, pyrite formation and the oceanic sulfur budget. In: Dryssen, D., and Jagner, D., (Eds.), *Proceedings of the Nobel Symposium 20*, Almquist and Wiskell, Stockholm. pp. 347-361.
- Berner, R.A., 1984. Sedimentary pyrite formation: an update. *Geochim. Cosmochim. Acta* 48, 605-615.

- Bethke, C.M., 1996. *Geochemical reaction modeling*. Oxford University Press. New York, pp. 397.
- BGS and DPHE, 2001. *Arsenic contamination of groundwater in Bangladesh*, Kinniburgh, D.G., and Smedley, P.L., (Eds.). Vol. 2. Final Report, BGS Technical Report WC/00/19. British Geological Survey, Keyworth.
- Bhattacharya, P., Claesson, M., Fagerberg, J., Bundschuh, J., Storniolo, A.R., Martin, R.A., Thir, J.M., Sracek, O., 2005. Natural arsenic in the groundwater of the alluvial aquifers of Santiago del Estero Province, Argentina. In: Bundschuh, J., Bhattacharya, P. and Chandrasekharam, D. (Eds.), *Natural Arsenic in Groundwater: Occurrence, Remediation and Management*. Taylor & Francis Group, London, UK. 57-65.
- Blanchard, M., Alfredsson, M., Brodholt, J., Wright, K., Catlow, C.R.A., 2007. Arsenic incorporation into FeS₂ pyrite and its influence on dissolution: A DFT study. *Geochim. Cosmochim. Acta.* 71, 624-630.
- Bostick, B.C., and Fendorf, S., 2003. Arsenite sorption on troilite (FeS) and pyrite (FeS₂). *Geochim. Cosmochim. Acta.* 67, 909-921.
- Bostick, B.C., Landis, J.D., Hadzima, E., 2006. Sulfate reduction rates impact on arsenic concentrations in Cambodia. *Abstracts with Programs, Geological Society of America.* 38 (7), 242.
- Bostick, B.C., Fendorf, S., Brown, G.E.Jr., 2005. In situ analysis of thioarsenate complexes in neutral to alkaline arsenic sulphide solutions in aquifers in Bengal and Cambodia. *Mineral. Mag.* 69, 825-839.
- Broecker, W.S., Peng, T.-H., 1982. *Tracers in the Sea*; Lamont- Doherty Geological Observatory. Columbia University. New York.
- Butler, I.A., and Rickard, D., 2000. Framboidal pyrite formation via the oxidation of iron (II) monosulfide by hydrogen sulfide. *Geochim. Cosmochim. Acta.* 64(15), 2665-2672.
- Chapelle, F.H., and Lovley, D.R., 1992. Competitive exclusion of sulfate reduction by Fe (III)-reducing bacteria: a mechanism for producing discrete zones of high-iron groundwater. *Ground Water* 30 (1), 29-36.
- Chatain, V., Bayard, R., Sanchez, F., Moszkowicz, P., Gourdon, R., 2005. Effect of indigenous bacterial activity on arsenic mobilization under anaerobic conditions. *Environ. Int.* 31, 221-226.

- Chen, H.W., and Frey, M.M., 1999. Arsenic treatment considerations. *J. of Am. Water Works Association* 91 (3), 74-85.
- Cole, J.M., Ryan, M.C., Smith, S., Bethune, D., 2005. Arsenic contamination of the Salamanca aquifer system in Mexico: a risk analysis. In: Bundeschuh, J., Bhattacharya, P. and Chandrasekharam, D. (Eds.), *Natural Arsenic in Groundwater: Occurrence, Remediation and Management*. Taylor & Francis Group, London, UK. 67-75.
- Creclius, E.A., Bloom, N.S., Cowan, C.E., Jenne, E.A., 1986. Speciation of selenium and arsenic in natural waters and sediments: arsenic speciation. *Electric Power Research Institute (EA-4641, Project 2020-2)*. 2.
- Cullen, W.R., and Reimer, K.J., 1989. Arsenic speciation in the environment. *Chem. Rev.* 89, 713-764.
- Dhakal, P., Saunders, J.A., Lee, M.-K., Savage, K., 2007. Arsenian pyrite: the most important solid arsenic phase in groundwater under sulfate reducing conditions. *Abstracts with programs, Geol. Soc. of Am.* 39(6), pp. 466.
- Dhakal, P., Saunders, J.A., Lee, M.-K., 2008. Arsenic sequestration in arsenian pyrite in low temperature iron-bearing groundwater conditions: field bioremediation, laboratory investigations, and geochemical modeling approaches. *Abstracts with programs, Geol. Soc. of Am.* 40(4), pp. 56.
- Donald, R., and Southam, G., 1999. Low temperature anaerobic bacterial diagenesis of ferrous monosulfide to pyrite. *Geochim. Cosmochim. Acta* 63, 2019-2023.
- Dowdle, P.R., Laverman, A.M., Oremland, R.S., 1996. Bacterial dissimilatory reduction of arsenic (V) to arsenic (III) in anoxic sediments. *Appl. Environ. Microbio.* 62 (5), 1664-1669.
- Dowling, C.B., Poreda, R.J., Basu, A.R., Peters, S.L., 2002. Geochemical study of arsenic release mechanism in the Bangal Basin groundwater. *Water Resources Research* 38, 1-20.
- Drever, J.I., 1997. *The geochemistry of natural waters: surface and groundwater environments*. Prentice Hall, New Jersey. pp. 436.
- Driehaus, W., 2005. Technologies for arsenic removal from potable water. In: Bundeschuh, J., Bhattacharya, P. and Chandrasekharam, D. (Eds.), *Natural Arsenic in Groundwater: Occurrence, Remediation and Management*. Taylor & Francis Group, London, UK. 189-203.

- Dzombak, D.A., and Morel, A.M.M., 1990. Surface complexation modeling: hydrous ferric oxide. Wiley-Interscience. New York.
- EPA, 2003. List of drinking water contaminants & MCLs, Environmental Protection Agency, USA. (available online at: <http://www.epa.gov/safewater/mcl.html>, accessed on June 12, 2008).
- Farquhar, M.L., Charnock, J.M., Livens, F.R., Vaughan, D.J., 2002. Mechanisms of arsenic uptake from aqueous solution by interaction with goethite, lepidocrocite, mackinawite, and pyrite; an x-ray absorption spectroscopy study. *Environ. Sci. Technol.* 36, 1757-1762.
- Fleet, M.E., MacLean, P.J., Barbier, J., 1989. Oscillatory-zoned As-bearing pyrite from strata-bound and stratification gold deposits: an indicator of ore fluid evolution. *Eco. Geol. Monograph.* 6, 356-362.
- Fleet, M.E., and Mumin, A.H., 1997. Gold-bearing arsenian pyrite, marcasite and arsenopyrite from Carlin Trend gold deposits and laboratory synthesis. *Am. Mineralogist.* 82, 182-193.
- Gallegos, T.J., Hyun, S.P., Hayes, K.F., 2007. Spectroscopic investigation of the uptake of arsenite from solution by synthetic mackinawite. *Environ. Sci. Technol.* 41, 7781-7786.
- Goldhaber, M.B., Lee, B.C., Hatch, J.R., Pashin, J.C., Treworgy, J., 2003 Role of large scale fluid-flow in subsurface arsenic enrichment. In: Welch, A.H., and Stollenwerk, K.G. (Eds.), *Arsenic in Groundwater*. Kulwer Academic Publishers. Massachusetts, USA. pp. 127-164.
- Harvey, C.F., Swartz, C.H., Badruzzman, B., Keon, N.E., Yu. W., Ali, A., Jay, J., Beckie, R., Niedan, V., Brabander, D, Oates, P., Ashfaq, K., Islam, S., Hemond, H.F., Ahmed, F., 2002. Arsenic mobility and groundwater extraction in Bangladesh. *Science* 298, 1602-1606.
- Hem, J.D., 1985. Study and interpretation of the chemical characteristics of natural water. Third eds. U.S. Geological Survey Water-Supply paper. Vol. 2254. pp. 264.
- Huerta-Diaz, M.A., and Morse, J.W., 1992. Pyritization of trace metals in anoxic marine sediments. *Geochim. Cosmochim. Acta* 56, 2681-2702.
- Huerta-Diaz, M.A., Tessier, A., Carignan, R., 1998. Geochemistry of trace metals associated with reduced sulfur in freshwater sediments. *Appl. Geochem.* 13, 213-233.

- Hsia, T-H., Lo, S-L., Lin, C-F., Lee, D-Y., 1994. Characterization of arsenate adsorption on hydrous iron oxide using chemical and physical methods. *Colloids and Surface A: Physicochem. Eng. Aspects.* 85, 1-7.
- Keimowitz, A.R., Simpson, H.J., Stute, M., Datta, S., Chillrud, S.N., Ross, J., Tsang, M., 2005. Naturally occurring arsenic: mobilization at a landfill in Maine and implications for remediation. *Appl. Geochem.* 20, 1985-2002.
- Keimowitz, A.R., Mailloux, B.J., Cole, P., Stute, M., Simpson, H.J., Chillrud, S.N., 2007. Laboratory investigations of enhanced sulfate reduction as a groundwater arsenic remediation strategy. *Environ. Sci. Technol.* 41, 6718-6724.
- Kirk, M.F., Holm, T.R., Park, J., Jin, Q., Sanford, R.A., Fouke, B.W., Bethke, C.M., 2004. Bacterial sulfate reduction limits natural arsenic contamination in groundwater. *Geology.* 32, 953-956.
- Kolker, A., Haack, S.K., Cannon, W.F., Westjohn, D.B., Kim, M.J., Nriagu, J., Woodruff, L.G., 2003. Arsenic in southeastern Michigan. In: Welch, A.H., and Stollenwerk, K.G. (Eds.), *Arsenic in Groundwater*. Kulwer Academic Publishers. Massachusetts, USA. pp. 281-294.
- Korte, N., 1991. Naturally occurring arsenic in groundwaters of the Midwestern United States. *Environ. Geol. Water Sci.* 18, 137-141.
- Lee, M.-K., and Saunders, J.A., 2003. Effect of pH on metals precipitation and sorption: field bioremediation and geochemical modeling approaches. *Vadose Zone J.* 2, 177-185.
- Lee, M.-K., Saunders, J.A., Wilkin, R.T., Mohammad, S., 2005. Geochemical modeling of arsenic speciation and mobilization: implications for bioremediation. In: O'Day, P. A., Vlassopoulos, D., Meng, X. and Benning, L. G. (Eds.), *Advances in arsenic research*. American Chemical Society, Washington, DC. 398-413.
- Lee, M.-K., Griffin, J., Saunders, J.A., Wang, Y., Jean, J., 2007. Reactive transport of trace elements and isotopes in Alabama coastal plain aquifers. *J. Geophys. Res.* 112, G02026, (doi:10.1029/2006JG000238).
- Lovley, D.R., and Chapelle, F.H., 1995. Deep subsurface microbial processes. *Rev. of Geophys.* 33, 365-381.
- Lovley, D.R., 2001. Reduction of iron and humics in subsurface environments. In: Fredrickson, J.K., Fletcher, M., (Eds.), *Subsurface microbiology and biogeochemistry*. Wiley-Liss, Inc. New York. pp. 193-211.

- Lowers, H.A., Breit, G.N., Foster, A.L., Whitney, J., Yount, J., Uddin, M.N., Muneem, A.A., 2007. Arsenic incorporation into authigenic pyrite, Bengal Basin sediment, Bangladesh. *Geochim. Cosmochim. Acta* 71, 2699-2717.
- Masscheleyn, P.H., Delaune, R.D., Patrick, W.H., 1991. Effect of redox potential and pH on arsenic speciation and solubility in a contaminated soil. *Environ. Sci. Technol.* 25, 1414-1419.
- Morimoto, N., and Clark, L.A., 1961. Arsenopyrite crystal-chemical reactions. *Am. Mineral.* 46 (11-2). 1448-1469.
- Morse, J.W., Millero, F.J., Cornwell, J.C., Rickard, D., 1987. The chemistry of the hydrogen sulfide and iron sulfide systems in natural waters. *Earth-Science Rev.* 24, 1-42.
- Mullet, M., Boursiquot, S., Abdelmoula, M., Genin, J-M., Ehrhardt, J-J., 2002. Surface chemistry and structural properties of mackinawite prepared by reaction of sulfide ions with metallic iron. *Geochim. Cosmochim. Acta* 66(5), 829-836.
- Neumann, T., Rausch, N., Leipe, T., Dellwig, O., Berner, Z., Böttcher, E.M., 2005. Intense pyrite formation under low-sulfate conditions in the Acheterwasser lagoon, SW Baltic Sea. *Geochim. Cosmochim. Acta* 69(14), 3619-3630.
- Nickson, R., McArthur, J., Burgess, W., Ahmed, K.M., Ravenscroft, P., Rahman, M., 1998. Arsenic poisoning of Bangladesh groundwater. *Nature* 395, 338.
- Nickson, R.T., McArthur, J.M., Ravenscroft, P., Burgess, W.G., Ahmed, K.M., 2000. Mechanism of arsenic release to groundwater, Bangladesh and West Bengal. *Appl. Geochem.* 15, 403-413.
- Nordstrom, D.K., 2000. An overview of arsenic mass poisoning in Bangladesh and West Bengal, India. In: Young, C. (Eds.), *Minor elements 2000: processing and environmental aspects of As, Sb, Se, Te, and Bi*. Society for Mining, Metallurgy and Exploration, 21-30.
- Norman, D.I., Miller, G.P., Branvold, L., Thomas, H., Appiah, J., Ayamsegna, J., Rartey, R., 2001. Arsenic in Ghana, West Africa, ground waters. Extended abstracts, USGS workshop on arsenic in the environment, February 21-22, Denver, CO. (available online at: <http://wwwbrr.cr.usgs.gov/Arsenic/>, accessed on July 11, 2008).
- O'Day, P.A., 2006. Chemistry and mineralogy of arsenic. *Elements*. 2, 77-83.

- O'Day, P.A., Vlassopoulos, D., Root, R.A. and Rivera, N., 2004. The influence of sulfur and iron on dissolved arsenic concentrations in the shallow subsurface under changing redox conditions. *Proceedings of the National Academy of Science*. 101, 13703-13708.
- Onishi, H., 1969. *Handbook of geochemistry* (Wedepohl, K.H., Eds.). Springer-Verlag, Newyork.
- Panthi, S.R., Sharma, S., Mishra, A.K., 2006. Recent status of arsenic contamination in groundwater of Nepal-a review. *Kathmandu University J.of Sci. Engg. & Technol.* 2 (1), 1-11.
- Papacostas, N.C., Bostick, B.C., Landis, J.D., 2006. Establishing geologic controls on arsenic contamination of groundwater: Kandal province, Cambodia. *Abstracts with Programs, Geol. Soc. of Am.* 38 (7), 421.
- Perfetti, E., Pokrovski, G.S., Ballerat-Busserolles, K., Majer, V., Gibert, F., 2008. Densities and heat capacities of aqueous arsenious and arsenic acid solutions to 350°C and 300 bar, and revised thermodynamic properties of, and iron sulfur arsenide minerals. *Geochim. Cosmochim. Acta* 72, 713-731.
- Pierce, M.L., and Moore, C.B., 1982. Adsorption of arsenite and arsenate on amorphous iron hydroxide. *Water Resources* 16, 1247-1253.
- Pokrovski, G.S., Kara, S., Roux, J., 2002. Stability and solubility of arsenopyrite, FeAsS, in crustal fluids. *Geochim. Cosmochim. Acta* 66, 2361-2378.
- Ravenscroft, P., Burgess, W.G., Ahmed, K.M., Burren, M., Perrin, Jerome, 2005. Arsenic in groundwater of the Bengal Basin, Bangladesh: distribution, field relations, and hydrogeological setting. *Hydrogeo. J.* 13, 727-751.
- Reich, M., and Becker, U., 2006. First-principles calculations of the thermodynamic mixing properties of arsenic incorporation into pyrite and marcasite. *Chemical Geology* 225, 278-290.
- Rickard, D., 1968. The geological and microbiological formation of iron sulfides. Ph.D. Thesis, London University. pp. 283.
- Rickard, D., 1969. The chemistry of iron sulfide formation at low temperatures. *Stockholm Contrib. Geol.* 20, 67-95
- Rickard, D.T., 1975. Kinetics and mechanism of pyrite formation at low temperatures. *Am. J. of Sci.* 275, 636-652.

- Rickard, D., and Luther II, G.W., 1997. Kinetics of pyrite formation by the H₂S oxidation of iron (II) monosulfide in aqueous solutions between 25 and 125°C: The mechanism. *Geochim. Cosmochim. Acta* 61, 135-147.
- Rickard, D., and Morse, J.W., 2005. Acid volatile sulfide (AVS). *Marine Chem.* 97, 141-197.
- Rittle, K.A., Drever, J.I., Colberg, P., 1995. Precipitation of arsenic during bacterial sulfate reduction. *Geomicrobio. J.* 13, 1-11.
- Saunders, J.A., Pritchett, M.A., Cook, R.B., 1997. Geochemistry of biogenic pyrite and ferromanganese stream coatings: A bacterial connection? *Geomicrobio. J.* 14, 203-127.
- Saunders, J.A., Lee, M.-K., Mohammad, S., 2005(a). Geochemistry and geomicrobiology of arsenic in Holocene alluvial aquifers, USA. In: Bundeschuh, J., Bhattacharya, P., and Chandrasekharam, D., (Eds.), *Natural Arsenic in Groundwater: Occurrence, Remediation and Management*. Taylor & Francis Group, London, UK. 155-162.
- Saunders, J.A., Lee, M.-K., Uddin, A., Shamsudduha, M., Wilkin, R.T., Fayek, M., Korte, N.E., 2005(b). Natural arsenic contamination of Holocene alluvial aquifers by linked tectonic, weathering, and microbial processes. *Geochemistry, Geophysics and Geosystems (G³)*. 6, 1-7. (doi:10.1029/2004GC000803).
- Saunders, J.A., Lee, M.-K., Wolf, L.A., Morton, C.M., Feng, Y., Thomson, I., Park, S., 2005(c). Geochemical, microbiological, and geophysical assessments of anaerobic immobilization of heavy metals. *Bioremed. J.* 9, 33-48.
- Saunders, J.A., Mohammad, S., Korte, N.E., Lee, M.-K., Fayek, M., Castle, D., Barnett, M.O., 2005(d). Groundwater geochemistry, microbiology, and mineralogy in two arsenic-bearing Holocene alluvial aquifers from the United States. In: O'Day, P. A., Vlassopoulos, D., Meng, X., and Benning, L. G., (Eds.), *Advances in Arsenic Research*. American Chemical Society, Washington, DC. 191-205.
- Saunders, J.A., Lee, M.-K., Shamsudduha, M., Dhakal, P., Uddin, A., Chowdury, M.T., Ahmed, K.M., 2008. Geochemistry and mineralogy of arsenic in (natural) anaerobic groundwaters. *Appl. Geochem.* (in press). (doi: 10.1016/j.apgeochem.2008.07.002).
- Savage, K.S., Tingle, T.N., O'Day, P.A., Waychunas, G.A., Bird, D.K., 2000. Arsenic speciation in pyrite and secondary weathering phases, Mother Lode Gold District, Tuolumne County, California. *Appl. Geochem.* 15, 1219-1244.
- Schoonen, M.A., and Barnes, H.L., 1991. Reactions forming pyrite and marcasite from solution: II. Via FeS precursors below 100°C. *Geochim. Cosmochim. Acta* 55, 1505-1514.

- Sengupta, S., Mukherjee, P.K., Pal, T., Shone, S., 2004. Nature and origin of arsenic carriers in shallow aquifer sediments of Bengal delta, India. *Environ. Geol.* 45, 1071-1081.
- Shahnewaz, M., 2003. Universality of geochemical, microbiologic and hydro-geologic processes controlling the development of natural arsenic contamination of Holocene floodplain aquifers. M.S. Thesis, Auburn University. Auburn. pp. 127.
- Shamsudduha, M., 2007. Mineralogical and geochemical profiling of arsenic-contaminated alluvial aquifers in the Ganges-Brahmaputra flood plain Manikganj, Bangladesh. M.S. Thesis, Auburn University. Auburn. pp. 183.
- Smedley, P.L., and Kinniburgh, D.G., 2002. A review of the source, behaviour and distribution of arsenic in natural waters. *Appl. Geochem.* 17, 517-568.
- Southam, G., and Saunders, J.A., 2005. Geomicrobiology of ore deposits. *Econ. Geol.* 100, 1067-1084.
- Stumm, W., 1992. *Chemistry of the solid-water interface*. John Wiley & Sons, Inc. New York.
- Tandukar, N., Bhattacharya, P., Jacks, G., Valero, A.A., 2005. Naturally occurring arsenic in groundwater of Terai region in Nepal and mitigation options. In: Bundeschuh, J., Bhattacharya, P. and Chandrasekhar, D. (Eds.), *Natural Arsenic in Groundwater: Occurrence, Remediation and Management*. Taylor & Francis Group, London, UK. 41-48.
- Thomas, R.C., and Saunders, J.A., 1998. Arsenic coprecipitation in low-temperature pyrites; implications for bioremediation via sulfate reducing bacteria. *Abstracts with programs, Geol. Soc. of Am.* 30 (7), 58.
- Turner, J.P., 2006. Groundwater geochemistry, geology, and microbiology of arsenic-contaminated Holocene alluvial aquifers, Manikganj, Bangladesh. MS Thesis, Auburn University. pp. 76.
- Webster, J.G., 1990. The solubility of As_2S_3 and speciation of As in dilute and sulphide-bearing fluids at 25 and 90°C. *Geochim. Cosmochim. Acta* 54, 1009-1017.
- Welch, A.H., Westjohn, D.B., Helsel, D.R., Wanty, R.B., 2000. Arsenic in groundwater of the United States; occurrence and geochemistry. *Ground Water* 38, 589-604.
- Wharton, M.J., Atkins, B., Charnock, J.M., Livens, F.R., Patrick, R.A.D., Collison, D., 2000. An X-ray absorption spectroscopy study of coprecipitation of Tc and Re with mackinawite (FeS). *Appl. Geochem.* 15, 347-354.

- WHO, 1996. Guidelines for drinking-water quality, health criteria and other supporting information. Vol. 2: Geneva, World Health Organization.
- WHO, 2001. Arsenic and arsenic compounds, Environmental health criteria 224: Geneva, World Health Organization.
- Wilkin, R.T., Wallschläger, D., Ford, R.G., 2003. Speciation of arsenic in sulfidic waters. *Geochemical Transactions* 4, 1-7.
- Wilkin, R.T., and Barnes, H.L., 1996. Pyrite formation by reactions of iron monosulfides with dissolved inorganic and organic sulfur species. *Geochim. Cosmochim. Acta* 60(21), 4167-4179.
- Wolthers, M., Charlet, L., van Der Linde, P.R., Rickard, D., van Der Weijden, C.H., 2005(a). Surface chemistry of disordered mackinawite (FeS). *Geochim. Cosmochim. Acta* 69, 3469-3481.
- Wolthers, M., Butler, I.B., Rickard, D., Mason, P.R.D., 2005(b). Arsenic uptake by pyrite at ambient environmental conditions: A continuous-flow experiment. In: O'Day, P. A., Vlassopoulos, D., Meng, X., Benning, L. G. (Eds.), *Advances in Arsenic Research*. Am. Chem. Soc. Washington, DC. 60-76.
- Wolthers, M., Charlet, L., van Der Weijden, C.H., van der Linde, P.R., Rickard, D., 2005(c). Arsenic mobility in the ambient sulfidic environment: Sorption of arsenic (V) and arsenic (III) onto disordered mackinawite. *Geochim. Cosmochim. Acta* 69, 3483-3492.
- Wolthers, M., Butler, I.B., Rickard, D., 2007. Influence of arsenic on iron sulfide transformations. *Chem. Geol.* 236, 217-227.

APPENDIX 1: Laboratory results from batch experiments conducted to investigate sorption of As onto synthetic Fe-sulfide.

Sample	Blank concentration		6 hr				pH	Eh (mV)
	As in solution		As sorbed	As sorbed	%			
	µg/L	mg/L	µg/L	mg/L				
6A-1	197	0.197	34.14	0.034	0.163	83	6.95	-401
6A-2			39.56	0.040	0.157	80	12.65	-898
6A-3			40.42	0.040	0.157	79	12.5	-635
6B-1	1753	1.753	570.05	0.570	1.686	67	6.4	-406
6B-2			498.2	0.498	1.681	72	12.47	-632
6B-3			455.1	0.455	1.679	74	12.5	-648
6C-1	5835	5.835	3169	3.169	5.789	46	6.5	-400
6C-2			2877	2.877	5.784	51	12.5	-887
6C-3			3108	3.108	5.788	47	12.71	-644

Sample	Blank concentration		12 hr				pH	Eh (mV)
	As in solution		As sorbed	As sorbed	%			
	µg/L	mg/L	µg/L	mg/L				
12A-1	95	0.095	29.6	0.030	0.065	85	6.4	-391
12A-2			25.43	0.025	0.070	87	12.4	-858
12A-3			22.42	0.022	0.073	89	12.75	-625
12B-1	1002	1.002	598.4	0.598	0.936	66	6.25	-397
12B-2			497.6	0.498	0.930	72	12.55	-610
12B-3			579	0.579	0.935	67	12.75	-635
12C-1	9874	9.874	3500.6	3.501	9.834	40	6.43	-398
12C-2			3330.8	3.331	9.831	43	12.55	-899
12C-3			3408.5	3.409	9.832	42	12.75	-645

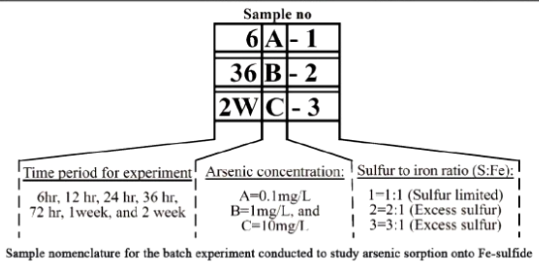
Sample	Blank concentration		24 hr				pH	Eh (mV)
	As in solution		As sorbed	As sorbed	%			
	µg/L	mg/L	µg/L	mg/L				
24A-1	101.4	0.1014	31.03	0.031	0.070	84	6.5	-401
24A-2			29.14	0.029	0.072	85	12.5	-909
24A-3			40	0.040	0.061	80	12.55	-690
24B-1	1010.4	1.0104	645.8	0.646	0.947	63	6.35	-410
24B-2			572.4	0.572	0.943	67	12.55	-698
24B-3			614.3	0.614	0.945	65	12.74	-710
24C-1	10080.6	10.08	3608.14	3.608	10.043	38	6.45	-445
24C-2			2980.2	2.980	10.032	49	12.55	-913
24C-3			3208.3	3.208	10.036	45	12.6	-625

Sample	Blank concentration		36 hr				pH	Eh (mV)
	As in solution		As sorbed	As sorbed	%			
	µg/L	mg/L	µg/L	mg/L				
36A-1	94.3	0.0943	29.24	0.029	0.065	85	6.6	-425
36A-2			30.5	0.031	0.064	85	12.65	-872
36A-3			40.42	0.040	0.054	79	12.71	-860
36B-1	968.1	0.9681	567	0.567	0.900	68	6.57	-424
36B-2			614.5	0.615	0.903	65	12.58	-825
36B-3			587.37	0.587	0.902	66	12.75	-735
36C-1	9845	9.845	4005.4	4.005	9.814	31	6.65	-418
36C-2			3245.3	3.245	9.801	44	12.05	-942
36C-3			3401	3.401	9.803	42	12.71	-670

Sample	Blank concentration		72 hr				pH	Eh (mV)
	As in solution		As sorbed	As sorbed	%			
	µg/L	mg/L	µg/L	mg/L				
72A-1	108	0.108	19.5	0.020	0.089	90	6.5	-430
72A-2			36.2	0.036	0.072	82	12.6	-720
72A-3			32.09	0.032	0.076	84	12.75	-765
72B-1	978.3	0.9783	627.32	0.627	0.914	64	6.47	-439
72B-2			612.8	0.613	0.913	65	12.42	-785
72B-3			589.2	0.589	0.912	66	12.6	-745
72C-1	7943	7.943	4169	4.169	7.914	29	6.25	-397
72C-2			3687.4	3.687	7.906	37	12.55	-895
72C-3			3945.06	3.945	7.911	32	12.75	-720

Sample	Blank concentration		1 Week				pH	Eh (mV)
	As in solution		As sorbed	As sorbed	%			
	µg/L	mg/L	µg/L	mg/L				
1WA-1	103.2	0.1032	30.4	0.030	0.073	85	6.46	-294
1WA-2			23.3	0.023	0.080	88	12.45	-615
1WA-3			25.03	0.025	0.078	87	12.52	-635
1WB-1	1063.04	1.06304	671.3	0.671	1.001	62	6.41	-230
1WB-2			438.4	0.438	0.988	75	12.39	-620
1WB-3			426.43	0.426	0.987	76	12.58	-640
1WC-1	8765	8.765	4006.1	4.006	8.734	31	6.67	-255
1WC-2			3106.3	3.106	8.718	47	12.28	-627
1WC-3			3279.24	3.279	8.721	44	12.42	-658

Sample	Blank concentration		2 Week				pH	Eh (mV)
	As in solution		As sorbed	As sorbed	%			
	µg/L	mg/L	µg/L	mg/L				
2WA-1	89	0.089	18.14	0.018	0.071	91	6.4	-298
2WA-2			26.7	0.027	0.062	86	12.4	-592
2WA-3			23.7	0.024	0.065	88	12.48	-612
2WB-1	978	0.978	370.6	0.371	0.899	79	6.32	-317
2WB-2			296.7	0.297	0.895	83	12.26	-601
2WB-3			243.6	0.244	0.892	86	12.43	-609
2WC-1	10340.01	10.340	2889	2.889	10.290	50	6.52	-246
2WC-2			2638.3	2.638	10.285	55	12.21	-618
2WC-3			3051.7	3.052	10.292	48	12.38	-639



APPENDIX 2: Tabulated data from laboratory experiments carried out to find the most suitable chemical solution to wash pyrite crystals that can maximize the adsorption of As with minimum changes in pH.

6 hr						12 hr					
Pyrite crystal washed with	Sample No	As (solution) ppm	As (sorbed) ppm	As (sorbed) %	pH	Pyrite crystal washed with	Sample No	As (solution) ppm	As (sorbed) ppm	As (sorbed) %	pH
Ethanol (C ₂ H ₆ O, 10%)	A-1U	0.489	3.55E-05	3.55	6.81	Ethanol (C ₂ H ₆ O, 10%)	B-1U	0.498	1.17E-04	11.67	6.68
Acid (0.5M HNO ₃)	A-1V	0.421	1.71E-04	17.06	6.1	Acid (0.5M HNO ₃)	B-1V	0.393	3.03E-04	30.31	5.9
Ethanol and then with DIW	A-1W	0.501	1.18E-05	1.18	6.32	Ethanol and then with DIW	B-1W	0.541	4.13E-05	4.13	6.1
Acid and then with DIW	A-1X	0.497	1.97E-05	1.97	6.31	Acid and then with DIW	B-1X	0.505	1.04E-04	10.37	6.2
DIW	A-1Y	0.494	2.56E-05	2.56	6.29	DIW	B-1Y	0.563	1.77E-06	0.18	6.15
Blank	A-1Z	0.507	0.00E+00	0.00	6.99	Blank	B-1Z	0.564	0.00E+00	0.00	6.99

24 hr						36 hr					
Pyrite crystal washed with	Sample No	As (solution) ppm	As (sorbed) ppm	As (sorbed) %	pH	Pyrite crystal washed with	Sample No	As (solution) ppm	As (sorbed) ppm	As (sorbed) %	pH
Ethanol (C ₂ H ₆ O, 10%)	C-1U	0.506	2.56E-05	2.56	5.72	Ethanol (C ₂ H ₆ O, 10%)	D-1U	0.825	2.89E-04	28.88	6.55
Acid (0.5M HNO ₃)	C-1V	0.510	1.75E-05	1.75	5.25	Acid (0.5M HNO ₃)	D-1V	0.423	6.35E-04	63.50	5.2
Ethanol and then with DIW	C-1W	0.510	1.70E-05	1.70	5.55	Ethanol and then with DIW	D-1W	0.988	1.49E-04	14.87	5.8
Acid and then with DIW	C-1X	0.518	1.93E-06	0.19	6.3	Acid and then with DIW	D-1X	0.961	1.71E-04	17.14	6.2
DIW	C-1Y	0.509	1.93E-05	1.93	5.92	DIW	D-1Y	1.017	1.23E-04	12.33	6.3
Blank	C-1Z	0.519	0.00E+00	0.00	6.99	Blank	D-1Z	1.160	0.00E+00	0.00	7

72 hr					
Pyrite crystal washed with	Sample No	As (solution) ppm	As (sorbed) ppm	As (sorbed) %	pH
Ethanol (C ₂ H ₆ O, 10%)	E-1U	0.696	2.91E-04	29.10	6.34
Acid (0.5M HNO ₃)	E-1V	0.365	6.28E-04	62.80	5.16
Ethanol and then with DIW	E-1W	0.850	1.34E-04	13.40	5.76
Acid and then with DIW	E-1X	0.815	1.69E-04	16.90	6.21
DIW	E-1Y	0.897	8.60E-05	8.60	6.1
Blank	E-1Z	0.981	0.00E+00	0.00	6.97

Summary of the results		
Pyrite crystal washed with	Drop in pH value	Max. As adsorbed
Ethanol (C ₂ H ₆ O, 10%)	7 to 5.72 (18.28%)	3.8μM/gm of FeS ₂ (29.1%)
Acid (0.5M HNO ₃)	7 to 5.16 (26.28%)	9.83μM/gm of FeS ₂ (63.5%)
Ethanol and then by DIW	7 to 5.55 (20.71%)	2.3μM/gm of FeS ₂ (14.87%)
Acid and then by DIW	7 to 6.2 (11.42%)	2.73μM/gm of FeS ₂ (17.14%)
DIW	7 to 5.72 (18.28%)	1.9μM/gm of FeS ₂ (12.33%)

APPENDIX 3: Laboratory data obtained from the adsorption kinetic experiment on pyrite.

Grain size	Est. As conc. (mg/L)	Sample No	Blank conc. (As) (µg/L)	15 min		30 min		1 hr		3 hr		6 hr		12 hr		24 hr		36 hr		72 hr		
				pH	As (T)	pH	As(T)	pH	As(T)	pH	As(T)	pH	As(T)	pH	As(T)	pH	As(T)	pH	As(T)	pH	As(T)	pH
Fine	0.1	F-1/1	88.46	7.00		6.96		6.93		6.70		6.72		6.68		6.45		6.32		6.39		
		As in solution (µg/L)			78.23		50.75		31.01		21.20		16.14		12.11		11.19		10.32		9.71	
		As Adsorbed (%)			11.56		42.63		64.94		76.04		81.76		86.31		87.35		88.33		89.02	
			As Adsorbed (µM/gm)			0.02		0.08		0.13		0.15		0.16		0.17		0.17		0.17		0.18
	1	F-1/2	891.30	6.99		6.99		6.95		6.43		6.69		6.68		6.48		6.51		6.40		
		As in solution (µg/L)			881.94		872.23		805.91		721.51		637.90		569.36		568.56		565.62		558.31	
		As Adsorbed (%)			1.05		2.14		9.58		19.05		28.43		36.12		36.21		36.54		37.36	
			As Adsorbed (µM/gm)			0.02		0.04		0.19		0.38		0.56		0.72		0.72		0.72		0.74
	10	F-1/3	9538.00	7.00		7.00		6.93		6.66		6.65		6.63		6.55		6.54		6.33		
		As in solution (µg/L)			9531.32		9453.11		9317.67		9218.48		9034.39		9014.36		8980.98		8964.77		8958.09	
		As Adsorbed (%)			0.07		0.89		2.31		3.35		5.28		5.49		5.84		6.01		6.08	
			As Adsorbed (µM/gm)			0.01		0.19		0.49		0.71		1.12		1.16		1.24		1.28		1.29
Intermediate	0.1	I-1/1	94.12	6.68		6.98		7.00		6.88		6.78		6.74				6.43		6.42		
		As in solution (µg/L)			90.06		70.83		51.60		29.05		17.50		12.05	6.58	10.99		9.60		9.09	
		As Adsorbed (%)			4.31		24.74		45.17		69.14		81.41		87.20		88.32		89.81		90.35	
			As Adsorbed (µM/gm)			0.01		0.06		0.10		0.15		0.18		0.19		0.19		0.19		0.19
	1	I-1/2	940.50	7.00		7.00		6.98		7.00		6.82		6.80				6.50		6.52		
		As in solution (µg/L)			923.19		916.33		891.88		855.38		797.26		729.55	6.49	716.66		716.00		708.76	
		As Adsorbed (%)			1.84		2.57		5.17		9.05		15.23		22.43		23.80		23.87		24.64	
			As Adsorbed (µM/gm)			0.04		0.05		0.11		0.19		0.32		0.47		0.50		0.50		0.52
	10	I-1/3	11251.00	7.00		6.89		6.92		6.77		6.72		6.64				6.54		6.38		
		As in solution (µg/L)			11247.96		11242.67		11145.24		11122.74		11084.49		10938.22	6.55	10921.35		10902.22		10889.84	
		As Adsorbed (%)			0.03		0.07		0.94		1.14		1.48		2.78		2.93		3.10		3.21	
			As Adsorbed (µM/gm)			0.01		0.02		0.24		0.29		0.37		0.70		6.58		0.78		0.80
Coarse	0.1	C-1/1	92.34	7.00		7.00		6.72		6.82		6.68		6.72		6.60		6.58		6.47		45.18
		As in solution (µg/L)			89.05		83.63		72.45		61.20		53.55		46.36		46.30		46.06		45.18	
		As Adsorbed (%)			3.56		9.43		21.54		33.72		42.01		49.79		49.86		50.12		51.07	
			As Adsorbed (µM/gm)			0.01		0.02		0.04		0.07		0.09		0.10		0.10		0.10		0.10
	1	C-1/2	913.70	7.00		7.00				6.92				6.76		6.58		6.52		6.48		
		As in solution (µg/L)			906.21		904.11	7.00	904.38		898.72	6.80	869.29		811.37		808.35		807.07		806.34	
		As Adsorbed (%)			0.82		1.05		1.02		1.64		4.86		11.20		11.53		11.67		11.75	
			As Adsorbed (µM/gm)			0.02		0.02		0.02		0.03		0.10		0.23		0.23		0.24		0.24
	10	C-1/3	913.70	7.00		7.00				6.85		6.79		6.73		6.68		6.58		6.50		
		As in solution (µg/L)			10255.59		10246.87	6.93	10185.23		10127.80		10114.47		10098.06		10067.29		10054.98		10044.73	
		As Adsorbed (%)			-1022.42		-1021.47		-1014.72		-1008.44		-1006.98		-1005.18		-1001.82		-1000.47		-999.35	
			As Adsorbed (µM/gm)			0.00		0.02		0.16		0.29		0.31		0.35		0.42		0.45		0.47

APPENDIX 4: Data derived from the adsorption isotherm experiment.

Batch experiment on fine grained pyrite crystals									
Assumed initial conc. mg/L	Sample No	As Adsorbed							
		Blank mg/L	As in solution mg/L	As Adsorbed (%)	Initial As conc μ M/L	As in Soln μ M/L	As Adsorbed μ M/gm	Ins Error %	
0.1	M-1/1	0.09	0.00	96.62	1.18	0.04	0.19	1.1	
1	M-1/2	0.97	0.06	94.20	12.97	0.75	2.04	0.7	
10	M-1/3	9.24	6.41	30.67	123.36	85.52	6.31	1.2	
20	M-1/4	18.81	15.74	16.30	251.04	210.11	6.82	1.3	
30	M-1/5	26.58	23.43	11.86	354.77	312.71	7.01	2.0	
40	M-1/6	38.90	35.73	8.16	519.26	476.87	7.07	5.0	
50	M-1/7	46.16	42.97	6.91	616.11	573.54	7.10	1.0	
100	M-1/8	93.54	90.32	3.44	1248.51	1205.59	7.15	1.1	
Batch experiment on intermediate grained pyrite crystals									
Assumed initial conc. mg/L	Sample No	As Adsorbed							
		Blank mg/L	As in solution mg/L	As Adsorbed (%)	Initial As conc μ M/L	As in Soln μ M/L	As Adsorbed μ M/gm	Ins Error %	
0.1	M-2/1	0.09	0.00	98.06	1.22	0.02	0.20	0.3	
1	M-2/2	0.96	0.04	95.89	12.83	0.53	2.05	0.7	
10	M-2/3	8.73	7.27	16.80	116.55	96.97	3.26	1.8	
20	M-2/4	18.42	16.78	8.91	245.91	223.99	3.65	2.5	
30	M-2/5	28.88	27.12	6.07	385.44	362.05	3.90	1.1	
40	M-2/6	36.89	35.09	4.86	492.36	468.41	3.99	1.0	
50	M-2/7	48.12	46.28	3.82	642.21	617.67	4.09	1.7	
100	M-2/8	103.24	101.31	1.87	1377.98	1352.19	4.30	3.6	
Batch experiment on coarse grained pyrite crystals									
Assumed initial conc. mg/L	Sample No	As Adsorbed							
		Blank mg/L	As in solution mg/L	As Adsorbed (%)	Initial As conc μ M/L	As in Soln μ M/L	As Adsorbed μ M/gm	Ins Error %	
0.1	M-3/1	0.08	0.00	96.58	1.03	0.04	0.17	4.0	
1	M-3/2	0.89	0.17	80.68	11.91	2.30	1.60	1.9	
10	M-3/3	9.82	8.67	11.78	131.12	115.68	2.57	2.5	
20	M-3/4	19.82	18.46	6.87	264.54	246.36	3.03	1.0	
30	M-3/5	23.52	22.13	5.90	313.93	295.42	3.09	0.5	
40	M-3/6	40.88	39.42	3.57	545.64	526.16	3.25	0.4	
50	M-3/7	45.55	44.08	3.23	607.97	588.35	3.27	1.0	
100	M-3/8	93.60	92.07	1.63	1249.31	1228.92	3.40	1.2	

APPENDIX 5: Tabulated data from laboratory experiments conducted to investigate changes in As concentration as a function of pH and grain size.

36 Hrs observation											
Size of Pyrite crystals	pH							Blank As (III)			
Fine grained	4	5	6	7	8	9	10	mg/L	µg/gm	µM/L	Max SD
0.1mg/L	F-4/1	F-5/1	F-6/1	F-7/1	F-8/1	F-9/1	F-10/1				
As in Solution (mg/L)	0.073	0.008	0.003	0.002	0.003	0.002	0.002	0.096	96.04	1.28	3.2
As adsorbed (mg)	0.02	0.09	0.09	0.09	0.09	0.09	0.09				
As Adsorbed (%)	24.20	92.00	96.52	97.75	97.23	98.42	98.41				
As Adsorbed µM/gm	0.31	1.18	1.24	1.25	1.25	1.26	1.26				
1mg/L	F-4/2	F-5/2	F-6/2	F-7/2	F-8/2	F-9/2	F-10/2				
As in Solution (mg/L)	0.82	0.08	0.06	0.04	0.04	0.04	0.02	1.022	102.21	13.64	2.03
As adsorbed (mg)	0.20	0.94	0.96	0.99	0.99	0.98	1.00				
As Adsorbed (%)	19.38	92.20	93.83	96.40	96.54	96.24	97.82				
As Adsorbed µM/gm	2.64	12.57	12.80	13.15	13.17	13.13	13.34				
10mg/L	F-4/3	F-5/3	F-6/3	F-7/3	F-8/3	F-9/3	F-10/3				
As in Solution (mg/L)	8.57	2.27	1.28	1.18	1.08	1.08	1.01	9.846	98.46	131.38	2.47
As adsorbed (mg)	1.28	7.57	8.57	8.67	8.76	8.76	8.83				
As Adsorbed (%)	12.97	76.91	87.00	88.01	88.99	89.01	89.73				
As Adsorbed µM/gm	17.04	101.07	114.33	115.66	116.95	116.97	117.92				
Intermediate grained											
0.1mg/L	I-4/1	I-5/1	I-6/1	I-7/1	I-8/1	I-9/1	I-10/1				
As in Solution (mg/L)	0.08	0.02	0.01	0.01	0.01	0.00	0.01	0.088	88.12	1.18	0.58
As adsorbed (mg)	0.01	0.07	0.08	0.08	0.08	0.09	0.08				
As Adsorbed (%)	13.20	79.68	93.01	94.18	94.10	96.52	94.00				
As Adsorbed µM/gm	0.16	0.94	1.09	1.11	1.11	1.14	1.11				
1mg/L	I-4/2	I-5/2	I-6/2	I-7/2	I-8/2	I-9/2	I-10/2				
As in Solution (mg/L)	0.83	0.23	0.10	0.07	0.06	0.07	0.07	0.941	94.12	12.56	1.05
As adsorbed (mg)	0.11	0.71	0.85	0.87	0.88	0.87	0.87				
As Adsorbed (%)	11.88	75.17	89.90	92.50	93.31	92.21	92.80				
As Adsorbed µM/gm	1.49	9.44	11.29	11.62	11.72	11.58	11.66				
10mg/L	I-4/3	I-5/3	I-6/3	I-7/3	I-8/3	I-9/3	I-10/3				
As in Solution (mg/L)	9.77	4.71	2.88	2.64	2.72	2.70	2.68	10.841	108.41	144.66	3.16
As adsorbed (mg)	1.07	6.13	7.96	8.21	8.12	8.15	8.16				
As Adsorbed (%)	9.84	56.53	73.40	75.69	74.91	75.14	75.30				
As Adsorbed µM/gm	14.24	81.80	106.20	109.52	108.40	108.72	108.96				
Coarse grained											
0.1mg/L	C-4/1	C-5/1	C-6/1	C-7/1	C-8/1	C-9/1	C-10/1				
As in Solution (mg/L)	0.09	0.03	0.02	0.01	0.01	0.01	0.01	0.102	102.4	1.37	5.2
As adsorbed (mg)	0.01	0.07	0.08	0.09	0.09	0.09	0.09				
As Adsorbed (%)	13.36	72.45	81.40	87.29	87.92	89.50	91.32				
As Adsorbed µM/gm	0.18	0.99	1.11	1.19	1.20	1.22	1.25				
1mg/L	C-4/2	C-5/2	C-6/2	C-7/2	C-8/2	C-9/2	C-10/2				
As in Solution (mg/L)	0.87	0.41	0.14	0.12	0.12	0.11	0.11	0.925	92.52	12.35	0.83
As adsorbed (mg)	0.06	0.52	0.79	0.81	0.81	0.81	0.81				
As Adsorbed (%)	6.02	56.00	85.39	87.52	87.37	87.63	88.00				
As Adsorbed µM/gm	0.74	6.92	10.54	10.81	10.79	10.82	10.87				
10mg/L	C-4/3	C-5/3	C-6/3	C-7/3	C-8/3	C-9/3	C-10/3				
As in Solution (mg/L)	10.787	8.517	4.578	4.462	4.278	4.325	4.343	11.262	112.62	150.28	1.84
As adsorbed (mg)	0.48	2.75	6.68	6.80	6.98	6.94	6.92				
As Adsorbed (%)	4.22	24.38	59.35	60.38	62.01	61.60	61.44				
As Adsorbed µM/gm	6.34	36.64	89.21	90.77	93.22	92.60	92.35				